Aus dem

Lübecker Institut für Experimentelle Dermatologie

Direktor: Prof. Dr. Ralf Ludwig

Innovative Anti-IL-33 Receptor Blocking: A Novel Intrapulmonary Therapeutic Approach for the Treatment of Steroid-Hyporesponsive Severe Asthma

Inauguraldissertation

Zum Erwerb des Doktorgrades

der Universität zu Lübeck

-Aus der Sektion Medizin-

vorgelegt von

Baraa Khalid Salah Al-Sheakly

aus Baghdad, Irak

Lübeck 2025

1. Berichterstatter*in: Prof. Dr. med. vet. Jennifer Hundt

Ko-Betreuer*in: PD Dr. rer. nat. Yves Laumonnier

2. Berichterstatter*in: Prof. Dr. rer. nat. Olaf Jöhren

Tag der mündlichen Prüfung: 10.07.2025

Zum Druck genehmigt. Lübeck, den 11.07.2025

-Promotionskommission der Sektion Medizin-

Table of Contents

LIST OF ABBREVIATIONS

AHR - Airway Hyperresponsiveness

AMP - Ampicillin

AST - Astegolimab (monoclonal antibody)

BALF - Bronchoalveolar Lavage Fluid

BSA - Bovine Serum Albumin

cDNA - Complementary DNA

COPD - Chronic Obstructive Pulmonary Disease

CXCL8 - Chemokine (C-X-C motif) Ligand 8 (also known as IL-8)

DAPI - 4′,6-Diamidino-2-Phenylindole (a fluorescent nuclear stain)

DEX - Dexamethasone

ΔΔCT - Delta Delta Cycle Threshold

ECL - Enhanced Chemiluminescence

EDTA - Ethylenediaminetetraacetic acid (a chelating agent)

ELISA - Enzyme-Linked Immunosorbent Assay

FACS - Fluorescence-Activated Cell Sorting

FDA - Food and Drug Administration

FeNO - Fractional Exhaled Nitric Oxide

GLU - Glucose

GR - Glucocorticoid Receptor

GRα - Glucocorticoid Receptor Alpha

GRβ - Glucocorticoid Receptor Beta

HCAb - Heavy-Chain Antibody

HDAC2 - Histone Deacetylase 2

HDM - House Dust Mite

HSP - Hidradenitis Suppurativa

HRP - Horseradish Peroxidase

IHC - Immunohistochemistry

IC_{50} - Half Maximal Inhibitory Concentration

IL-1R AcP - Interleukin-1 Receptor Accessory Protein

IL-18Rα - Interleukin-18 Receptor Alpha

IL-33 - Interleukin-33

IL-36R - Interleukin-36 Receptor

IMAC - Immobilized Metal Affinity Chromatography

IV - Intravenous

KD - Dissociation Constant

LB - Luria-Bertani (a nutrient-rich bacterial growth medium)

MAPK - Mitogen-Activated Protein Kinase

NB - Nanobody (e.g., NB7)

NF-κB - Nuclear Factor Kappa B

NS-NB - Nonspecific Nanobody

OVA - Ovalbumin

PAS - Periodic Acid-Schiff (a staining method)

PBS-Tween - Phosphate-Buffered Saline with Tween

PCR - Polymerase Chain Reaction

PEGylation - Polyethylene Glycol Modification

p-ERK - Phosphorylated Extracellular Signal-Regulated Kinase

p-IκBα - Phosphorylated Inhibitor of Nuclear Factor Kappa B Alpha

PI3K/AKT - Phosphoinositide 3-Kinase/Protein Kinase B

qRT-PCR - Quantitative Real-Time Polymerase Chain Reaction

RNA - Ribonucleic Acid

RSV - Respiratory Syncytial Virus

SC - Subcutaneous

SOC - Super Optimal Broth with Catabolite Repression (a bacterial growth medium)

ST2 - Suppressor of Tumorigenicity 2

SYK - Spleen Tyrosine Kinase

TES - Tris-EDTA-Sucrose buffer

Th - T Helper (e.g., Th2, Th17)

Th2/Th17 - T Helper Cell Type 2/Type 17

TMB - Tetramethylbenzidine (a substrate for HRP enzyme in ELISA)

TPP - Thrombotic Thrombocytopenic Purpura

TSLP - Thymic Stromal Lymphopoietin

VHH - Variable Heavy-Chain Domain of Heavy-Chain Antibodies

List of Figures

List of Tables

Abstract

Severe asthma remains a critical healthcare challenge due to its complex pathophysiology and poor response to corticosteroids. IL-33, a potent alarmin, plays a central role in promoting airway inflammation through its receptor, ST2. Targeting the IL-33/ST2 axis is emerging as a promising therapeutic strategy for severe asthma. While monoclonal anti-ST2 antibodies such as astegolimab show potential in severe asthma, their high cost, limited tissue penetration, and immunogenicity highlight the need for innovative alternatives. This study addresses these limitations by developing novel anti-ST2 nanobodies and evaluating their therapeutic potential through intrapulmonary delivery, which offers localized treatment with superior tissue penetration, reduced side effects, and enhanced efficiency. Mechanistic studies revealed that IL-33/ST2 signaling drives steroid hypo-responsiveness by activating MAPK/ERK and NF-κB pathways and disrupting the GRα/GRβ balance. To counteract these effects, we generated a high-affinity anti-ST2 nanobody library using phage display technology. NB7, the top-performing nanobody, demonstrated exceptional binding specificity and affinity for ST2. Functional evaluations in primary human lung epithelial cells confirmed NB7's ability to block ST2, reduced MAPK/ERK and NF-κB activation, and suppress key pro-inflammatory cytokines, including IL-17 and IL-8. Notably, NB7 restored the GRα/GRβ balance and reversed steroid hypo-responsiveness *in vitro*. *In vivo*, intrapulmonary delivery of NB7 demonstrated enhanced localized action, significantly reducing airway inflammation, mucus production, and cytokine levels, while improving lung mechanics and restoring steroid responsiveness with lower systemic exposure and side effects. NB7 demonstrated superior efficacy to astegolimab across multiple parameters at a lower dose. This research is the first to develop anti-ST2 nanobodies that specifically target the IL-33 receptor and evaluate their efficacy via intrapulmonary delivery compared to

monoclonal antibodies. By addressing key limitations of existing therapies, this study offers a transformative and localized approach to improving the management of severe asthma.

Zusammenfassung

Hintergrund: Schweres Asthma bleibt eine bedeutende gesundheitliche Herausforderung aufgrund seiner komplexen Immunpathologie und der Resistenz gegenüber Kortikosteroidtherapien. Die IL-33/ST2-Signalkaskade spielt eine entscheidende Rolle bei der Förderung von Atemwegsentzündungen und trägt zur Chronizität der Erkrankung sowie zur Steroid-Hyporesponsivität bei. IL-33, ein epithelialer Alarmin, löst durch Bindung an seinen Rezeptor ST2 eine Kaskade entzündlicher Reaktionen aus, die zur Aktivierung der MAPK/ERK- und NF-κB-Signalwege führt. Diese Signalwege verstärken nicht nur die Atemwegsentzündung, sondern verringern auch die Wirksamkeit von Kortikosteroiden. Während monoklonale Antikörper (mAbs) gegen ST2, wie Astegolimab, in klinischen Studien vielversprechende Ergebnisse zeigten, wird ihre therapeutische Anwendung durch hohe Produktionskosten, eine begrenzte Gewebepenetration und mögliche Immunogenität erschwert. Um diese Herausforderungen zu bewältigen, zielte diese Studie darauf ab, eine neuartige Klasse von anti-ST2-Nanobodies mit verbesserter Gewebepenetration, erhöhter Stabilität und reduzierten systemischen Nebenwirkungen bei intrapulmonaler Verabreichung zu entwickeln.

Methoden: Eine hochaffine anti-ST2-Nanobody-Bibliothek wurde durch Immunisierung eines Kamels mit rekombinantem humanem ST2 und anschließender Selektion mittels Phagen-Display-Technologie erstellt. Die Nanobodies wurden hinsichtlich ihrer Bindungsspezifität und Affinität gescreent, wobei NB7 als vielversprechendster Kandidat identifiziert wurde. Funktionelle Tests wurden an primären humanen Lungenepithelzellen durchgeführt, um die Auswirkungen von NB7 auf die IL-33-induzierte Entzündungssignalisierung, die MAPK/ERK- und NF-κB-Aktivierung sowie die Zytokinsekretion, insbesondere IL-17 und IL-8, zu untersuchen. Zudem wurde geprüft, ob

NB7 das GRα/GRβ-Gleichgewicht wiederherstellen und die Steroid-Hyporesponsivität umkehren kann. In vivo-Experimente wurden an einem murinen Modell für schweres Asthma durchgeführt, in dem NB7 intrapulmonal verabreicht wurde. Die Analyse umfasste Atemwegsentzündung, Schleimproduktion, Zytokinspiegel, Lungenmechanik und Steroidreaktivität, um die therapeutische Wirksamkeit von NB7 im Vergleich zu Astegolimab zu bewerten.

Ergebnisse: NB7 zeigte eine außergewöhnliche Bindungsspezifität und hohe Affinität für ST2 und hemmte effektiv die IL-33-induzierten Signalwege. In vitro führte die Behandlung mit NB7 zu einer signifikanten Reduktion der MAPK/ERK- und NF-κB-Aktivierung, was mit einer starken Unterdrückung der proinflammatorischen Zytokine IL-17 und IL-8 einherging. Bemerkenswerterweise stellte NB7 das GRα/GRβ-Gleichgewicht wieder her und kehrte die Steroid-Hyporesponsivität in primären Lungenepithelzellen um. In vivo führte die intrapulmonale Verabreichung von NB7 zu einer signifikanten Reduktion der Atemwegsentzündung, der Schleimüberproduktion und der proinflammatorischen Zytokinspiegel. Zudem verbesserte NB7 die Lungenmechanik und stellte die Steroidreaktivität mit reduzierter systemischer Exposition und geringeren Nebenwirkungen im Vergleich zu Astegolimab wieder her. Besonders hervorzuheben ist, dass NB7 eine überlegene Wirksamkeit bei der Minderung der Atemwegsentzündung und der Verbesserung der Kortikosteroidantwort bei einer niedrigeren Dosis als die monoklonale Antikörpertherapie zeigte.

Schlussfolgerung: Diese Studie beschreibt erstmals die Entwicklung und Evaluierung von anti-ST2-Nanobodies, die gezielt den IL-33-Rezeptor für die Behandlung von schwerem Asthma adressieren. Durch den Einsatz der Phagen-Display-Technologie wurde NB7 als hochwirksamer Nanobody identifiziert, der die ST2-Signalübertragung blockiert, Entzündungen reduziert und die Kortikosteroid-Sensitivität wiederherstellt. Die

intrapulmonale Verabreichung von NB7 bietet eine lokal begrenzte Therapie mit überlegener Gewebepenetration und minimalen systemischen Nebenwirkungen, wodurch zentrale Einschränkungen aktueller monoklonaler Antikörpertherapien überwunden werden. Diese Ergebnisse unterstreichen das Potenzial von Nanobody-basierten Therapien als innovative Strategie zur Behandlung von schwerem Asthma und ebnen den Weg für weitere klinische Entwicklungen.

1. Introduction

1.1 General Overview of Asthma

Asthma is a heterogeneous chronic inflammatory condition marked by airway hyper-responsiveness (AHR), inflammation, remodelling, and reversible airflow limitation, often triggered by environmental or occupational exposures to microbes, industrial products, or allergens (Wenzel, 2012). It affects approximately 300 million people globally, and this number is expected to rise by 100 million by 2025 (Auckland, 2018). It ranks 28th among the leading causes of disease burden and 16th globally in terms of disability-adjusted life years, highlighting its significant impact on quality of life (Auckland, 2018). In the UAE, 4.9% of the population suffers from asthma (Tarraf et al., 2018).

Several factors contribute to the prevalence of asthma, including genetic predisposition, tobacco smoke exposure, viral infections, air pollution, obesity, and certain allergens like dust mites (Toskala & Kennedy, 2015). Other factors such as stress, lack of beneficial microbial exposure, socioeconomic status, and occupational hazards in adults also play a role (Toskala & Kennedy, 2015; von Mutius & Smits, 2020). Asthma varies in its causes, severity, and response to treatment, which is why it is classified based on clinical, physiological, and immunobiological characteristics (Toskala & Kennedy, 2015; von Mutius & Smits, 2020).

1.2 Asthma Pathophysiology

1.2.1 Clinical Traits and Disease Mechanisms

Asthma is characterized by symptoms such as dyspnoea, wheezing, cough, phlegm production, and frequent exacerbations (Hashmi & Cataletto, 2024). These symptoms reflect complex interactions between structural and immune cells, resulting in airway inflammation, hyperresponsiveness, and remodelling (Wenzel, 2012). Loss of lung function and asthma severity often vary, highlighting the heterogeneity of the disease (Carr & Bleecker, 2016).

1.2.2 Type 2 (T2) Inflammation

Type (T2) inflammation is a dominant feature in asthma, marked by eosinophilic airway infiltration and the overproduction of cytokines like IL-4, IL-5, and IL-13 (Robinson et al., 2017). Each cytokine plays a distinct role in fuelling the inflammatory process. IL-4 is essential for B cell class switching, leading to IgE production that binds to mast cells and triggers allergic sensitization (Akar-Ghibril, Casale, Custovic, & Phipatanakul, 2020). IL-5 promotes the growth, activation, and survival of eosinophils, intensifying airway inflammation (Nakagome & Nagata, 2024; Pelaia et al., 2022). IL-13 contributes to mucus overproduction, airway remodelling, and smooth muscle contraction, all of which worsen airflow obstruction and bronchial hyperreactivity (Nakagome & Nagata, 2024; Pelaia et al., 2022). In allergic asthma, TH2 cells release IL-5 and IL-13 in response to allergens, driving inflammation and early-onset symptoms (Jonckheere, Bullens, & Seys, 2019). In contrast, non-allergic T2-high asthma is often triggered by environmental factors, with ILC2 cells playing a central role in promoting eosinophilic inflammation and airway hyperresponsiveness (Ciprandi, Tosca, Silvestri, & Ricciardolo, 2017). This form of asthma tends to develop later in life and is usually more severe and persistent (Ciprandi et al., 2017). T2 asthma usually responds well to corticosteroids, which suppress IL-4, IL-5, and IL-13, reducing eosinophilic inflammation and improving symptoms (Hussain & Liu, 2024). In

severe cases with persistent eosinophilia, response may be limited, requiring targeted biologics (Peters et al., 2019) **(Figure 1.1)**.

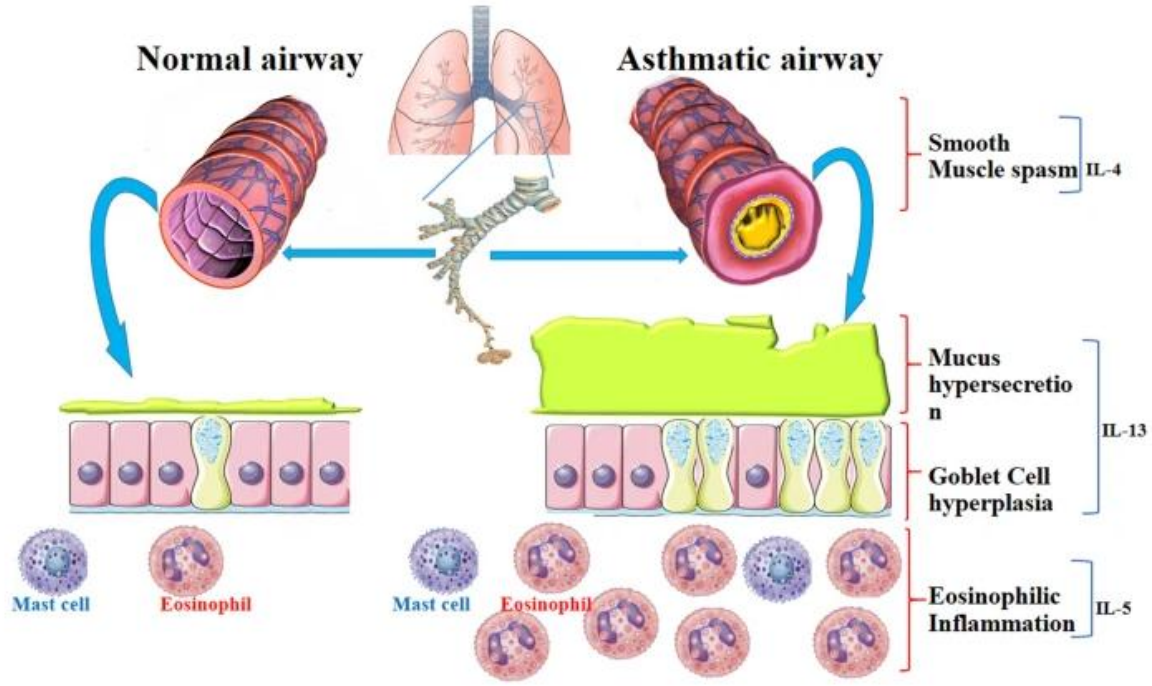

Figure 1.1 Type2 inflammation (Athari, 2019): The image compares a normal airway with an asthmatic airway, highlighting smooth muscle spasm (IL-4), mucus hypersecretion (IL-13), goblet cell hyperplasia (IL-13), and eosinophilic inflammation (IL-5). Key immune cells include mast cells and eosinophils. Airways in asthma become narrowed, inflamed, and mucus-filled, impairing airflow.

1.2.3 Type 2-Low Inflammation

T2-low asthma is often characterized by neutrophilic inflammation (≥40-60%) and is typically resistant to corticosteroids (Nair, Surette, & Virchow, 2021). This phenotype has been linked to Th1 and Th17 activation, with evidence suggesting that Th17/Treg imbalance may contribute to severe, steroid-resistant, neutrophilic asthma (X. Liu et al., 2015). Mechanisms driving neutrophilic inflammation are unclear but may involve chronic bacterial

infection, obesity, smoking, smooth muscle dysfunction, and activation of the NLRP3 inflammasome with elevated IL-1β (Hudey, Ledford, & Cardet, 2020). However, Th17-driven asthma, associated with IL-17A/F elevation, manifests as steroid-refractory disease with neutrophilic inflammation, airway remodelling, and increased collagen deposition (Newcomb & Peebles, 2013). IL-8-driven neutrophil recruitment further amplify airway hyperresponsiveness and inflammation in severe asthma (Norzila, Fakes, Henry, Simpson, & Gibson, 2000). This complex interplay underscores the need to better define T2-low asthma endotypes for more targeted therapeutic approaches (Kuruvilla, Lee, & Lee, 2019) **(Figure 1.2).**

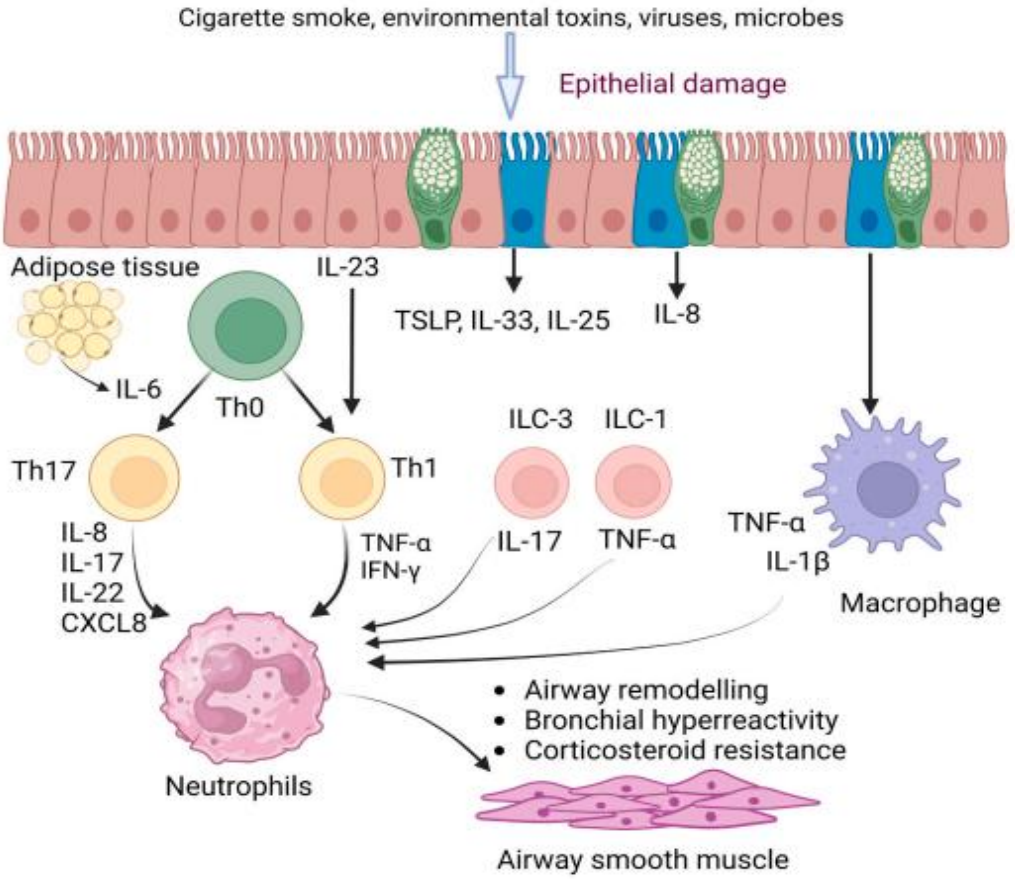

Figure 1.2 Type 2-low inflammation (Hudey et al., 2020): Epithelial damage from cigarette smoke, toxins, viruses, and microbes induces TSLP, IL-33, IL-25, and IL-8 release. IL-23 and

IL-6 drive Th0 differentiation into Th17 (IL-8, IL-17, IL-22, CXCL8) and Th1 (TNF-α, IFN-γ), promoting neutrophil recruitment. ILC-3 (IL-17) and ILC-1 (TNF-α) contribute to inflammation, while macrophages (TNF-α, IL-1β) amplify immune responses. These processes lead to airway remodeling, bronchial hyperreactivity, and corticosteroid resistance.

1.2.4 Airway Hyperresponsiveness

Mast cells play a critical role in asthma by releasing broncho-constrictive mediators such as histamine and leukotrienes (Banafea, Bakhashab, Alshaibi, Natesan Pushparaj, & Rasool, 2022). These cells infiltrate airway smooth muscle in both Type 2-high and Type 2-low asthma, contributing to airway hyperresponsiveness and inflammation (Kuruvilla et al., 2019). Asthma is marked by hypertrophy and hypercontractility of airway smooth muscle, leading to bronchospasm and airflow limitation (O'Byrne & Inman, 2003). This hyperresponsiveness is amplified by inflammatory mediators such as IL-5, IL-13, and IL-8, which contribute to muscle thickening and airway remodelling (Chapman & Irvin, 2015). Sensory nerve dysfunction, associated with eosinophilic inflammation, increases airway sensitivity, exacerbating symptoms like chronic cough (M. G. Drake, Cook, Fryer, Jacoby, & Scott, 2021).

1.2.5 Airway Remodeling

In asthma, the airways undergo abnormal changes in the epithelial and submucosa, known as airway remodelling, which are linked to a progressive and permanent loss of function (Tai et al., 2014). The epithelium undergoes alterations, such as the metaplasia of goblet cells and the accumulation of extra mucus (Hough et al., 2020). Submucosal alterations include excess collagen type I, III, and V accumulation, greater number of the gland cells, smooth muscular cell growth and proliferation, and an increase in the quantity

of blood vessels (Wadsworth, Sin, & Dorscheid, 2011). Due to baseline constricted airways and greater susceptibility to respiratory exacerbates like allergens, these anatomical alterations are thought to contribute to asthma exacerbations. It is still debatable how lung remodelling, inflammation, and AHR are related (Dougherty & Fahy, 2009) **(Figure 1.3)**.

Research in both humans and animals has long confirmed that persistent inflammation in asthma patients drives airway remodelling (Ward et al., 2002). This is supported by findings showing that glucocorticoid therapy not only reduces airway inflammation but also positively affects airway remodelling (Hoshino et al., 1998).

1.2.6 Alarmins: Key Responders to Cellular Stress and Regulators of Asthma Pathogenesis

The airway epithelium plays a crucial role in asthma, acting as the first line of defence against environmental triggers like allergens, viruses, and smoke (Lambrecht & Hammad, 2012). When this barrier is compromised, it leads to the release of key epithelial cytokines—TSLP, IL-33, and IL-25—collectively known as alarmins (Gauvreau et al., 2023). These alarmins activate immune cells such as Th2 cells and ILC2s, driving inflammation, mucus production, and airway constriction (Gauvreau et al., 2023). Beyond Th2 pathways, alarmins can directly activate mast cells, intensifying inflammation and airway hyperresponsiveness (Hansi, Ranjbar, Whetstone, & Gauvreau, 2024) **(Figure 1.3)**. IL-25 and TSLP are particularly important in amplifying airway inflammation following epithelial damage, whether from allergens, pollutants, or infections (Whetstone, Ranjbar, Omer, Cusack, & Gauvreau, 2022). They stimulate ILC2s, mast cells, and dendritic cells, triggering the release of type 2 cytokines like IL-4, IL-5, and IL-13, which fuel eosinophilic inflammation, excessive mucus, and airway remodelling—key characteristics of asthma (Stanbery, Shuchi, Jakob von, Tait Wojno, & Ziegler, 2022). TSLP enhances dendritic cell activity, pushing T

cells toward a Th2 response and reinforcing chronic inflammation (He & Geha, 2010), while IL-25 promotes eosinophil recruitment and mucus secretion through ILC2 activation (Deng et al., 2021). IL-33 is well-established as a driver of eosinophilic inflammation in asthma, but its role in neutrophilic asthma remains less understood (Kakkar & Lee, 2008). Emerging evidence suggests that it can also contribute to neutrophilic inflammation, potentially through the activation of Th17 cells and the induction of IL-17A (Curren et al., 2023). This dual role of IL-33 makes it an important player in both eosinophilic and neutrophilic forms of this alarmin shapes non-type 2 asthma, potentially revealing novel therapeutic targets for severe cases.

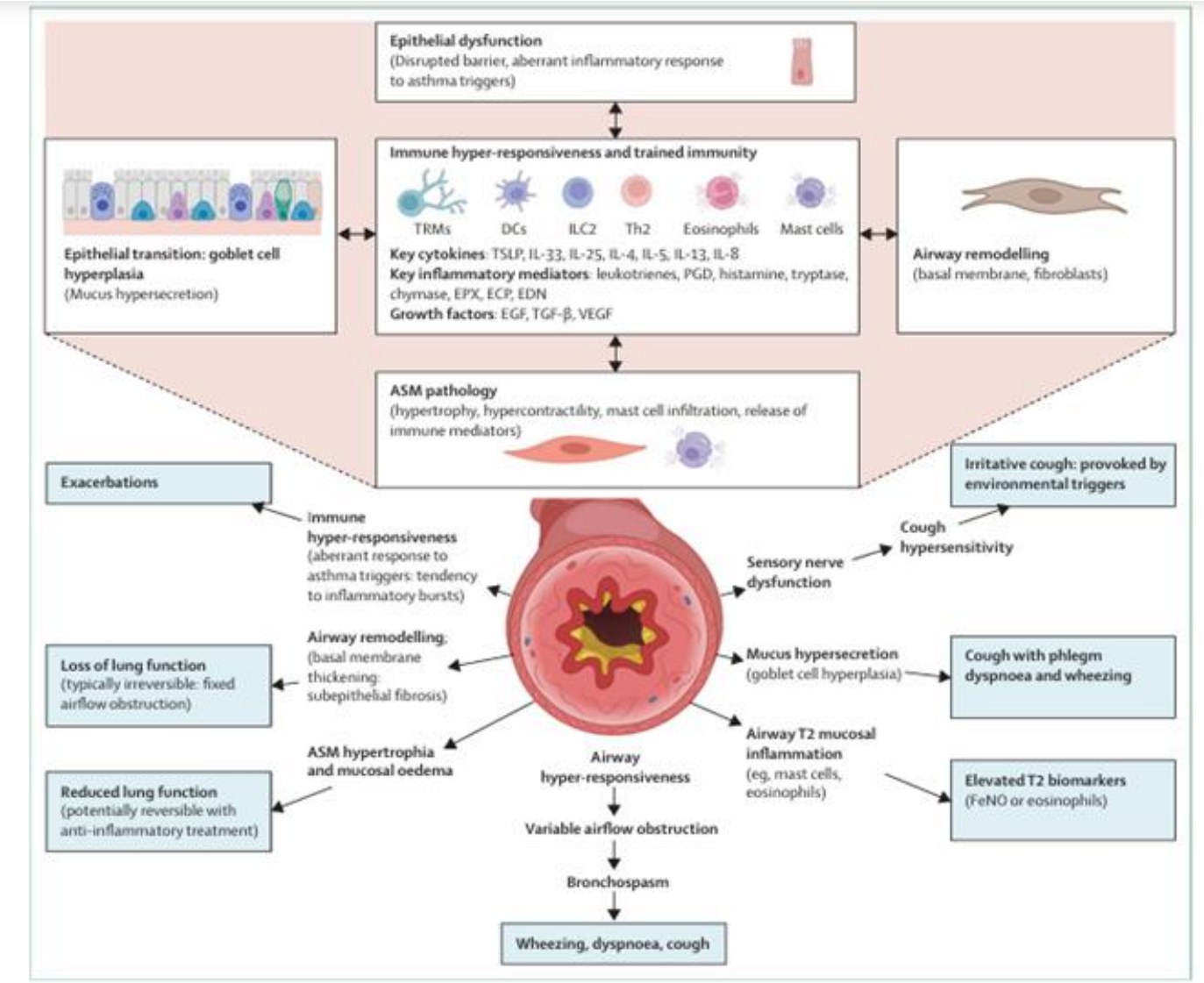

Figure 1.3 Asthma Pathophysiology (Wenzel, 2012): Asthma pathology involves epithelial dysfunction, immune hyper-responsiveness (TRMs, DCs, ILC2, Th2, eosinophils, mast cells), and airway remodeling. Key mediators include TSLP, IL-33, IL-25, IL-4, IL-5, IL-13, IL-8, leukotrienes, histamine, and growth factors (EGF, TGF-β, VEGF). ASM pathology leads to hypercontractility, hypertrophy, and immune infiltration, causing mucus hypersecretion, T2 mucosal inflammation, airway hyper-responsiveness, bronchospasm, and airflow obstruction. Clinically, this manifests as wheezing, dyspnea, cough, exacerbations, and lung function loss, with FeNO and eosinophils as T2 biomarkers.

1.3 IL-33/ST2 Pathway in Asthma

Interleukin-33 (IL-33), a member of the IL-1 cytokine family, plays a crucial role in immune regulation (Cayrol & Girard, 2018), particularly in promoting type 2 immune responses (Löhning et al., 1998). Encoded by the IL33 gene on chromosome 9 (9p24.1)(Tsuda et al., 2012), IL-33 is primarily expressed in epithelial and endothelial cells, smooth muscle cells, adipocytes, and various tissues, including the lungs, gut, and skin (Liew, Girard, & Turnquist, 2016; Moussion, Ortega, & Girard, 2008; Talabot-Ayer et al., 2012). The release of IL-33 is induced by pro-inflammatory cytokines like TNF-α, IFN-γ, IL-4, and by pathogen-associated molecular patterns (PAMPs) and ATP (Liew et al., 2016; Miller, 2011; Pinto et al., 2018). IL-33 functions as an alarmin, rapidly released in response to cellular damage or inflammation(Moussion et al., 2008). It signals through the ST2 receptor (Lingel et al., 2009), activating immune cells such as mast cells, eosinophils, and ILC2s (Cherry, Yoon, Bartemes, Iijima, & Kita, 2008; Hsu & Bryce, 2012; Olguín-Martínez et al., 2022). This leads to the production of type 2 cytokines, including IL-4, IL-5, and IL-

13, driving eosinophilic inflammation, mucus secretion, and airway hyperresponsiveness—hallmarks of asthma and allergic diseases(L. Y. Drake & Kita, 2017; Piehler et al., 2016).

IL-33 signals through a heterodimeric receptor complex composed of IL-1 receptor-like 1 (IL1RL1, known as ST2) and IL-1 receptor accessory protein (IL1RAcP) (Lingel et al., 2009). IL-33/ST2 interactions lead to the recruitment of adaptor proteins, such as MyD88 and IRAK, activating downstream pathways like MAPK, NF-κB, PI3K/AKT, JAK2, and SYK, which are critical for immune cell activation and cytokine production (Andrade et al., 2011; Schmitz et al., 2005). Dysregulated IL-33 signalling is implicated in various diseases, including asthma, allergies, rheumatoid arthritis, fibrosis, cardiovascular diseases, and autoimmune disorders (Gaurav & Poole, 2022; Xiuxing Liu et al., 2019; Murdaca et al., 2019). IL-33 plays a dual role as both an alarmin, released during cellular stress, and a cytokine, amplifying inflammatory responses (L. Y. Drake & Kita, 2017). Ongoing research into IL-33's signalling mechanisms continues to reveal its significance in immune modulation and its potential as a therapeutic target for inflammatory and autoimmune diseases (L. Y. Drake & Kita, 2017). Blocking alarmins with monoclonal antibodies or receptor inhibitors offers a promising approach to reducing airway inflammation and improving control, particularly for patients with severe asthma (Gauvreau et al., 2023).

1.4 Current Treatments for Asthma

Asthma management relies on a combination of long-term control therapies and quick-relief medications to reduce airway inflammation, prevent exacerbations, and provide symptom relief. Inhaled corticosteroids (ICS), such as fluticasone, mometasone, and budesonide, are the cornerstone of asthma treatment, offering effective inflammation control by inhibiting cytokine production and immune cell recruitment (Barnes, 2006). ICS therapy is

generally well-tolerated, with minimal systemic side effects compared to oral corticosteroids, as glucocorticoids act at the nuclear level by impairing histone acetyltransferase activity and recruiting histone deacetylase-2, ultimately suppressing inflammatory gene expression (Barnes, 2006; Ito, Barnes, & Adcock, 2000).

Combination inhalers that pair ICS with long-acting beta-agonists (LABAs), like fluticasone/salmeterol or budesonide/formoterol, enhance asthma control by providing both anti-inflammatory effects and sustained bronchodilation (Nannini, Lasserson, & Poole, 2012). These combinations significantly reduce the risk of exacerbations and improve lung function in patients with moderate to severe asthma (Nannini et al., 2012).

For immediate symptom relief during acute asthma attacks, short-acting beta2-agonists (SABAs) like albuterol and levalbuterol rapidly alleviate bronchoconstriction, while anticholinergic agents such as ipratropium and tiotropium relax airway muscles to improve breathing (Papi et al., 2020; Sobieraj et al., 2018). Long-term control strategies also include leukotriene receptor antagonists like montelukast, which prevent smooth muscle contraction by blocking leukotriene D4 receptors (Hamid, Tulic, Liu, & Moqbel, 2003), and theophylline, a daily bronchodilator that helps maintain open airways by relaxing smooth muscles (Mahemuti, Zhang, Li, Tieliwaerdi, & Ren, 2018). Despite these therapies, some patients with severe asthma experience persistent symptoms and frequent exacerbations, necessitating the use of advanced biologics for more targeted intervention (Abrams, Becker, & Szefler, 2018).

Monoclonal antibodies (mAbs) have transformed the treatment landscape for severe asthma by selectively modulating immune pathways implicated in disease progression (Kardas, Panek, Kuna, Damiański, & Kupczyk, 2022). Omalizumab, the first anti-IgE therapy, reduces allergic inflammation and has been shown to decrease oral corticosteroid use, exacerbation rates, and hospitalizations in patients with severe allergic asthma (W. Busse

et al., 2001). It remains the only biologic approved for children as young as six. Anti-IgE antibody ligelizumab, which binds IgE with more affinity than omalizumab, has shown promising results in clinical trials (Katsaounou et al., 2019).

Anti-IL-5 therapies such as mepolizumab, reslizumab, and benralizumab have emerged as effective options for eosinophilic asthma measures (Bleecker et al., 2016; Nair et al., 2009; Pavord et al., 2012).While mepolizumab and reslizumab target IL-5 to reduce eosinophil counts and prevent exacerbations, benralizumab uniquely induces eosinophil apoptosis by targeting the IL-5 receptor, offering broader benefits across eosinophilic asthma subtypes (Bleecker et al., 2016; Nair et al., 2009).

More recently, dupilumab, an IL-4 receptor monoclonal antibody, blocks both IL-4 and IL-13 signalling pathways, addressing key drivers of type 2 inflammation and demonstrating significant reductions in exacerbations and oral steroid dependence (W. W. Busse et al., 2018). Although other IL-13 inhibitors, such as lebrikizumab and tralokinumab, have not consistently shown efficacy in asthma, dupilumab remains a promising therapeutic option for severe patients (Nakamura, Sugano, Ohta, & Takaoka, 2017). Additionally, emerging therapies targeting epithelial-derived alarmins like TSLP are reshaping severe asthma treatment (Corren et al., 2017). Tezepelumab, an anti-TSLP monoclonal antibody, has shown encouraging results in clinical trials by mitigating airway inflammation at an upstream level, regardless of eosinophil count (Corren et al., 2017). Other novel agents, such as astegolimab, an anti-ST2 monoclonal antibody, are under investigation (Kelsen et al., 2021; Yousuf et al., 2022). This agent targets the IL-33/ST2 axis, which plays a crucial role in both eosinophilic and neutrophilic inflammation in asthma (Kelsen et al., 2021; Yousuf et al., 2022). Despite the variety of available treatments, some patients still face poor asthma control due to several challenges in asthma treatment (Onyedum, Ukwaja, Desalu, & Ezeudo, 2013).

1.5 Challenges in Asthma Treatment: Addressing Pulmonary Drug Delivery, Heterogeneity, and Steroid Hypo-responsiveness

1.5.1 The Heterogeneity of Asthma

Asthma is not a single disease but a collection of distinct phenotypes, each with its own pathophysiological mechanisms (Borish & Culp, 2008). Some patients, particularly those with severe asthma, exhibit steroid-hypo-responsive inflammation, making them less responsive to conventional treatments like ICS (Henderson, Caiazzo, McSharry, Guzik, & Maffia, 2020). This variability in disease characteristics requires tailored approaches to treatment, both in terms of medication choice and delivery strategies. The variability in lung structure and function across individuals can affect how drugs are deposited and absorbed, further complicating the development of effective therapies (Labiris & Dolovich, 2003a). For example, patients with obstructed or inflamed airways may face more difficulty in achieving deep lung deposition, while those with steroid-hypo-responsive asthma may not respond adequately to existing therapies, even if the drug reaches its target site (Labiris & Dolovich, 2003a).

1.5.2 Steroid Hypo-responsiveness Asthma

Bronchial asthma is a complex condition that ranges from mild and intermittent to severe and chronic forms, with the latter often presenting significant treatment challenges and, in some cases, fatal outcomes (Ukena, Fishman, & Niebling, 2008). A distinct subgroup within asthma, known as steroid hyporesponsive asthma defined by a lack of improvement in forced expiratory volume in 1 second (FEV1) after 14 days of oral steroid treatment, according to updated diagnostic criteria (Lommatzsch & Virchow, 2014). It affects 5-10% of asthma patients and is associated with more severe symptoms and increased healthcare costs

(Adcock, Ford, Bhavsar, Ahmad, & Chung, 2008; Barnes & Adcock, 2009). Patients with steroid hyporesponsive asthma often face inadequate disease control with conventional therapies, leading to frequent exacerbations, hospitalizations, and a reduced quality of life (Castillo, Peters, & Busse, 2017). Understanding the underlying mechanisms of steroid hyporesponsive asthma and identifying alternative treatment strategies is crucial for improving outcomes in these patients (Castillo et al., 2017).

In contrast to mild to moderate asthma, where corticosteroids effectively reduce inflammation through both genomic and non-genomic pathways, steroid hyporesponsive asthma fails to benefit from these mechanisms (Poon & Hamid, 2016; Ramamoorthy & Cidlowski, 2016; Wadhwa et al., 2019). Genomic effects occur when corticosteroids bind to the glucocorticoid receptor (GR), enabling it to translocate into the nucleus and influence gene transcription (Poon & Hamid, 2016; Ramamoorthy & Cidlowski, 2016; Wadhwa et al., 2019). Non-genomic effects are faster, involving kinases such as AKT and MAPKs that regulate cellular processes like proliferation and apoptosis (Ramamoorthy & Cidlowski, 2016; Samarasinghe, Witchell, & DeFranco, 2012). However, in steroid hyporesponsive asthma, key pathways, such as the ERK1/ERK2 and p38 MAPK, remain activated, leading to continued inflammation and recruitment of neutrophils via CXCL8 synthesis (Alam & Gorska, 2011; Robins et al., 2011).

A critical aspect of steroid hyporesponsive asthma is the imbalance between the two isoforms of the glucocorticoid receptor—GRα, which binds corticosteroids, and GRβ, a non-binding isoform that inhibits GRα function (Vazquez-Tello, Halwani, Hamid, & Al-Muhsen, 2013). In steroid hyporesponsive asthma, inflammation mediated by cytokines like IL-2 and IL-4 leads to decreased GRα expression, while IL-17 increases GRβ expression, disrupting the GRα/GRβ ratio (Ramakrishnan, Al Heialy, & Hamid, 2019; Vazquez-Tello et al., 2013; Vazquez-Tello et al., 2010). This dysregulation, combined with reduced binding affinity and

impaired nuclear translocation of GR-bound steroids, compromises the anti-inflammatory action of corticosteroids (Al Heialy et al., 2020; Poon & Hamid, 2016). Furthermore, histone acetylation, which is necessary for gene repression upon GR binding to DNA, is diminished in steroid hyporesponsive asthma due to oxidative stress and upregulation of GRβ (Matthews, Ito, Barnes, & Adcock, 2004). This reduction in histone deacetylase 2 (HDAC2) activity further limits the efficacy of corticosteroids, contributing to the steroid hyporesponsive asthma observed in these patients (Li, Leung, Martin, & Goleva, 2010).

These challenges underscore the need for innovative strategies to improve lung-targeted drug delivery. Approaches such as developing nanoparticles and liposomes for better drug encapsulation, protection against enzymatic degradation, and sustained release, as well as designing personalized inhaler devices, are being explored to enhance therapeutic efficacy and minimize systemic side effects (Cheng, Xie, & Sun, 2023; P. Liu, Chen, & Zhang, 2022). In this context, nanobodies—small single-domain antibody fragments derived from camelid antibodies—emerge as a promising solution (Arbabi-Ghahroudi, 2022).

1.5.3 Pulmonary Drug Delivery Barriers

These challenges in asthma heterogeneity and steroid hypo-responsiveness are further exacerbated by the complexities of pulmonary drug delivery barriers (Scherzer & Grayson, 2018). Despite the progress in targeted therapies, asthma treatment still encounters significant challenges (Caminati, Vaia, Furci, Guarnieri, & Senna, 2021). One of the major hurdles is achieving effective pulmonary drug delivery (Labiris & Dolovich, 2003a). This involves not only ensuring that medications reach the specific target sites within the lungs but also minimizing systemic exposure and potential side effects (Labiris & Dolovich, 2003a). Inhalation is the preferred route for delivering asthma medications, providing direct access to the respiratory tract and a rapid onset of action. However, barriers such as mucus,

mucociliary clearance, and the alveolar-capillary barrier can hinder drug deposition in the lungs (Guo et al., 2021; Labiris & Dolovich, 2003b).

Particle size is crucial for effective drug delivery (Thomas, 2013). Aerosolized particles that are too large may settle in the oropharynx and be swallowed, while particles that are too small can be exhaled before reaching the deeper regions of the lungs (Thomas, 2013). Optimal particle size for deep lung deposition is typically between 1 and 5 micrometers (Labiris & Dolovich, 2003b). The heterogeneous structure of the lungs, with its branching airways and varying airflow dynamics, further complicates uniform drug distribution (Fei, Bentley, Ghadiali, & Englert, 2023). Techniques such as using propellants in metered-dose inhalers (Holland et al., 2013) or designing dry powder inhalers and nebulizers are employed to enhance delivery efficiency, but each method has its limitations (Ye, Ma, & Zhu, 2022).

Pharmacokinetics also significantly impacts the effectiveness of asthma drug delivery (Derendorf, Nave, Drollmann, Cerasoli, & Wurst, 2006). Medications must be efficiently absorbed across the respiratory epithelium to achieve therapeutic levels (Labiris & Dolovich, 2003a). Factors such as the presence of lung surfactants, enzymatic degradation, and rapid clearance through the lymphatic system or bloodstream can reduce drug bioavailability (Labiris & Dolovich, 2003a). Additionally, patient-related factors including inhalation technique, lung capacity, and adherence to therapy influence treatment outcomes (J. Ma, Sun, Wang, Liu, & Shi, 2023).

1.6 Nanobodies: History, Structure and Characteristics:

1.6.1 History of Nanobodies

Antibodies are traditionally defined as molecules with two heavy chains and two light chains. However, there was an important change in the traditional understanding of antibodies

in 1989. This research conducted by Professor Raymond Hamers of the Vrije University Brussel (VUB) resulted in the unexpected discovery of heavy chain-only antibodies (HCAbs) which lack a light chain **(Figure 1.4).** This discovery happened via student-led research which formulated a sero-diagnostic assay in order to diagnose trypanosome infection in camels and water buffalos (Muyldermans, 2013).

The discovery of Camelid heavy-chain antibodies has prompted widespread interest in utilizing these antibody domains in a variety of applications such as research, diagnostics and therapeutics (Muyldermans, 2013). These camelid heavy-chain antibodies are also known as Variable Heavy-chain domains of Heavy-chain antibodies (VHHs), Single-domain Antibodies (sdAbs), or Nanobodies **(Figure 1.4).** The formation of camelid VHHs for medicinal purposes occurred in three separate stages. The first decade (1993-2003) could potentially be considered as the exploration period (Arbabi-Ghahroudi, 2017). During 1996 and 2001, numerous patents were granted to research institutions with an emphasis on potential commercial uses. The primary goal of advancing nanobody-based medications and examining their therapeutic potential (Arbabi-Ghahroudi, 2017) (**Figure 1.5)**.

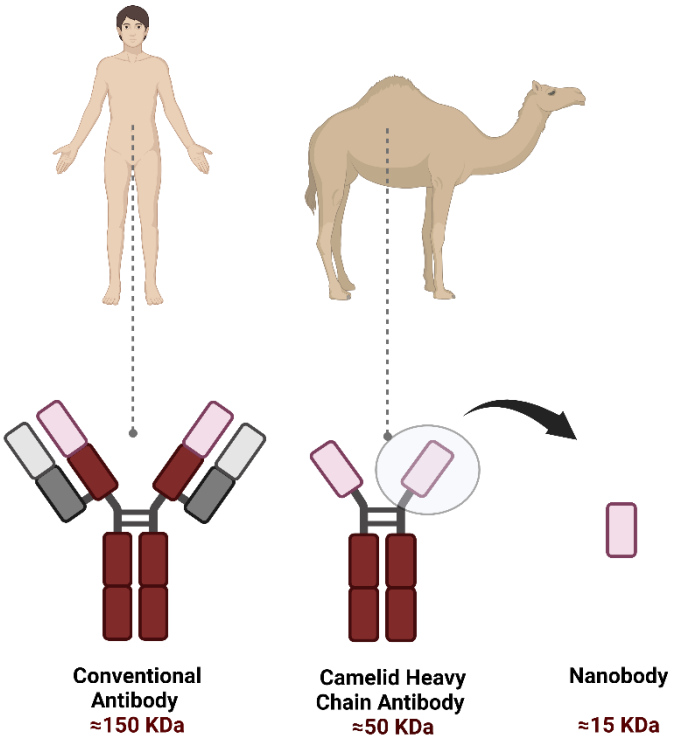

Figure 1.4: The image compares human IgG (≈150 kDa) with camelid heavy-chain IgG (≈50 kDa), which lacks light chains. From camelid IgG, a single-domain antibody (sdAb or nanobody, ≈15 kDa) can be isolated, offering a smaller and more stable binding domain, created with BioRender.com.

During the period of 2003 to 2013, a significant increase in publications surpassing 1,000 by 2013 was observed which suggests a substantial increase in attention and research focus on VHHs(Arbabi-Ghahroudi, 2017) (**Figure 1.5)**. There has been an evident increase in publications throughout the current developmental period starting from 2014 to the present and numerous VHHs have progressed into clinical trials or are getting ready for market release(Arbabi-Ghahroudi, 2017). The approval of the first nanobody medication known as caplacizumab (Cablivi) was obtained from the European Medicines Agency (EMA) and the Food and Drug Administration (FDA) in 2018 and 2019, respectively (Bergstrand et al., 2022; Scully et al., 2019). This novel drug cures a rare blood clotting disorder called the acquired thrombotic thrombocytopenic purpura (TPP) (Scully et al., 2019). Multiple variables

are accountable for the long duration that passed between the discovery of camelid single-domain antibodies (sdAbs) and their release into the market. One of the major variables is the novel nature of this approach (**Figure 1.5).**

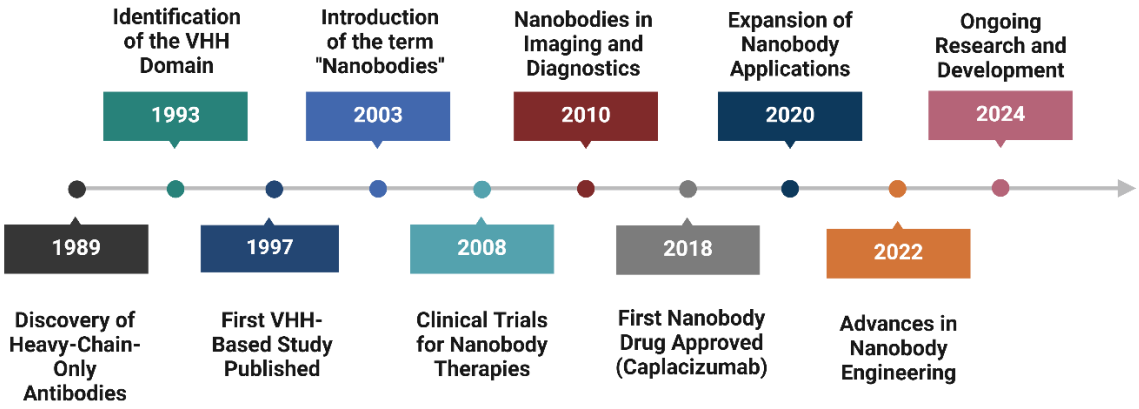

Figure 1.5 Summarized timeline of the discovery and development of nanobodies, created with BioRender.com.

1.6.2 Structure and Characteristics of Nanobodies

Camelidae species are immunized against specific targets or antigens which result in the production of heavy chain antibodies (HCAb) and conventional antibody repertoires *in vivo*. Phage-display libraries provide a reliable representation of the various *in vivo*-matured heavy chain repertoires since they are generated by cloning amplified VHH repertoires with barely any alteration (Arbabi-Ghahroudi, 2017).

The remarkable specificity and affinity of VHHs are similar to those of conventional antibodies. Also, they exhibit excellent solubility, stability at different temperatures and possess monomeric behaviour (Ikeuchi, Kuroda, Nakakido, Murakami, & Tsumoto, 2021). VHHs are extremely tiny, measuring around 2.5 nm in diameter and 4 nm in length with a molecular weight of about 15 kDa (Hoey, Eom, & Horn, 2019). They are easier to genetically engineer and can easily be produced for a relatively low price (Hoey et al., 2019). Moreover, they exhibit low immunogenicity and have improved tissue penetration properties

(Khodabakhsh, Behdani, Rami, & Kazemi-Lomedasht, 2018). The remarkable thermostability of nanobodies is demonstrated by their capacity to retain 80% of their activity even after exposure to 37°C for a week (Paul, Ghosh, Mitra, Banerjee, & Ghorui, 2023). Furthermore, they exhibit resistance to proteases, denaturing agents and high pH levels (Paul et al., 2023). Despite their extremely short development time, research suggests that nanobodies can be generated in large quantities by employing a microbiological system(de Marco, 2020). Nanobodies offer a promising alternative to conventional antibodies in disease diagnosis and treatment due to their unique advantages **Table 1.**

Table 1: Advantages and Limitations of Conventional Antibodies vs Nanobodies. *IV (Intravenous), SC (Subcutaneous), kD (Kilodalton)*

Characteristics	Conventional Aantibodies	Nanobodies
Structure	Possess 2 heavy chains and 2 light chains	Possess 2 heavy chains only, devoid of light chains.
Molecular Weight	150 kD (large size)	12~15 kD (small size)
Manufacturing Expenses	High	Moderate
Delivery Mode	IV and SC	IV, SC, oral and aerosol.
Target Binding	Generally, binds surface epitope	Can bind hidden or concave epitopes
specificity	High	High
Tissue penetration	Limit tissue penetration	Excellent tissue penetration
stability	Denature at high temperature and *pH*	Resistant to heat and *pH*
solubility	Moderate (hydrophobics)	High (no hydrophobics)

Half-life	Longer serum half-life	Shorter serum half-life

1.7 Nanobody in Diverse Disease Treatment

Nanobodies are demonstrating considerable potential across a spectrum of diseases, for instance, M1095, an anti-IL-17A/F nanobody, has shown effectiveness in treating moderate-to-severe plaque psoriasis by targeting IL-17A and IL-17F (Svecova et al., 2019). Furthermore, ALX-0061, a bispecific nanobody that targets the IL-6 receptor (IL-6R), is used for conditions involving excessive IL-6 signaling, such as rheumatoid arthritis (Van Roy et al., 2015). Similarly, Sonelokimab, which targets both IL-17A and IL-17F, shows promise in treating Hidradenitis Suppurativa (Hunt, Qian, Olds, & Daveluy, 2023). ALX-0171, a 42 kDa trivalent nanobody currently used in nebulizer solutions for respiratory syncytial virus (RSV) infections, targets the fusion (F) protein of RSV with high affinity, effectively inhibiting viral replication (Detalle et al., 2016).

1.8 Nanobodies in Asthma Treatment

Ongoing *in silico*, preclinical studies, and clinical trials are advancing the role of nanobodies in asthma treatment, presenting promising alternatives to traditional monoclonal antibodies as summarized in **Table 2.**

1.8.1 *In Silico* Nanobodies Development for asthma

Recent advances in *in-silico* approaches have greatly contributed to the design and optimization of nanobody based therapeutics for asthma. Using computational tools such as molecular dynamics simulations and homology modelling (Cheng et al., 2019), researchers

have focused on designing single-domain antibodies with enhanced stability, solubility, and specificity (Cheng et al., 2019).

One study utilized a camelization approach to create three specific mutated single-domain antibodies targeting a key pro-inflammatory cytokine implicated in allergic asthma. Using a monoclonal antibody structure as a template, these mutations significantly improved solubility and stability. Simulations revealed stable, long-lasting interactions mediated primarily by complementary-determining regions (CDRs). The engineered single-domain antibodies demonstrated improved binding affinity, stability, and solubility compared to their wild-type counterparts, highlighting their therapeutic potential (Araújo et al., 2023) **Table 2.**

1.8.2 Preclinical Nanobodies Development for Asthma

In recent preclinical studies, several promising nanobody-based therapies have been developed for the treatment of asthma and related allergic conditions, focusing on different therapeutic targets. For instance, Ma, L. et al. developed a trivalent bispecific nanobody targeting IL-5, a cytokine critical for eosinophil proliferation and activation, and albumin to improve efficacy and address limitations of current IL-5 therapies (L. Ma et al., 2022). This nanobody showed superior efficacy over existing IL-5 therapies like mepolizumab, being 58 times more effective in inhibiting TF-1 cell proliferation. It also demonstrated excellent pharmacokinetics and sustained eosinophil suppression in primates. These results suggest the nanobody's potential as a next-generation therapeutic for severe eosinophilic asthma, offering improved efficacy and longer-lasting effects (L. Ma et al., 2022). Similarly, Li, Shijie et al. engineered nanobodies suitable for inhalation administration that target IL-5. Among the candidates, AIL-A96-Fc was identified as a highly effective nanobody that blocked the IL-5/IL-5Rα interaction and demonstrated cross-species activity with both human and

cynomolgus IL-5. AIL-A96-Fc exhibited significant blocking effects, underscoring its potential as an inhaled therapeutic for eosinophilic asthma (Shijie et al., 2024) **Table 2**.

Additionally, Qiu, W. et al. produced a bispecific antibody targeting both IL-4Rα and IL-5, utilizing humanized VHHs derived from alpacas (Qiu, Meng, Su, Xie, & Song, 2024). They further investigated the epitope interactions of these VHHs with IL-4Rα and IL-5. Structural and biochemical analyses demonstrated that the nanobodies effectively inhibited the interactions between IL-4, IL-5, IL-13, and their respective receptors. Compared to dupilumab, which targets only IL-4Rα and has limited efficacy in severe disease, this bispecific antibody simultaneously attenuates the activity of three cytokines (IL-4, IL-5, and IL-13), offering enhanced therapeutic potential (Qiu et al., 2024) **Table 2**.

Furthermore, Zhu, M. et al. designed an inhalable nanobody targeting the IL-4Rα chain for asthma treatment, capitalizing on the inherent stability and efficacy advantages of nanobodies. By utilizing three immunized Nb libraries, they created the bivalent Nb, LQ036, which exhibited high affinity and specificity for human IL-4Rα. Preclinical tests in humanized mice demonstrated that LQ036 effectively inhibited key asthma-related biomarkers, including IgE and CCL17, reduced airway inflammation, and showed favourable pharmacokinetics and safety profiles. These findings underscore the potential of LQ036 as an effective inhalable biologic for the treatment of asthma (Zhu et al., 2024).

Meanwhile, Gevenois, P. J. Y. et al. developed nanobodies targeting IL-13, a key cytokine in allergy, inflammation, and fibrosis. While the initial nanobodies showed good affinity, they were ineffective at inhibiting IL-13 biological activity *in vitro*. To enhance efficacy, multimeric constructs were created, resulting in a significant increase in both affinity and biological activity, suggesting that multimeric nanobodies could be a promising approach for more effective IL-13 targeting (Gevenois et al., 2021) **Table 2**.

In a similar manner, Rinaldi, M. et al. constructed ALX-0962, a bispecific nanobody targeting IgE and human serum albumin to extend plasma half-life (Rinaldi et al., 2013). Unlike Omalizumab, ALX-0962 demonstrated dual functionality, effectively neutralizing soluble IgE with higher potency while displacing preformed IgE-FcεRI complexes on basophils. This dual action significantly reduced basophil degranulation at nanomolar concentrations. These findings highlight ALX-0962's potential to provide a faster onset of clinical improvement in asthma treatment (Rinaldi et al., 2013) **Table 2**.

In addition, Bauernfeind, C. et al. developed high-affinity Bet v 1-specific nanobody trimers to outcompete IgE binding and prevent allergic reactions. The engineered trimers showed enhanced cross-reactivity, slower dissociation rates, and better inhibition of IgE-allergen interactions compared to monomers. They effectively reduced IgE binding to Bet v 1 and related allergens while suppressing allergen-induced basophil degranulation. These results highlight the potential of nanobody trimers as a promising therapeutic strategy to prevent allergic reactions caused by Bet v 1 and its cross-reactive allergens (Bauernfeind et al., 2024) **Table 2**.

Likewise, a study produced an anti-IgE nanobody derived from the Indian dromedarius camel to reduce hypersensitivity in allergic asthma. Using an ovalbumin-induced mouse model, the nanobody significantly suppressed IgE production and alleviated symptoms of airway inflammation, including bronchoconstriction and airway hyperresponsiveness. The results suggest that this camelid-derived nanobody could be a promising therapeutic strategy for allergic inflammation (Paul et al., 2023) **Table 2**.

1.8.3 First Clinical Study of Nanobodies for Asthma

SAR443765 is the first and only nanobody to date to reach a Phase 1 clinical trial for asthma treatment, marking a significant advancement in biologics targeting type 2 airway

inflammation (Deiteren et al., 2023). This bifunctional NANOBODY®, designed to block both TSLP and IL-13, demonstrated promising safety and efficacy results in the trial (NCT05366764). In 36 mild-to-moderate asthma patients with elevated FeNO, a single subcutaneous dose significantly reduced FeNO at week 4, outperforming the effects of monovalent biologics targeting either pathway. Reductions in blood biomarkers, such as IL-5 and IgE, aligned with these findings, and numerical improvements in prebronchodilator FEV1 were observed. The treatment was well-tolerated, with only mild to moderate Treatment-emerging adverse events such as nasopharyngitis and injection site reactions. These results highlight SAR443765's potential as a groundbreaking therapeutic for asthma (Deiteren et al., 2023).

The advancement of SAR443765 into clinical trials marks a significant milestone, demonstrating the transformative potential of nanobodies as promising therapeutic agents for asthma. This success highlights the urgent need for further research and development to translate more preclinical breakthroughs into clinical applications, paving the way for nanobodies to revolutionize asthma treatment and address critical unmet medical needs **Table2**.

Table 2: Summary of Key Studies on Nanobody Development in Asthma Treatment

Study Type	Objectives	Key Findings	Conclusion	Reference
***In Silico* Development**	To design and optimize nanobody-based therapeutics for asthma using computational tools.	Utilized molecular dynamics simulations and homology modelling to improve stability, solubility, and specificity of	*In silico* methods can effectively design stable, high affinity nanobodies for asthma treatment.	Araújo, P. *et al. (2023)*

		nanobodies. Engineered single-domain antibodies showed improved binding affinity, stability, and solubility.		
Preclinical Development	To develop a bispecific nanobody targeting IL-5 and albumin for enhanced efficacy in asthma treatment.	The bispecific nanobody showed 58 times higher efficacy than current IL-5 therapies, with excellent pharmacokinetics and sustained eosinophil suppression.	The bispecific nanobody could be a next-generation therapy for eosinophilic asthma.	Ma, L. *et al. (2022)*
Preclinical Development	To engineer inhalable nanobodies targeting IL-5 for asthma treatment.	AIL-A96-Fc effectively blocked the IL-5/IL-5Rα interaction and demonstrated cross-species activity with human and cynomolgus IL-5.	AIL-A96-Fc shows promise as an inhaled therapeutic for eosinophilic asthma.	Shijie, L. I. *et al. (2024)*

Preclinical Development	To produce a bispecific nanobody targeting both IL-4Rα and IL-5.	The bispecific nanobody inhibited IL-4, IL-5, and IL-13 interactions, showing enhanced therapeutic potential compared to dupilumab.	Bispecific antibodies could improve efficacy in treating asthma by targeting multiple cytokines.	Qiu, W., *et al. (2024)*
Preclinical Development	To design an inhalable nanobody targeting IL-4Rα for asthma treatment.	LQ036 effectively inhibited asthma-related biomarkers, reduced airway inflammation, and showed favorable pharmacokinetics and safety.	LQ036 could be an effective inhalable biologic for asthma treatment.	Zhu, M. *et al. (2024)*
Preclinical Development	To develop nanobodies targeting IL-13 for better asthma management.	Multimeric nanobodies showed enhanced affinity and biological activity, improving IL-13 inhibition.	Multimeric nanobodies offer a more effective approach for targeting IL-13 in asthma.	Gevenois, P. J. Y. *et al. (2021)*
Preclinical Development	To develop a bispecific nanobody targeting IgE and human serum	ALX-0962 effectively neutralized IgE and displaced preformed IgE-FcεRI complexes,	ALX-0962 may provide faster clinical improvement in	Rinaldi, M. *et al. (2013)*

	albumin for asthma treatment.	reducing basophil degranulation.	asthma with dual functionality.	
Preclinical Development	To develop Bet v 1-specific nanobody trimers for preventing allergic reactions.	Nanobody trimers showed enhanced cross-reactivity and better inhibition of IgE-allergen interactions than monomers.	Nanobody trimers could be a promising strategy for preventing allergic reactions.	Bauernfeind, C. *et al. (2024)*
Preclinical Development	To produce an anti-IgE nanobody from the Indian dromedarius camel for asthma.	The nanobody significantly reduced IgE production and alleviated airway inflammation, bronchoconstriction, and hyperresponsiveness in a mouse model.	This camelid-derived nanobody may be an effective therapeutic strategy for allergic inflammation.	Paul, P., *et al. (2023)*
Clinical Trial	To evaluate the safety and efficacy of SAR443765, a bifunctional nanobody targeting TSLP and IL-13.	A single dose of SAR443765 significantly reduced FeNO, IL-5, and IgE levels, with improvements in	SAR443765 shows potential as a groundbreaking therapeutic for type 2 asthma.	Deiteren, A. *et al. (2023)*

		FEV1. The treatment was well-tolerated.		

1.9 Future Directions for Nanobodies in Asthma Treatment

The future of nanobodies in asthma treatment is set to bring innovative solutions, addressing both clinical and therapeutic gaps in current asthma management.

1.9.1 Expansion of Targeted Inflammatory Mediators

Currently, nanobody based therapies primarily target mediators such as IL-4, IL-5 and IgE. However, the expansion of this therapeutic approach to include other inflammatory biomarkers such as IL-1β, IL-6, IL-25, IL-33, and TGF-β presents an opportunity to manage more severe and resistant forms of asthma, including steroid hyporesponsive asthma (Calderon et al., 2023; Lambrecht, Hammad, & Fahy, 2019; Sim, Choi, & Park, 2024; Stanbery et al., 2022). These molecules are involved in various stages of the inflammatory response in asthma and could offer more comprehensive control over the disease's complex pathophysiology. By targeting multiple cytokines, nanobodies could prevent the exacerbation of asthma symptoms in patients who do not respond well to current treatments (**Figure 1.6**).

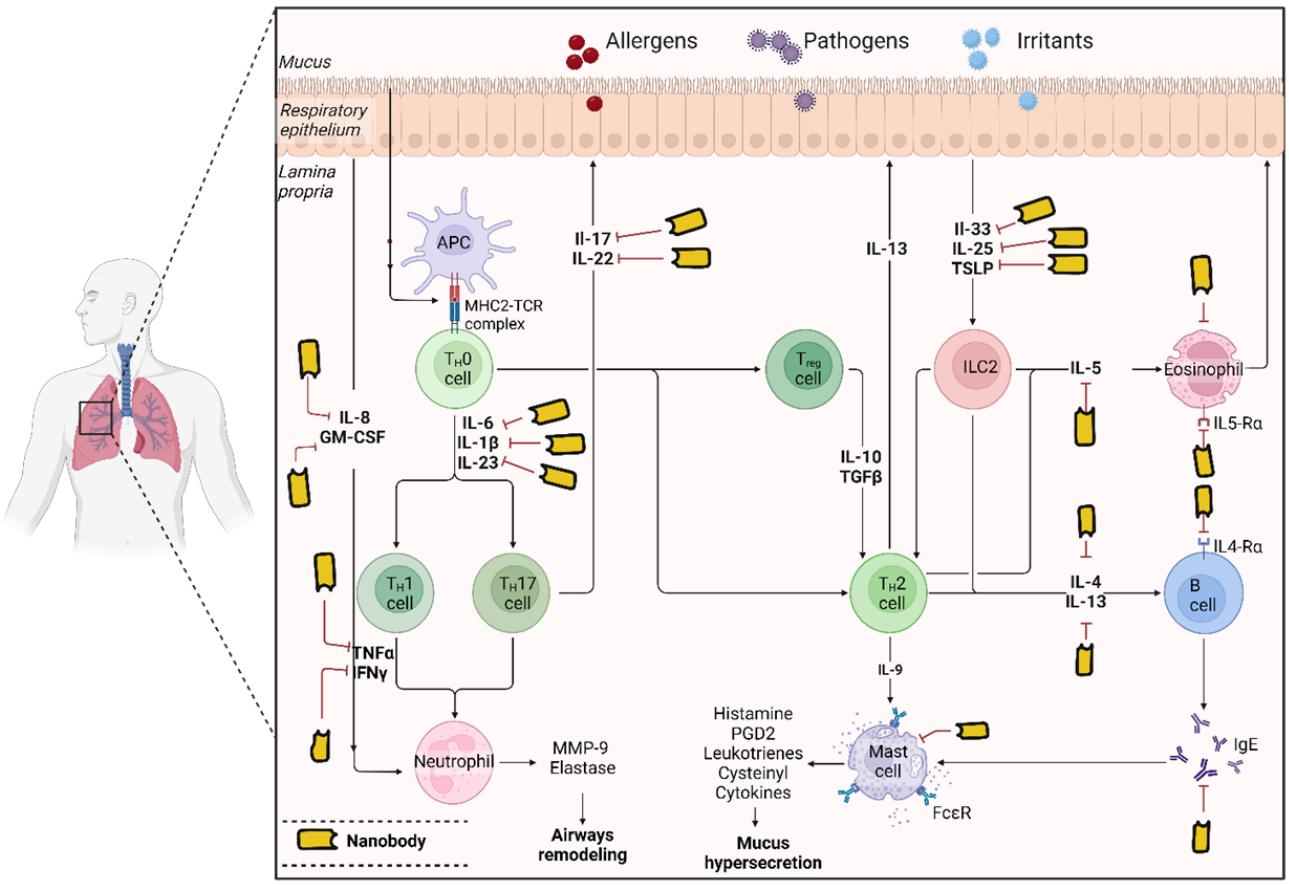

Figure 1.6: Possible Targets of Nanobodies in Asthma Treatment. Created with BioRender.com

1.9.2 Combination Therapies

The use of nanobodies in combination with existing therapies, such as corticosteroids, biologics, or bronchodilators, could enhance treatment efficacy (Jovcevska & Muyldermans, 2020). Nanobodies may address multiple inflammatory pathways simultaneously, increasing the effectiveness of asthma treatment (Jovcevska & Muyldermans, 2020). Combination therapies could help tackle both the underlying inflammatory mechanisms and the symptoms of asthma, offering a more holistic approach to management (Saleh, 2008).

1.9.3 Targeted Delivery Systems

Aerosolized nanobodies, designed for direct pulmonary delivery, are an exciting direction for the future of asthma treatment (Mustafa & Ahmed, 2023; Van Heeke et al., 2017). This delivery method ensures that nanobodies are precisely targeted to the lungs, enhancing therapeutic efficacy while minimizing systemic side effects (Labiris & Dolovich, 2003a). Aerosolized nanobodies could improve treatment compliance by offering a more convenient and localized approach to asthma management (Labiris & Dolovich, 2003a).

1.9.4 Improving Stability and Delivery Mechanisms

Nanobody stability and pharmacokinetics are critical factors for their clinical application. Current research is focused on improving the shelf-life, stability, and delivery of nanobodies through advanced formulations (Dingus, Tang, Amamoto, Wallick, & Cepko, 2022; Mir, Mehraj, Sheikh, & Hamdani, 2020). These innovations may include using engineered carriers or nanoparticles to enhance the bioavailability and efficacy of nanobodies, allowing for sustained release and optimal dosing intervals (Dingus et al., 2022). Such advancements would make nanobody treatments more effective and easier to administer, contributing to better patient outcomes (Dingus et al., 2022; Jin, Odongo, Radwanska, & Magez, 2023; Kunz et al., 2018).

1.9.5 Long-Term Studies and Clinical Evaluation

While preclinical studies have shown promising results, long-term clinical studies are necessary to fully assess the safety, efficacy, and potential side effects of nanobody based asthma treatments (Jovčevska & Muyldermans, 2020). These studies should focus on evaluating sustained benefits and how nanobodies perform over extended periods of use. Furthermore, clinical trials should explore their impact on lung function, symptom control,

and quality of life in patients with asthma. Only through comprehensive clinical evaluation can the full potential of nanobodies be realized.

1.9.6 Cost-Effectiveness and Accessibility

As with any novel therapeutic, the cost of nanobody based treatments must be considered. Research is underway to identify ways to make nanobodies more cost-effective, which would increase accessibility to a larger number of patients (Fridy et al., 2014). Reducing the cost of nanobodies could make them viable alternatives to current expensive biologic therapies, providing patients with more affordable options for managing asthma (Fridy et al., 2014). Ensuring these treatments are widely accessible will be key to their adoption and success in clinical practice.

1.10 Rationale

Severe asthma characterized by corticosteroid hypo-responsiveness, remains a significant therapeutic challenge. IL-33 has emerged as a key driver of inflammation and corticosteroid hypo-responsiveness (Kearley et al., 2015; Prefontaine et al., 2009), yet the underlying mechanisms by which it mediates these effects remain underexplored. While monoclonal antibodies such as astegolimab, targeting ST2 (the IL-33 receptor), have shown promise in ongoing studies (Kelsen et al., 2021), their utility is limited by challenges including high production costs, poor tissue penetration, and immunogenicity (Kardas et al., 2022; Samaranayake, Wirth, Schenkwein, Räty, & Ylä-Herttuala, 2009). Nanobodies, with their smaller size, superior tissue penetration, reduced immunogenicity, and cost-effective production, represent a promising alternative (Hoey et al., 2019; Khodabakhsh et al., 2018). Despite these advantages, no nanobody-based therapies currently target the IL-33/ST2

pathway, with most research focusing on Th2-driven asthma phenotypes (Gevenois et al., 2021; L. Ma et al., 2022; Qiu et al., 2024; Shijie et al., 2024; Zhu et al., 2024). This critical gap highlights the necessity of developing locally delivered nanobody therapy targeting IL-33/ST2, offering a more efficient treatment with fewer side effects for severe asthma management.

1.11 Hypothesis

IL-33 regulates the response to steroids during steroid-hyporesponsive asthma, while intrapulmonary administration of anti-ST2 blocking nanobodies resolves inflammation and restores steroid responsiveness more effectively than astegolimab.

1.12 Aims and objectives

Objective 1: To investigate the role of IL-33 in promoting steroid hypo-responsiveness in a chronic HDM-induced asthma mouse model.

Aim 1.1: Establish a severe asthma mouse model using IL-33/HDM induction.

Aim 1.2: Treat the model with corticosteroids to determine steroid responsiveness.

Objective 2: To develop anti-ST2 nanobodies and evaluate their blocking capacity, binding affinity, and specificity as potential therapeutic agent.

Aim 2.1: Generate anti-ST2 nanobodies using phage display technology and purify them using Ni-NTA chromatography.

Aim 2.2: Determine the specificity of purified nanobodies for ST2 over related targets using ELISA-based assays.

Aim 2.3: Characterize the binding affinity (KD) and evaluate their blocking efficacy (IC50) using direct and competitive ELISA.

Objective 3: To determine the efficacy of anti-ST2 nanobodies in mitigating lung inflammation and restoring steroid responsiveness compared to astegolimab.

Aim 3.1: Assess the ability of anti-ST2 nanobodies to block ST2 *in vitro* using HDM/IL-33-stimulated primary human lung epithelial cells compared to astegolimab.

Aim 3.2: Evaluate the ability of anti-ST2 nanobodies to resolve inflammation *in vivo* using the chronic HDM-induced asthma mouse model compared to astegolimab.

Aim 3.3: Compare the effectiveness of anti-ST2 nanobodies and astegolimab in restoring steroid responsiveness both *in vitro* and *in vivo*.

1.13 Project Impacts

The study provides robust evidence linking IL-33/ST2 signalling to severe asthma pathogenesis, emphasizing its role in airway inflammation, mucus overproduction, and corticosteroid hypo-responsiveness. It identifies key mechanistic pathways, including MAPK/ERK, NF-κB, and GRα/GRβ dysregulation, deepening the understanding of steroid resistance. By pioneering the use of nanobodies, specifically NB7, targeting the IL-33 receptor ST2, the research introduces a smaller, cost-effective, and more tissue-penetrative alternative to monoclonal antibodies like astegolimab. NB7 demonstrated superior efficacy in reducing airway inflammation, restoring steroid responsiveness, and improving lung mechanics at a lower dose, showcasing its therapeutic promise. Intranasal delivery of NB7 ensures localized action, minimizes systemic side effects, and enhances treatment safety and efficacy. Its lower cost and reduced immunogenicity make advanced asthma treatments more accessible to broader patient populations. Beyond severe asthma, the findings have implications for other IL-33/ST2-driven conditions, such as chronic obstructive pulmonary disease, allergic rhinitis, and atopic dermatitis, contributing to the growing evidence supporting nanobodies as revolutionary biotherapeutic agents.

2. Methodology

2.1 Research Methods

This chapter outlines the methodologies employed to investigate the role of IL-33/ST2 signalling in asthma and evaluate the therapeutic potential of the NB7 nanobody. The experimental design was strategically developed to combine *in silico*, *in vivo*, and *in vitro* approaches, ensuring robustness and reproducibility. For example, *in silico* analysis was used to establish the clinical relevance of ST2 upregulation, while *in vivo* and *in vitro* experiments validated the mechanisms and explored therapeutic interventions. This chapter provides a comprehensive description of the materials and methods used.

2.2 *In Silico* Analysis

The transcriptomic dataset (GSE147881) was curated to evaluate ST2 expression levels in the bronchial biopsies from healthy controls (n=13) and patients with mild/moderate (n=18) and severe asthma (n=42). Read counts were normalized using Voom (Law, Chen, Shi, & Smyth, 2014). The statistical significance was assessed with Student's t-test. The results were visualized as box plots providing insights into the relationship between ST2 expression and disease severity.

2.3 *In Vivo* Studies

2.3.1 Mice

Mice experiments were performed following approval from Animal Care and Use Committee of University of Sharjah (agreement number: ACUC-20–02-11–1), per the

national guidelines for the care of laboratory animals. In this study, wild type female BALB/c mice 8-10 weeks old were obtained from the animal facility of University of Sharjah. All mice were housed under pathogen- and ovalbumin (OVA)-free conditions and kept in sterile, individually ventilated cages (TECNIPLAST). They were maintained on a 12-h light–dark cycle and fed a sterile, maintenance diet (Altromin 1324 TPF) and sterile-distilled water. Environmental enrichment was provided by autoclaved dust-free aspen bedding (ABEDD).

2.3.2 Chronic Asthma Model Development

A well-established mouse model of chronic airway inflammation (Woo et al., 2018) was adapted with modifications to create a novel model incorporating IL-33 stimulation and subsequent therapeutic interventions. Female BALB/c mice were randomly divided into three groups: HDM-only, HDM/IL-33, and a negative control group receiving PBS. The HDM extract (Dermatophagoides pteronyssinus extract, Citeq Biologics, 20A05) was re-suspended in PBS at a concentration of 25 µg in 35 µL. Recombinant mouse IL-33 (ab270066, Abcam) was prepared according to the manufacturer's instructions with PBS and diluted to a final dose of 0.1 µg/kg in 20 µL PBS for intranasal administration. Mice were lightly anesthetized with 5% isoflurane in an induction chamber, and HDM extract (35 µL) was delivered intranasally using a 10–100 µL pipette tip for 4 consecutive days weekly (Monday to Thursday) over 4 weeks. The HDM/IL-33 group received the same HDM treatment, along with an additional intranasal administration of recombinant IL-33 (0.1 µg/kg in 20 µL PBS) immediately following HDM exposure twice a week. The negative control group received PBS intranasally in place of HDM and IL-33 under the same conditions.

In the first part of the study, the HDM-only group was compared with the HDM/IL-33 group to evaluate the impact of IL-33 on airway inflammation and immune responses.To

assess the responsiveness to steroids, both the HDM-only and HDM/IL-33 groups were treated with dexamethasone (250 μg/kg) intranasally twice a week.

In the second part of the study, the HDM/IL-33 group was further divided into subgroups to evaluate the therapeutic potential of specific nanobody treatments, nonspecific nanobody treatments, and monoclonal antibodies. Mice in the specific nanobody group received intranasal administration of nanobodies (NB7) at dose of 100 μg/kg, delivered twice a week before each IL-33 stimulation. The nonspecific nanobody group received a control nanobody at the same concentrations (100 μg/kg), administered using the same schedule. For the monoclonal antibody treatment group, mice received monoclonal antibodies astegolimab (medchemexpress, HY-P99444) at a dose of 300 μg/kg, also delivered twice a week before each IL-33 stimulation. These treatment groups allowed for a comprehensive evaluation of the efficacy of specific nanobodies compared to nonspecific nanobody and monoclonal antibody treatments in modulating IL-33-driven airway inflammation and immune responses.

Endpoint evaluations were performed 24 hours after the final exposure, including the collection of bronchoalveolar lavage fluid (BALF) for cell counts and cytokine analysis, as well as lung tissues for histological examination, and RNA/protein extraction. This protocol established a robust neutrophil-dominant airway inflammation model, incorporated IL-33 stimulation to investigate its role in shifting the inflammatory phenotype and enabled the evaluation of steroid responsiveness and therapeutic efficacy of specific nanobody, nonspecific nanobody, and monoclonal antibody treatments.

A total of 8 groups of mice (n=5 per group) were included in the study:

1. **NC (Negative Control):** Mice receiving PBS only.
2. **HDM-only:** Mice treated with house dust mite (HDM) extract.
3. **HDM/IL-33:** Mice treated with HDM extract and recombinant IL-33.
4. **HDM-only + DEX:** Mice treated with HDM extract and dexamethasone.

5. **HDM/IL-33 + DEX:** Mice treated with HDM extract, recombinant IL-33, and dexamethasone.
6. **HDM/IL-33 + NB:** Mice treated with HDM extract, recombinant IL-33, and a specific nanobody.
7. **HDM/IL-33 + NS-NB:** Mice treated with HDM extract, recombinant IL-33, and a nonspecific nanobody.
8. **HDM/IL-33 + AST:** Mice treated with HDM extract, recombinant IL-33, and astegolimab, a monoclonal antibody targeting ST2.

2.3.3 Intranasal NB7 Delivery and Lung Retention

To evaluate the efficiency of intranasal delivery of NB7, a total of 12 mice were divided into four groups (n=3 per group) based on the time points of lung tissue collection: 0-, 24-, 48-, and 72-hours post-administration. NB7 was administered intranasally at a fixed therapeutic dose (100 μg/kg) to all groups. Mice in the 0-hour group served as the baseline, with lung tissue collected immediately after administration. Mice in the remaining groups were sacrificed at their respective time points (24-, 48-, and 72-hours post-administration). Lung tissues were collected from all mice and processed to detect the presence of NB7 by western blot using Anti-6X His tag® (Abcam, ab9108, 1:4000), confirming its delivery and retention in the tissue over time.

2.3.4 Airway Hyperresponsiveness

Lung function was assessed using the FlexiVent system (SCIREQ, Montreal, Quebec, Canada), a computer-controlled small animal ventilator that employs the forced oscillation technique to measure lung resistance and dynamic compliance in tracheostomized mice under anaesthesia. Mice were anesthetized with an intraperitoneal injection of ketamine (114.5

mg/kg) and xylazine (6.9 mg/kg) and administered the muscle relaxant rocuronium bromide (2.5 mg/kg) intraperitoneally after initiating mechanical ventilation. Airway hyperresponsiveness (AHR) was evaluated by sequentially exposing the mice to aerosolized PBS (baseline) followed by increasing concentrations of methacholine (6.25 to 50 mg/mL) in a stepwise manner, as previously described (McGovern, Robichaud, Fereydoonzad, Schuessler, & Martin, 2013). Total airway resistance was calculated in cm $H_2O \cdot s \cdot mL^{-1}$ using FlexiVent software (version 8.0.4).

2.3.5 Flow Cytometry

After measuring airway hyperresponsiveness (AHR), BALF was collected by sequentially flushing the lungs twice with 0.5 mL of ice-cold PBS supplemented with 0.05 mM EDTA, followed by a final flush with 1 mL of the same solution. The collected BALF was centrifuged at 1,400 rpm for 10 minutes at 4°C. The resulting pellet was resuspended in 300 µL of FACS buffer (PBS supplemented with 3 mM EDTA and 2% FBS). A 200 µL aliquot was transferred to a U-bottom 96-well plate for further analysis, while the remaining 100 µL was used for cytospin preparation. The plate was centrifuged at 350 rpm for 3 minutes at 4°C, and the supernatant was discarded. The pellet was then resuspended in 20 µL of a pre-prepared antibody mixture and incubated in the dark at 4°C for 30 minutes. Following incubation, 100 µL of FACS buffer was added to each well. The plate was centrifuged again, the supernatant discarded, and the pellet resuspended in 300 µL of FACS buffer before being transferred to flow cytometry tubes. Sample acquisition was performed using a Cytek Biosciences flow cytometer, and data were analyzed with FlowJo software (version 10).

The following antibodies, all purchased from BioLegend, were used to characterize immune populations in the BALF:

- APC/Cyanine7 anti-mouse CD45: 1:50 dilution (Clone: 30-F11; Cat. No. 103116)
- APC anti-mouse CD170 (Siglec F): 1:20 dilution (Clone: S17007L; Cat. No. 155508)
- PerCP-Cy5.5 anti-mouse CD11c: 1:20 dilution (Clone: N418; Cat. No. 117328)
- Alexa Fluor® 488 anti-mouse Ly-6G: 1:20 dilution (Clone: 1A8; Cat. No. 127626)
- PE anti-mouse/human CD11b: 1:50 dilution (Clone: M1/70; Cat. No. 101208)

2.3.6 BALF and cytospin

To collect Broncho alveolar lavage fluid (BALF) (Dua, Shukla, & Hansbro, 2017), mice were anesthetized and positioned with elevated heads. A small neck incision exposes the trachea, where a cannula is inserted to instil sterile PBS with 0.05mM EDTA into the lungs for fluid recovery. This lavage procedure is repeated multiple times to ensure thorough collection (3ml). BALF is then centrifuged to separate cells and debris, with the supernatant stored for analysis, while the cell pellet is resuspended for downstream applications.

For cytospin preparation, a portion of the cell pellet is transferred to a microscope slide and centrifuged to evenly distribute cells. Following this, cells were stained with Wright-Giemsa and air-dried. Stained cells are subsequently examined under a microscope for morphology and differential cell counting was performed by a histopathologist. The evaluation was based on the average of five visual fields per sample.

2.3.7 Histological examinations

The left lung lobes were fixed in 10% formalin and later embedded in paraffin blocks. Sections, 5µm thick, were acquired using a microtome made by SLEE Medical GmbH, Germany. These sections were subsequently stained either with haematoxylin and eosin (H&E) or Periodic Acid-Schiff (PAS) following the manufacturer's instructions. Assessment

of inflammation in perivascular and peri-bronchial regions, as well as goblet cell hyperplasia, was performed by a histopathologist.

Scoring values:

0: No evidence of peri-bronchial, perivascular, and parenchymal infiltration of inflammatory cells.

1: Evidence of a few peri-bronchial, perivascular, and parenchymal infiltration of inflammatory cells.

2: One layer of peri-bronchial, perivascular, and parenchymal infiltration of inflammatory cells.

3: 2-4 layers of inflammatory cells in peri-bronchial, perivascular, areas.

4: Extensive inflammatory infiltration (>4 layers of cell rings) in peri-bronchial, perivascular, and the parenchymal areas.

Mucus secretion was evaluated based on the visual field average of 5 fields per sample of the PAS-positive mucus-containing cells compared to the total number of epithelial cells.

2.3.7.1 Immunohistochemistry (IHC)

Tissue samples are fixed in 10% neutral-buffered formalin for 24 hours, embedded in paraffin, sectioned (4 μm), and mounted on slides, which are deparaffinized in xylene and rehydrated through graded ethanol. Antigen retrieval is performed in citrate buffer (pH 6.0) using heat, followed by cooling and PBS washes. Endogenous peroxidase activity is blocked with Hydrogen Peroxide Block (10 minutes), and nonspecific binding is minimized using Protein Block (20 minutes). The primary antibody is applied, incubated (overnight at 4°C), and washed in PBS. The HRP secondary antibody is added, incubated (15 minutes), and followed by DAB chromogen development for brown signal detection, monitored

microscopically. Hematoxylin counterstaining is performed for nuclear visualization. Slides were dehydrated through a graded series of ethanol, cleared in xylene, and mounted with a permanent mounting medium. Stained slides were examined under a microscope, where antigen sites appeared brown, and nuclei appeared blue. Evaluation was performed by a histopathologist, based on the average of five visual fields per sample. The Mouse and Rabbit Specific HRP/DAB Detection IHC Kit (Abcam, Cat. No. Noab64264) was used for immunohistochemical staining.

2.4 Nanobody Development (Pardon et al., 2014)

2.4.1 Immunization of Camelids

A camel (Camelus dromedarius) was immunized subcutaneously with human ST2 recombinant protein as the antigen (1 mg/mL). The antigen was prepared in aliquots and stored at -20°C until use. Prior to each immunization, an aliquot was thawed, mixed with an equal volume of adjuvant, and injected subcutaneously in up to five spots, with a maximum of 2 mL per spot. The immunization was performed weekly for a total of 5 weeks.

2.4.2 Collection of Peripheral Blood Lymphocytes (PBLs)

Three to four days after the final immunization, approximately 100 mL of anticoagulated blood was collected from the jugular vein of the immunized camelid. The blood was diluted 1:1 with 0.9% NaCl and layered into Leucosep® tubes. Following centrifugation at 1,000 x g for 10 minutes, lymphocytes were collected from the interphase, washed three times in PBS (10 volumes of PBS per pellet), and pelleted. The cells were then used for total RNA isolation using TRIzol reagent, following the manufacturer's instructions. RNA concentration was determined by UV spectrophotometry.

2.4.3 Synthesis of First Strand Cdna

The isolated RNA was immediately used for the synthesis of first-strand cDNA or stored at -80°C for later use. The resulting cDNA was either used directly for PCR amplification of VHH sequences or stored at -20°C for future experiments.

2.4.4 Amplification of VHH Sequences

VHH sequences were amplified in two steps. The first PCR, using CALL001 and CALL002 primers, generated two amplicons (~0.7 kb and ~0.9 kb). The ~0.7 kb band, corresponding to heavy chain-only antibody mRNA, was purified using the QIAquick Gel Extraction Kit. Nested PCR was then performed with VHH-BACK-SAPI and VHH-FORWARD-SAPI primers to amplify VHH-only sequences (~400 bp) while introducing Sap I restriction sites. PCR products were analyzed on agarose gels, purified, and quantified using a Nanodrop spectrophotometer. The purified VHH products were either used immediately for downstream applications or stored at -20°C.

2.4.5 Preparation of Electro-competent TG1 Cells

TG1 cells were streaked on a minimal medium plate and incubated overnight at 37°C. A single colony was inoculated into 5 mL 2× TY medium and shaken overnight at 37°C and 250 rpm. The overnight culture (2 mL) was used to inoculate 300 mL 2× TY medium in a baffled flask and shaken at 37°C until the OD_{600} reached 0.8–1.0 (~3–4 hours). The culture was chilled on ice for 1 hour, pelleted by centrifugation at 2200 × g for 7 minutes at 4°C, and resuspended in ice-cold 1 mM HEPES (pH 7.0). After two washes with 10% glycerol and repeated centrifugation, the final pellet was resuspended in 10% glycerol to a final volume of 1 mL. Aliquots of 50 µL were prepared and either used immediately or stored on ice for electroporation.

2.4.6 Restriction Digestion and Ligation of VHH Sequences to pMECS-GG Vector

The purified nested PCR product (~400 bp) was mixed with the pMECS-GG vector (~3 µg) and incubated with SapI restriction enzyme, T4 DNA ligase, and CutSmart Buffer. The reaction underwent cycling (30 min at 37°C, 30 min at 18°C for 18 cycles) followed by a final ligation step (60 min at 18°C) and enzyme inactivation at 50°C and 80°C. DNA was purified using phenol-chloroform extraction, precipitated with ethanol, and dissolved in H_2O for subsequent electroporation.

2.4.7 Electroporation and Library Construction

Purified ligation products were mixed with 50 µL electro-competent TG1 cells and electroporated at 1.8 kV. SOC medium (1 mL) was added, and the mixture was incubated at 37°C for 1 hour at 200 rpm. Transformed cells were plated on LB/AMP-GLU agar plates and incubated overnight at 37°C. Colony counts were used to assess ligation efficiency, and colonies were picked for library preparation. Colonies from transformation plates were picked and subjected to colony PCR using MP57 and GIII primers targeting the VHH insert **Table 3**. PCR conditions included an initial denaturation at 95°C for 5 minutes, followed by 28 cycles (94°C for 45 s, 55°C for 45 s, 72°C for 45 s) and a final extension at 72°C for 10 minutes. PCR products were analyzed on a 1% agarose gel, and clones with the expected VHH insert size (~700 bp) were confirmed for inclusion in the library. The VHH library was stored or used for further downstream applications.

Table 3*:* Primer sequences used for colony PCR

Primer Name	Sequence (5′→3′)
CALL001	GTCCTGGCTGCTCTTCTACAAGG
CALL002	GGTACGTGCTGTTGAACTGTTCC
VHH-BACK-SAPI	CTTGGCTCTTCTGTGCAGCTGCAGGAGTCTGGRGGAGG
VHH-FORWARD-SAPI	TGATGCTCTTCCGCTGAGGAGACGGTGACCTGGGT

MP57	TTATGCTTCCGGCTCGTATG
GIII	CCACAGACAGCCCTCATAG

2.4.8 Enrichment and Identification of Antigen-Specific Nanobodies from a Phage-Displayed VHH Library

The library of phage-displayed VHHs was generated by infecting *E. coli* TG1 cells containing the VHH library with M13K07 helper phages, followed by overnight growth in 2×TY medium with ampicillin and kanamycin to produce phages. Purified phages were tittered and used for panning on antigen-coated ELISA wells, with blocking by skimmed milk to prevent non-specific binding. After incubation, unbound phages were washed away, and bound phages were eluted with triethylamine, neutralized, and used to infect *E. coli* TG1 cells for amplification and subsequent rounds of panning. Polyclonal ELISA monitored antigen-specific enrichment across rounds, while monoclonal ELISA tested periplasmic extracts from individual colonies for antigen binding. Positive clones, identified by a >2-fold absorbance increase in antigen-coated wells compared to controls, were selected for further analysis. Nanobody inserts were sequenced using MP57 or GIII primers to confirm antigen specificity. Verified clones were stored as glycerol stocks and transformed into *E. coli* WK6 cells for expression and purification of antigen-specific Nanobodies.

2.4.9 Expression and purification of Antigen-Specific Nanobodies

Recombinant *E. coli* WK6 cells harboring pMECS vectors with VHH genes were cultured in LB/AMP medium and shaken overnight at 37°C. A starter culture was inoculated into TB/AMP-GLU-MG medium, grown to an OD_{600} of 0.6–0.9, and induced with IPTG (1 mM final concentration) at 28°C overnight. Cells were harvested by centrifugation, and the

pellet was resuspended in TES buffer for osmotic shock extraction of periplasmic proteins. A second osmotic shock was optionally performed to maximize Nanobody yield.

Periplasmic extracts were purified using HIS-Select affinity resin for immobilized metal affinity chromatography (IMAC). The resin was equilibrated with PBS, incubated with the periplasmic extract, and washed with PBS to remove non-specific proteins. Nanobody was eluted with PBS containing 500 mM imidazole and further purified by dialysis, Vivaspin concentration, or size-exclusion chromatography to remove imidazole and aggregates.

Purity and identity of the purified Nanobody were assessed by SDS-PAGE stained with Coomassie blue and confirmed by Western blot using an anti-6×His antibody. The purified Nanobody was suitable for downstream applications such as ELISA, Western blot, or structural studies.

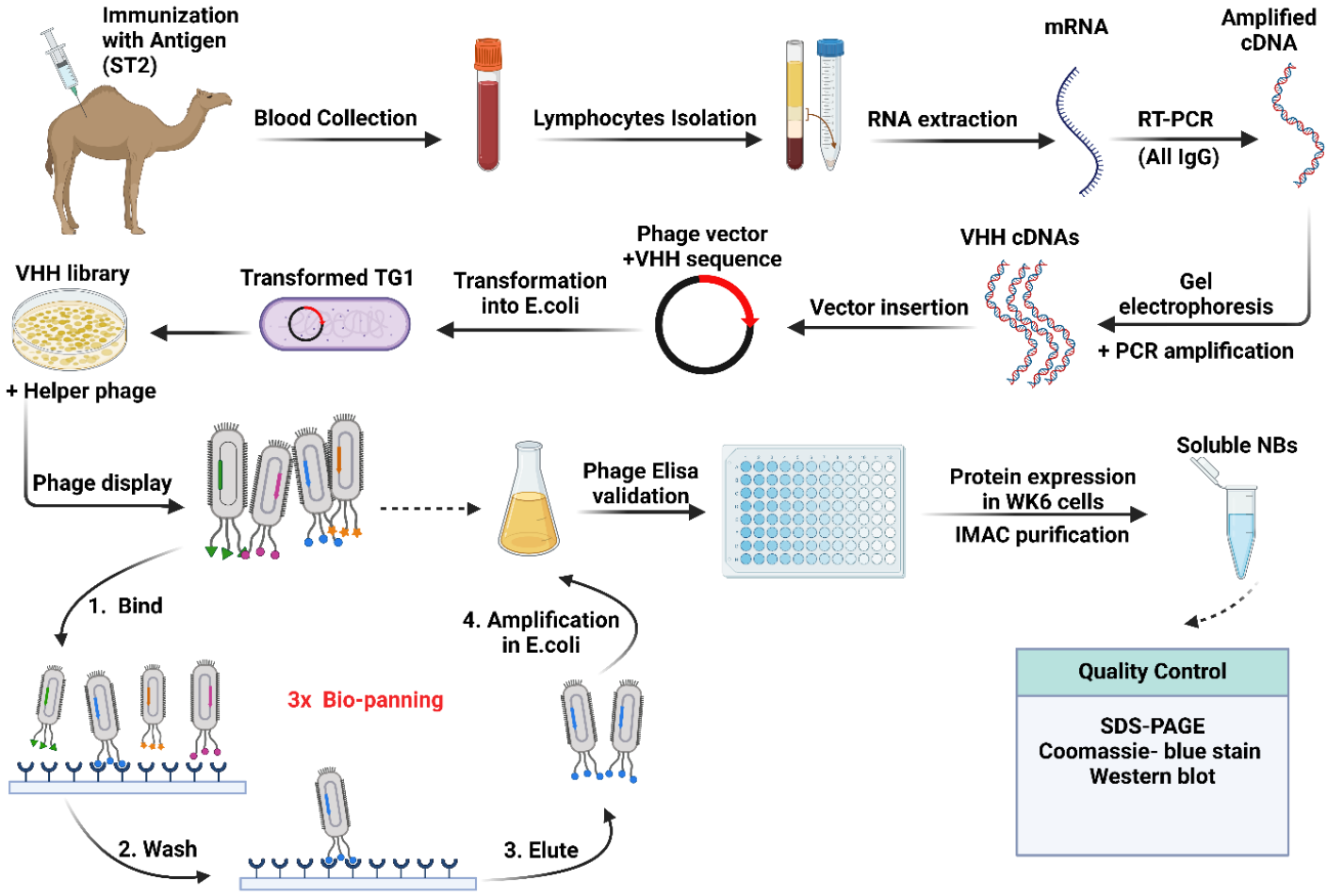

Figure 2.1 VHH production steps, Created with BioRender.com

2.4.10 Binding Specificity, Affinity, IC50

The specificity and cross-reactivity of the selected nanobody were assessed using ELISA. Antigens, including ST2 and a panel of control proteins from the IL-1 receptor family IL-18Rα, IL-36R, IL-1RAcP, and BSA, were coated onto 96-well ELISA plates at a concentration of 1 μg/mall Nanobody binding to the antigens was detected using an HRP-conjugated anti-His antibody, followed by the addition of an HRP substrate for signal development. This assay evaluated the Nanobody's specificity for ST2 and potential cross-reactivity with related proteins.

The Direct Ligand-Receptor Interaction Assay (Direct LRA) (Syedbasha et al., 2016) involves coating a 96-well plate with recombinant receptor (100 ng/μL) in carbonate buffer, incubating overnight at 4°C, washing with PBS-Tween, and blocking with 5% BSA for 2 hours at room temperature (RT). Serial dilutions of His-tagged ligands were added (100 μL/well) and incubated for 2 hours at RT to allow binding. After washing, primary anti-His mouse monoclonal antibody (1:1,000) was added and incubated for 2 hours, followed by HRP-conjugated goat anti-mouse IgG secondary antibody (1:5000) for 45 minutes. Signal development was achieved using TMB substrate for 15–30 minutes, stopped with stop solution, and absorbance was measured at 450 nm. Data were background-corrected, normalized, and plotted as a binding curve using ligand concentrations on a log10 scale. The dissociation constant was estimated using the Hill equation, representing the ligand concentration at which half of the receptor binding sites are occupied.

For the competitive ELISA, 96-well plates were coated with ST2 antigen (1 μg/mL) and incubated overnight at 4°C, with BSA-coated wells serving as negative controls. Wells were blocked with 5% BSA for 2 hours at room temperature (RT). Soluble ST2 antigen was prepared at increasing concentrations (0, 0.1, 0.2, 0.5, 1 μg/mL) and mixed with a fixed concentration of nanobodies (1 μg/mL) for 30 minutes at RT to allow complex formation.

The mixtures were added to antigen-coated wells and incubated for 2 hours at RT to evaluate competitive binding. After washing with PBS-Tween, bound nanobodies were detected using an anti-His primary antibody (1:1000) followed by an HRP-conjugated goat anti-mouse IgG secondary antibody (1:5000). TMB substrate was added for color development, and the reaction was stopped with sulfuric acid. Absorbance at 450 nm was recorded and analyzed to demonstrate the reduction in nanobody binding to immobilized ST2 with increasing concentrations of soluble ST2.

2.5 *In Vitro* Studies

2.5.1 Viability Assessment of Human Lung Epithelial Cells

Primary human lung epithelial cells purchased from PromoCell, were seeded into 96-well plates allowed to adhere overnight. Nanobodies were prepared at increasing concentrations (0, 1, 5, 10, and 50 µg/mL) in complete cell culture medium. The cells were treated with these nanobody concentrations for 24, 48, and 72 hours, with untreated cells (0 µg/mL) serving as the 100% viability control. At each time point, cell viability was measured using the CellTiter-Glo® Luminescent Cell Viability Assay, following the manufacturer's protocol. The assay involved adding an equal volume of CellTiter-Glo reagent to each well, gently mixing for 2 minutes to induce cell lysis, and incubating at room temperature for 10 minutes to stabilize the luminescent signal. Luminescence was measured using the GloMax® luminometer. The relative viability of treated cells was calculated as a percentage of the untreated control (0 µg/mL).

2.5.2 Cell Culture and Stimulation

Primary human lung epithelial cells purchased from PromoCell were cultured in complete growth medium at 37°C with 5% CO_2 until they reached 70–90% confluency. To evaluate the effects of NB7, the cells were first blocked with one of three treatments: NB7 at 1 µg/mL, astegolimab at 3 µg/mL as a positive control, or a non-specific nanobody at 1 µg/mL as a negative control. Blocking was performed for 1 hour at 37°C in serum-free medium to ensure receptor binding.

After the blocking step, the cells were stimulated with house dust mite (HDM) extract at a concentration of 50 µg/mL and recombinant human IL-33 (Abcam, ab281811) at 10 ng/mL. The stimulation cocktail was applied directly to the cells without removing the blocking agents to allow competitive interaction. This incubation was carried out under the following conditions based on the analysis type: 4 hours for RNA-based analyses, 24 hours for ST2 expression and cytokine release, and 30 minutes for phosphorylated protein detection.

Control cells, which were treated only with serum-free medium without any blocking or stimulation, were included to establish baseline expression levels. This setup was designed to mimic inflammatory conditions and assess the effectiveness of the blocking agents in modulating ST2 receptor activity under stimulated conditions.

2.5.3 Immunofluorescence (IF)

After the 24-hour stimulation, cells were fixed with 4% paraformaldehyde for 15 minutes at room temperature and washed three times with PBS. Permeabilization was performed using 0.1% Triton X-100 for 10 minutes, followed by blocking in 1% bovine serum albumin (BSA) in PBS for 1 hour at room temperature. Primary antibodies specific to the ST2 receptor were added and incubated overnight at 4°C. After washing with PBS, cells were incubated with fluorophore-conjugated secondary antibodies for 1 hour at room

temperature in the dark. Nuclei were counterstained with DAPI for 5 minutes before mounting with an anti-fade mounting medium. Fluorescence imaging was performed using a confocal microscope (Keyence BZ9000 BioRevo) at 20× magnification to visualize ST2 expression. This setup allowed evaluation of the functional impact of NB7 in reducing ST2 receptor expression compared to the controls under inflammatory stimulation conditions

2.6 Common Molecular and Immunoassays Used in *In Vivo* and *In Vitro* Investigations

2.6.1 Western Blot Analysis

Western blot analysis was performed for both cultured cells and tissue samples using standardized protocols based on a prior study(Mahmood & Yang, 2012). For cultured cells, the cells were washed twice with cold PBS to remove media and contaminants, then scraped into ice-cold RIPA buffer (50 mM Tris, 150 mM NaCl, 1% sodium deoxycholate, 0.1% SDS, 1% Triton X-100, pH 7.5) supplemented with protease and phosphatase inhibitors, including 1x Protease Inhibitor Cocktail and 1 mM phenylmethylsulfonyl fluoride (Sigma-Aldrich, Germany). The lysates were incubated on ice for 10 minutes, followed by sonication using two 5-second pulses to ensure complete lysis. The lysates were then centrifuged at 12,000 x g for 20 minutes at 4°C to remove debris, and the clear supernatant was collected. Protein concentrations were determined using a BCA protein assay (Thermo-Scientific Pierce BCA Protein Assay Kit) and normalized to a uniform concentration.

For lung tissue samples from both treated and untreated groups, approximately 10–30 mg of tissue was homogenized in ice-cold RIPA buffer with protease and phosphatase inhibitors and subsequently processed as described above. For both cells and tissues, 20–30 µg of total protein was denatured with Laemmli buffer, heated at 95°C for 5 minutes, and

resolved on 8%, 10%, or 12.5% SDS-PAGE gels. Proteins were transferred to nitrocellulose membranes (Bio-Rad) using a semi-dry transfer system. Membranes were blocked in 5% skim milk in TBST (TBS with 0.1% Tween-20) for 1 hour at room temperature to prevent non-specific binding. Primary antibodies (detailed below) were diluted as per the manufacturer's instructions and incubated with the membranes overnight at 4°C. After washing with TBST, membranes were incubated with horseradish peroxidase (HRP)-conjugated secondary antibodies for 1 hour at room temperature.

The primary antibodies used included Anti-6X His tag® (Abcam, ab9108, 1:4000), p.ERK (Cell Signaling, 9101S, 1:1000), ERK (Cell Signaling, 56955, 1:1000), IκBα (Cell Signaling, 4812S, 1:1000), p.IκBα (Cell Signaling, 2859S, 1:1000), GR alpha (Thermo Fisher, PA1-516, 1:500), GR beta (Thermo Fisher, PA3-514, 1:500), ST2 (MyBioSource, MBS150471, 1:1000), and GAPDH (Cell Signaling, 2118L, 1:1000) as a loading control. Secondary antibodies included anti-rabbit IgG-HRP (Cell Signaling, 7074S, 1:1000) and anti-mouse IgG-HRP (Cell Signaling, 7076S, 1:1000).

Blots were developed using chemiluminescent substrates, such as the Clarity Western ECL Substrate (Bio-Rad), and visualized using AZURE Sapphire (CA 94568 USA). Protein bands were quantified using ImageJ software, with GAPDH serving as a loading control.

2.6.2 Quantitative Real-Time PCR Analysis (qRT-PCR)

Total RNA was extracted from the cells or lung homogenates using TRIzol reagent (Invitrogen), following the manufacturer's instructions. The RNA quality and concentration were evaluated using a NanoDrop™ spectrophotometer (Thermo Scientific). Following cDNA synthesis using the High-Capacity cDNA Reverse Transcription Kit (Applied Biosystems) on the Veriti™ Thermal Cycler, qRT-PCR was carried out using SuperMix (Solis BioDyne) and performed on a QuantStudio™ 3 Real-Time PCR System (Applied

Biosystems, USA). Gene expression levels were evaluated using the comparative CT (ΔΔCT) method and normalized to the housekeeping gene β-actin or 18S rRNA. The mRNA expression data were presented as fold change relative to unstimulated controls, serving as baseline measurements for the therapy. Specific primer sequences are detailed in **Table 4**.

Table 4: Forward (F) and reverse (R) primer sequences for qPCR analysis.

Target genes	Forward sequence (F)	Reverse sequence (R)
mIL-4	GCATTTTGAACGAGGTCACAGG	CTCTCTGTGGTGTTCTTCGTTG
mIL-5	ATGGAGATTCCCATGAGCAC	AGCCCCTGAAAGATTTCTCC
mIL-13	ACACAAGACCAGACTCCCCT	GGGAATCCAGGGCTACACAG
mIL-17	ACCGCAATGAAGACCCTGAT	TCCCTCCGCATTGACACA
mGRα	AAAGAGCTAGGAAAAGCCATTGTC	TCAGCTAACATCTCTGGGAATTCA
mGRβ	AAAGAGCTAGGAAAAGCCATTGTC	CTGTCTTTGGGCTTTTGAGATAGG
mβ-ACTIN	CATTGCTGACAGGATGCAGAAGG	TGCTGGAAGGTGGACAGTGAGG
hIL-17	ATCCCTCAAAGCTCAGCGTGTC	GGGTCTTCATTGCGGTGGAGAG
hIL-1RL1	GTGATAGTCTTAAAAGTGTTCTGG	TCAAAAGTGTTTCAGGTCTAAGCA
hIL-8	CCACACTGCGCCAACACAG	CTTCTCCACAACCCTCTGC
hGRα	CAAAGAGCTAGGAAAAGCCAT	CAATACTCATGGTCTTATCCAA
hGRβ	TCAGTTCCTAAGGACGGTCT	ACCACATAACATTTTCATGCAT
h18s	CTACCACATCCAAGGAAGCA	TTTTTCGTCACTACCTCCCCG

2.6.3 Enzyme-Linked Immunosorbent assay (ELISA)

Cytokine levels in BALF and cell culture supernatants were measured using ELISA kits according to the manufacturer's instructions. The ELISA kits included Mouse IL-4 (R&D Systems, DY404), Mouse IL-5 (R&D Systems, DY405), Mouse IL-13 (R&D Systems, DY413), Mouse IL-17 (R&D Systems, DY421), Human IL-8 (Invitrogen, KAC1301), and

Human IL-17A (Invitrogen, BMS2017). These analyses were performed to determine cytokine concentrations under specific experimental conditions.

2.7 Statistics

We used GraphPad Prism software (version 8.0; GraphPad Software, La Jolla, Calif) to generate figures and perform statistical analyses. In the study, data are expressed as means ± SEM. For comparisons between the means of two groups, independent samples t-tests were used if the data were normally distributed, and Mann–Whitney U-tests were used for skewed data. For comparisons among more than two groups, one-way ANOVA was performed, followed by Bonferroni post hoc tests for multiple comparisons. Respiratory system mechanics were analyzed using two-sided ANOVA, followed by Bonferroni post hoc tests for multiple comparisons. All tests were two-tailed, and a P value of less than 0.05 was considered statistically significant. Furthermore, power analysis for comparing two independent sample means indicated that a sample size of 5 per group was required to detect differences with a power of 0.9 at a significance level of 0.05. All power analyses and sample size calculations were conducted using G*Power 3.1 (Faul, Erdfelder, Buchner, & Lang, 2009; Serdar, Cihan, Yücel, & Serdar, 2021).

3. Results

3.1 ST2 Expression Is Upregulated in Asthma

To explore the role of IL-33/ST2 signalling in asthma pathogenesis, we conducted comprehensive experimental approaches to investigate the expression and functional implications of ST2 in severe asthma. *In silico* analysis of transcriptomic datasets revealed a significant upregulation of ST2 expression in lung biopsies from patients with moderate and severe asthma compared to healthy controls **(Figure 3.1 A).** Notably, ST2 expression was progressively higher in the severe asthma group compared to the moderate asthma group ($p < 0.05$), highlighting a potential correlation between disease severity and IL-33 levels. This observation suggested a pivotal role of IL-33/ST2 signalling in driving asthma progression and formed the basis for further experimental validation.

To investigate this, we developed a novel chronic HDM-induced asthma mouse model and stimulated the mice with recombinant IL-33. The experimental setup and timeline are illustrated in the schematic representation **(Figure 3.1 B).** In the mouse model, recombinant IL-33 stimulation significantly increased ST2 expression in lung tissues compared to the HDM-only group 3-fold increase ($p< 0.0001$) **(Figures 3.1 C, D),** reflecting the increase in ST2 levels observed in the *in silico* analysis.

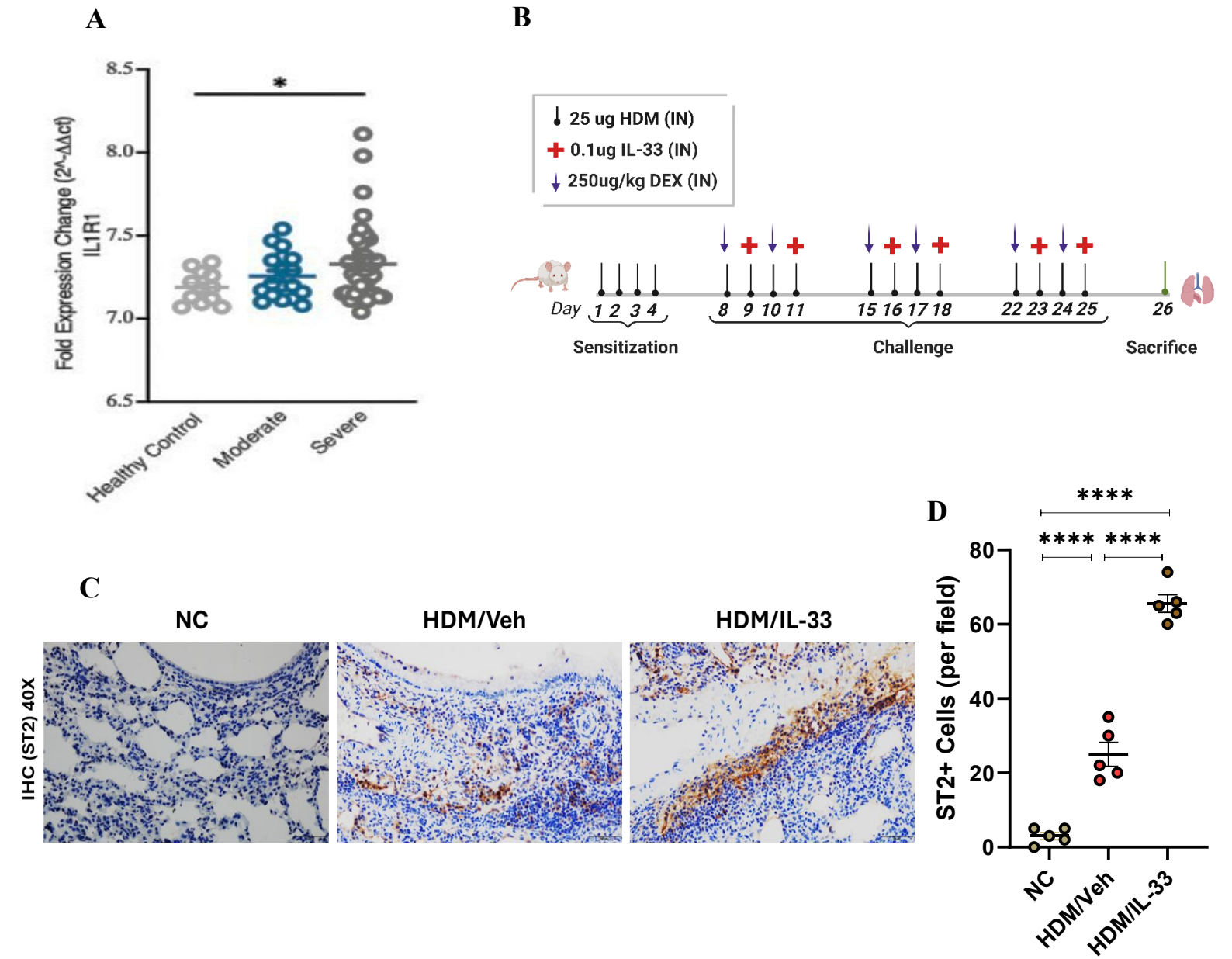
A
B
C
D
Fold Expression Change (2^-ΔΔct)
IL1R1
8.5
8.0
7.5
7.0
6.5
*
Healthy Control
Moderate
Severe
25 ug HDM (IN)
0.1ug IL-33 (IN)
250ug/kg DEX (IN)
Day
1 2 3 4
8 9 10 11
15 16 17 18
22 23 24 25
26
Sensitization
Challenge
Sacrifice
NC
HDM/Veh
HDM/IL-33
IHC (ST2) 40X
ST2+ Cells (per field)
80
60
40
20
0
****
****
****
NC
HDM/Veh
HDM/IL-33

Figure 3.1: ST2 is upregulated during asthma

(A) ST2 expression levels in bronchial biopsies from healthy controls (n=13), mild/moderate (n=18), and severe asthma patients (n=42). Data from GSE147881 were normalized using Voom, and statistical significance was assessed with Student's *t*-test. Box plots show the distribution of ST2 expression across groups. (B) Experimental procedure illustrated with BioRender.com. Mice were sensitized intranasally with HDM (25 μg) four times per week for 4 weeks. Recombinant IL-33 (0.1 μg) was administered intranasally twice weekly. The negative control (NC) group received no HDM or IL-33. Lung tissues were collected 24 hours after the final sensitization for analysis. (C, D) IHC analysis of mouse lung tissues showing $ST2^+$ cells (40× magnification, scale bar = 50 μm) per visual field. The recombinant IL-33-stimulated group displayed significantly higher ST2 expression compared to the HDM-only group. n = 5 mice per group. Statistical analyses: Two-way comparisons were performed using Student's *t*-test or the Mann–Whitney test for skewed

3.2 Elevated IL-33 Exacerbate Airway Inflammation, Enhance Hyperresponsiveness, and Drive a Shift to Neutrophilic Inflammation in the HDM/IL-33 Asthma Model

Stimulating HDM group with IL-33 was associated with extensive peri-bronchial and perivascular inflammation in lung tissues compared to the HDM-only group (2-fold increase, $p = 0.002$) **(Figure 3.2 A, D)**. This inflammation featured pronounced goblet cell hyperplasia and a marked increase in mucus production (2- fold increase, $p = 0.003$) (**Figure 3.2 B, E**). Additionally, there was a significant increase in the recruitment of total inflammatory cells, showing a (1.5-fold increase, $p = 0.002$) (**Figure 3.2 C, F**). Notably, the inflammatory cell profile shifted from predominantly eosinophilic inflammation in the HDM-only group to neutrophilic inflammation in the HDM/IL-33 group (3-fold increase, $p < 0.0001$) (**Figure 3.2 G-I**). These findings underscore the significant enhancement of airway pathology in the HDM/IL-33 group, driven by IL-33 stimulation, which exacerbate inflammation and alter its cellular profile.

Our results also revealed that stimulating HDM group with IL-33 significantly increased airway hyperresponsiveness (AHR) in a methacholine dose-dependent manner, with markedly elevated AHR observed in the HDM/IL-33 group compared to the HDM-only group ($p = 0.0002$, **Figure 3.2 J**). These findings underscore the significant enhancement of airway pathology in the HDM/IL-33 group, driven by IL-33, which exacerbate inflammation, alter the cellular profile, and worsen airway hyperresponsiveness.

IL-33 is known to promote Th2 cytokines such as IL-4, IL-5, and IL-13 through its receptor, ST2 (Murakami-Satsutani et al., 2014), a finding confirmed in our study. Elevated ST2 levels in the HDM/IL-33 group were associated with a significant increase in IL-4, showing a 2-fold increase ($p = 0.003$; **Figure 3.2 K**), and IL-13, showing a 1.3-fold increase

($p = 0.03$; **Figure 3.2 L**), but not IL-5, at both mRNA and protein levels in the BALF compared to the HDM-only group. Interestingly, IL-5 protein levels were significantly higher in the HDM-only group ($p < 0.0001$; **Figure 3.2 M**), with no corresponding changes at the mRNA level

Furthermore, it was shown that IL-33 signalling promotes Th17 differentiation *in vitro*, highlighting an important link between IL-33 and Th17 immunity (Cho et al., 2012). Interestingly, our study found a significant increase in IL-17 levels in both mRNA (2-fold increase, $p < 0.0001$; **Figure 3.2 N**) and protein levels (3-fold increase, $p < 0.0001$; **Figure 3.2 N**) in the HDM/IL-33 group compared to the HDM-only group.

3.2.1 IL-33 Drives Steroid Hypo-responsiveness in the HDM/IL-33 Asthma Model

Previous studies have demonstrated that memory-type $ST2^+$ T cells are steroid-resistant and appear to play a critical role in steroid-resistant types of lung inflammation (Mato et al., 2017). Furthermore, IL-33 has been identified as a novel inflammatory marker associated with severe asthma, highlighting the potential interplay between IL-33/ST2 signalling and steroid resistance (Prefontaine et al., 2009). Building on this knowledge, we sought to evaluate the impact of IL-33/ST2 signalling on steroid responsiveness in our chronic asthma model.

To investigate this, mice from both the HDM-only and HDM/IL-33 groups were treated intranasally with dexamethasone (DEX), as shown in the schematic representation **(Figure 3.1 B**). This approach allowed us to explore how IL-33/ST2 signalling contributes to impaired steroid responsiveness, providing insights into the mechanisms underlying severe asthma and its hypo-responsiveness to standard corticosteroid therapy.

Interestingly, we observed that DEX treatment significantly reduced overall lung inflammation in the BALF of the HDM-only group but not in the HDM/IL-33 group. This was evident by a 2-fold decrease ($p = 0.001$; **Figure 3.2 A.1, D**), as well as a reduction in mucus production, also by 2-fold ($p = 0.03$; **Figure 3.2 B.1, E**). Additionally, DEX markedly reduced the total inflammatory cell count in the BALF of the HDM-only group, with a 2-fold reduction ($p = 0.0004$; **Figure 3.2 C.1, F**), while eosinophil and neutrophil counts remained unaffected in both groups.

Accordingly, DEX treatment led to a reduction in cytokine levels at both mRNA and protein levels in the HDM-only group but not in the HDM/IL-33 group, compared to their untreated DEX counterparts. This reduction was observed for Th2 cytokines, including IL-4, IL-5, and IL-13 (approximately 5- to 4-fold reduction, $p < 0.0001$; **Figure 3.2 K–M**), as well as IL-17 (approximately 4-fold reduction, $p = 0.03$; **Figure 3.2 N**). However, in the HDM/IL-33

group, DEX treatment showed no significant effect on any of these parameters, indicating a complete lack of therapeutic efficacy in this group. **These findings indicate that IL-33 contributes to steroid hypo-responsiveness in this asthma model by maintaining elevated inflammation despite dexamethasone treatment**.

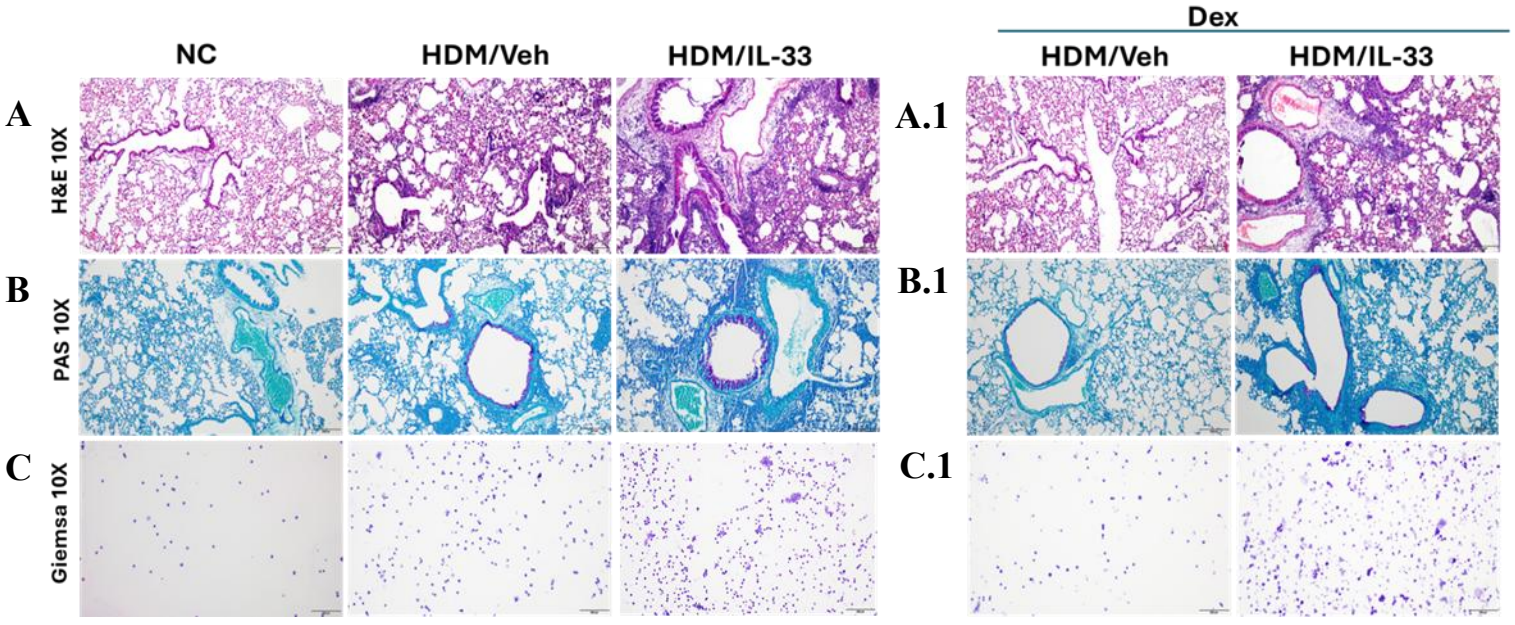

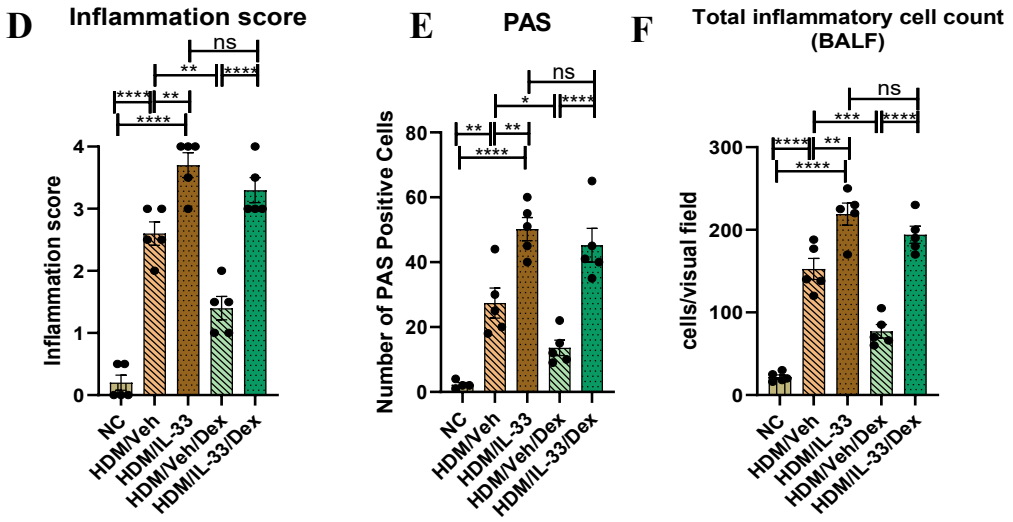

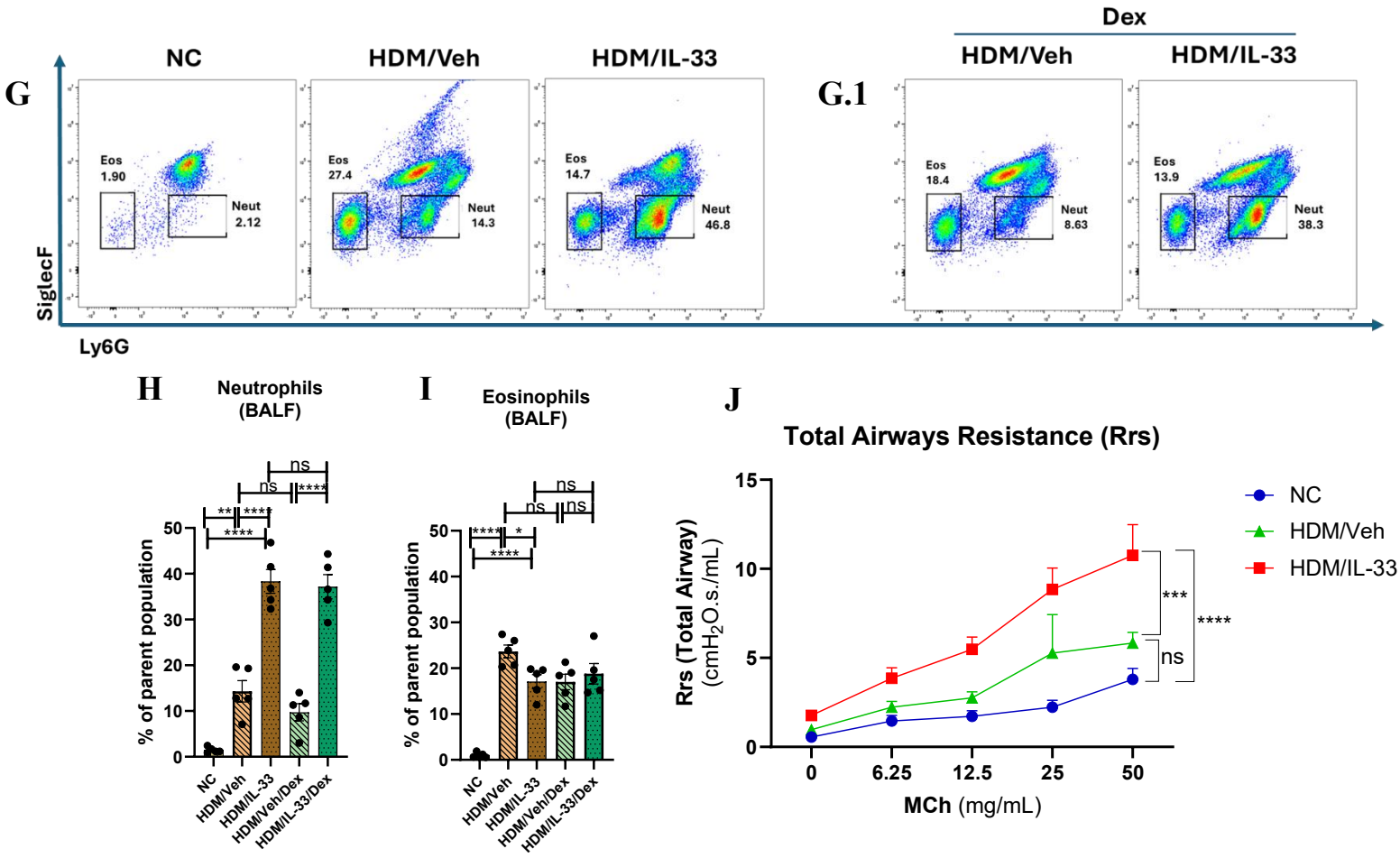
G
NC
HDM/Veh
HDM/IL-33
Eos
1.90
Neut
2.12
Eos
27.4
Neut
14.3
Eos
14.7
Neut
46.8
SiglecF
Ly6G
G.1
Dex
HDM/Veh
HDM/IL-33
Eos
18.4
Neut
8.63
Eos
13.9
Neut
38.3
H
Neutrophils
(BALF)
% of parent population
NC
HDM/Veh
HDM/IL-33
HDM/Veh/Dex
HDM/IL-33/Dex
I
Eosinophils
(BALF)
% of parent population
NC
HDM/Veh
HDM/IL-33
HDM/Veh/Dex
HDM/IL-33/Dex
J
Total Airways Resistance (Rrs)
Rrs (Total Airway)
(cmH2O.s./mL)
MCh (mg/mL)
NC
HDM/Veh
HDM/IL-33
ns
***
****

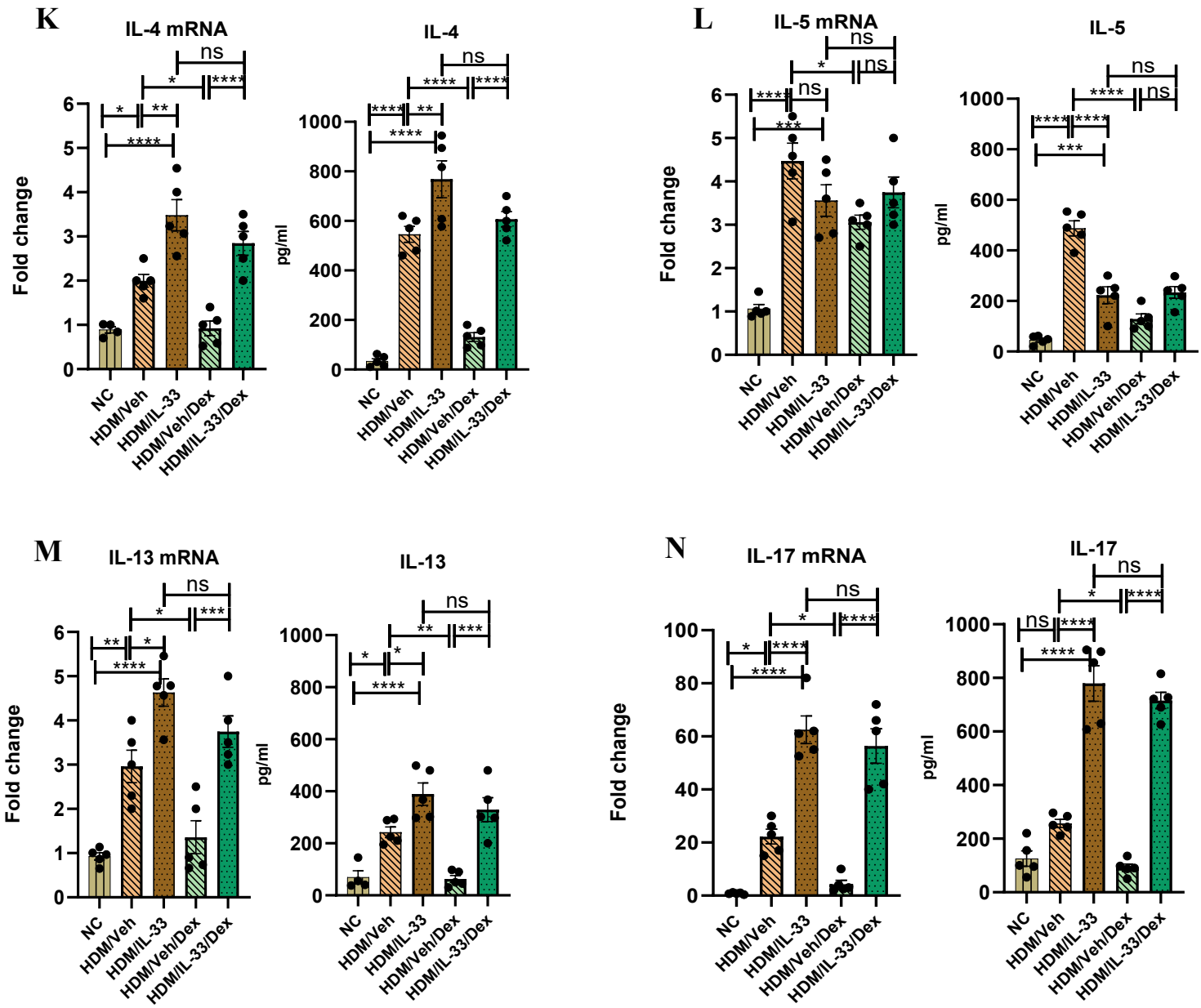
K
IL-4 mRNA
Fold change
IL-4
pg/ml
L
IL-5 mRNA
Fold change
IL-5
pg/ml
M
IL-13 mRNA
Fold change
IL-13
pg/ml
N
IL-17 mRNA
Fold change
IL-17
pg/ml
NC
HDM/Veh
HDM/IL-33
HDM/Veh/Dex
HDM/IL-33/Dex
ns

Figure 3.2: Elevated IL-33 Exacerbate Airway Inflammation, Enhance Hyperresponsiveness, and Drive a Shift to Neutrophilic Inflammation in the HDM/IL-33 Asthma Model. Upon treatment with DEX no response was shown.

(A) H&E staining of lung sections evaluated peri-bronchial and perivascular inflammation, (B) PAS staining evaluated mucus production in lung tissues, and (C) Wright-Giemsa staining of BALF cells analyzed inflammatory infiltrates (×10 magnification; scale bar = 200 μm). (D) Inflammation scores from lung sections (0–4 scale). (E) PAS staining quantified mucus-producing cells in lung tissue. (F) Total inflammatory cell infiltrates in BALF. (G) Flow cytometry of BALF. (H) Neutrophils in BALF analyzed using FlowJo. (I) Eosinophils in BALF analyzed using FlowJo. (J) AHR measured as airway resistance in response to escalating doses of methacholine (MCh). (K-N) Cytokine levels (IL-4, IL-5, IL-13, and IL-17) were quantified in BALF at both mRNA levels (qPCR) and protein levels (ELISA). (A.1, D) H&E staining of lung sections demonstrated that DEX treatment significantly reduced peri-bronchial and perivascular inflammation in the HDM-only group but had no effect in the HDM/IL-33 group. (B.1, E) PAS staining quantified mucus production, showing a significant reduction following DEX treatment in the HDM-only group, with no reduction observed in the HDM/IL-33 group. (C.1, F) Total inflammatory cell counts in BALF were significantly reduced by DEX in the HDM-only group, whereas no significant changes were observed in the HDM/IL-33 group. (G.1, H, I) Flow cytometry analysis showed that neutrophils and eosinophils remained elevated in the HDM/IL-33 group treated with DEX. (K-N) DEX treatment significantly reduced Th2 cytokines (IL-4, IL-5, IL-13) and IL-17 at both mRNA (qPCR) and protein (ELISA) levels in the HDM-only group but had no significant effect in the HDM/IL-33 group. **n** = 5 mice per group. Statistical analyses: Two-way comparisons used Student's t-test or Mann-Whitney test for skewed data; multiple group comparisons used two-sided ANOVA with post hoc Bonferroni tests. Data are presented as mean ± SEM. ns: non-significant, * $p < 0.05$, ** $p < 0.01$, *** $p < 0.001$, **** $p < 0.0001$. All analyses were performed using GraphPad Prism.

3.3 IL-33/ST2 Activation Counteracts Dexamethasone Suppression of MAPK/ERK and NF-κB Pathways

We next decided to investigate the molecular mechanisms underlying IL-33-induced steroid hypo-responsiveness. IL-33/ST2 signaling has been implicated in activating the MAPK/ERK and NF-κB pathways, which are critical regulators of inflammation in chronic respiratory diseases and are known to exhibit reduced responsiveness to corticosteroid treatment (T. Liu, Zhang, Joo, & Sun, 2017; van der Zwet et al., 2021). To explore their contribution to the observed resistance in the HDM/IL-33 group, we analyzed the activation of these pathways and their role in mediating IL-33-induced steroid hypo-responsive inflammation.

Our findings indicate that MAPK/ERK signalling was enhanced in lung tissue of HDM-only and HDM/IL-33 groups, as evidenced by a significant increase in the expression level of phosphorylated ERK (approximately 4-fold increase in p-ERK; $p < 0.0001$; **Figures 3.3 A, B**). Interestingly, NF-κB activation was more evident upon IL-33 stimulation, as the expression level of phosphorylated IκBα was higher in the HDM/IL-33 group than in the HDM-only group (higher fold change in p.IκBα upon IL-33 stimulation; $p < 0.0001$, **Figures 3.3 A, C**), further confirming robust NF-κB pathway activation.

Dexamethasone treatment effectively reversed these effects in the HDM-only group; p-ERK levels were significantly reduced (3-fold decrease; $p < 0.0001$, Figures 3A, B), and p-IκBα protein levels also showed a significant reduction compared to the untreated group (2-fold decrease; $p = 0.04$, **Figures 3.3 A,C**). However, dexamethasone treatment failed to reverse these effects in the HDM/IL-33 group (**Figures 3.3 A–C**). These results suggest that IL-33-induced activation of the MAPK/ERK and NF-κB pathways via ST2 signalling is hyporesponsive to dexamethasone.

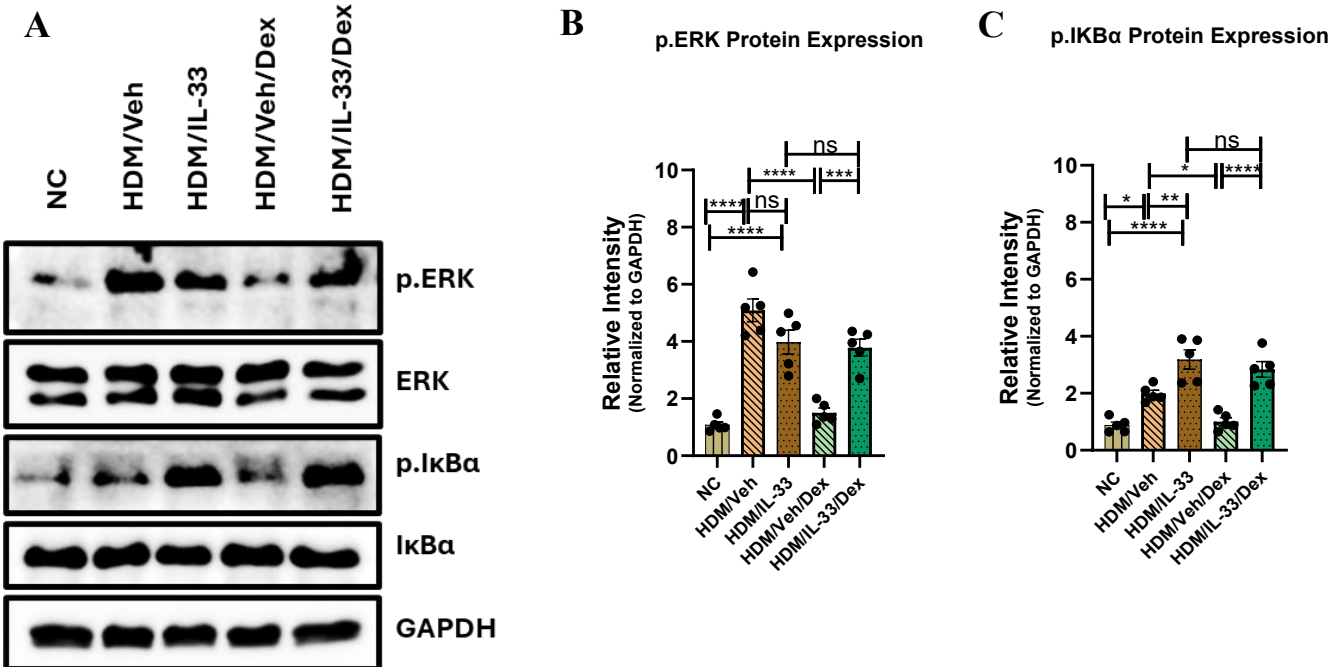

Figure 3.3: IL-33/ST2 Activation Counteracts Dexamethasone Suppression of MAPK/ERK and NF-κB Pathways

(A)Western blot analysis showed increased phosphorylated ERK (p-ERK) and phosphorylated IκBα (p-IκBα) levels in the HDM-only and HDM/IL-33 groups, normalized to GAPDH. (B) p-ERK levels were significantly elevated in both groups, with dexamethasone (DEX) reducing p-ERK in the HDM-only group but not in the HDM/IL-33 group. (C) p-IκBα levels were higher in the HDM/IL-33 group compared to the HDM-only group. DEX reduced p-IκBα levels in the HDM-only group but had no effect in the HDM/IL-33 group. Quantification was performed using ImageJ. Data are presented as mean ± SEM (n = 5). Statistical analyses Two-way comparisons used Student's t-test or Mann-Whitney test for skewed data. ns: non-significant, * $p < 0.05$, ** $p < 0.01$, *** $p < 0.001$, **** $p < 0.0001$. All analyses were performed using GraphPad Prism.

3.4 ST2 Signaling Induces Steroid Hypo-responsiveness by Regulating the GRα/GRβ Ratio

Building on previous findings linking reduced glucocorticoid sensitivity in asthma to glucocorticoid receptor (GR) dysfunction and activation of the MAPK and NF-κB pathways (Ayroldi et al., 2012; Barnes & Adcock, 2009), we hypothesized that ST2-mediated signalling in IL-33-challenged mice disrupts GRα and GRβ levels in lung tissues.

To test this hypothesis, we assessed the expression levels of the stimulatory GRα and inhibitory GRβ isoforms at both mRNA and protein levels. Our analysis revealed a significantly lower expression of GRα at both mRNA and protein levels in the lung tissue of the HDM/IL-33 group compared to the HDM-only group (2-fold decrease at both mRNA and protein levels, $p < 0.0001$; **Figure 3.4 A, D, F**). In contrast, GRβ expression was significantly upregulated at both mRNA and protein levels in the lung tissue of the HDM/IL-33 group compared to the HDM-only group (around 2-fold increase at both mRNA and protein levels, $p < 0.0001$; **Figure 3.4 B, E, F**). Given that the shift in the GRα/GRβ ratio was toward GRβ dominance (**Figure 3.4 C**).

Interestingly, following treatment, the HDM-only group—but not the HDM/IL-33 group—exhibited an effective recovery in GR expression, characterized by an increase in GRα levels and a reduction in GRβ levels (2-fold increase in GRα and 2-fold decrease in GRβ expression at both mRNA and protein levels, $p < 0.0001$; **Figure 3.4 A-F**). These findings highlight that ST2-mediated signalling in IL-33-challenged mice disrupts the GRα/GRβ balance, favouring GRβ dominance and contributing to reduced glucocorticoid sensitivity. Importantly, this imbalance was not reversed by treatment in the HDM/IL-33 group, underscoring the need for targeted therapeutic strategies.

The failure of standard dexamethasone treatment to suppress inflammation or restore the GRα/GRβ balance in the HDM/IL-33 group underscores the limitations of conventional corticosteroid therapies in IL-33/ST2-driven asthma, highlighting the urgent need for novel therapeutic strategies. To address this, **we developed, for the first time, novel anti-ST2 nanobodies as a pioneering therapeutic approach** to reduce inflammation and restore steroid responsiveness in IL-33/ST2-driven asthma.

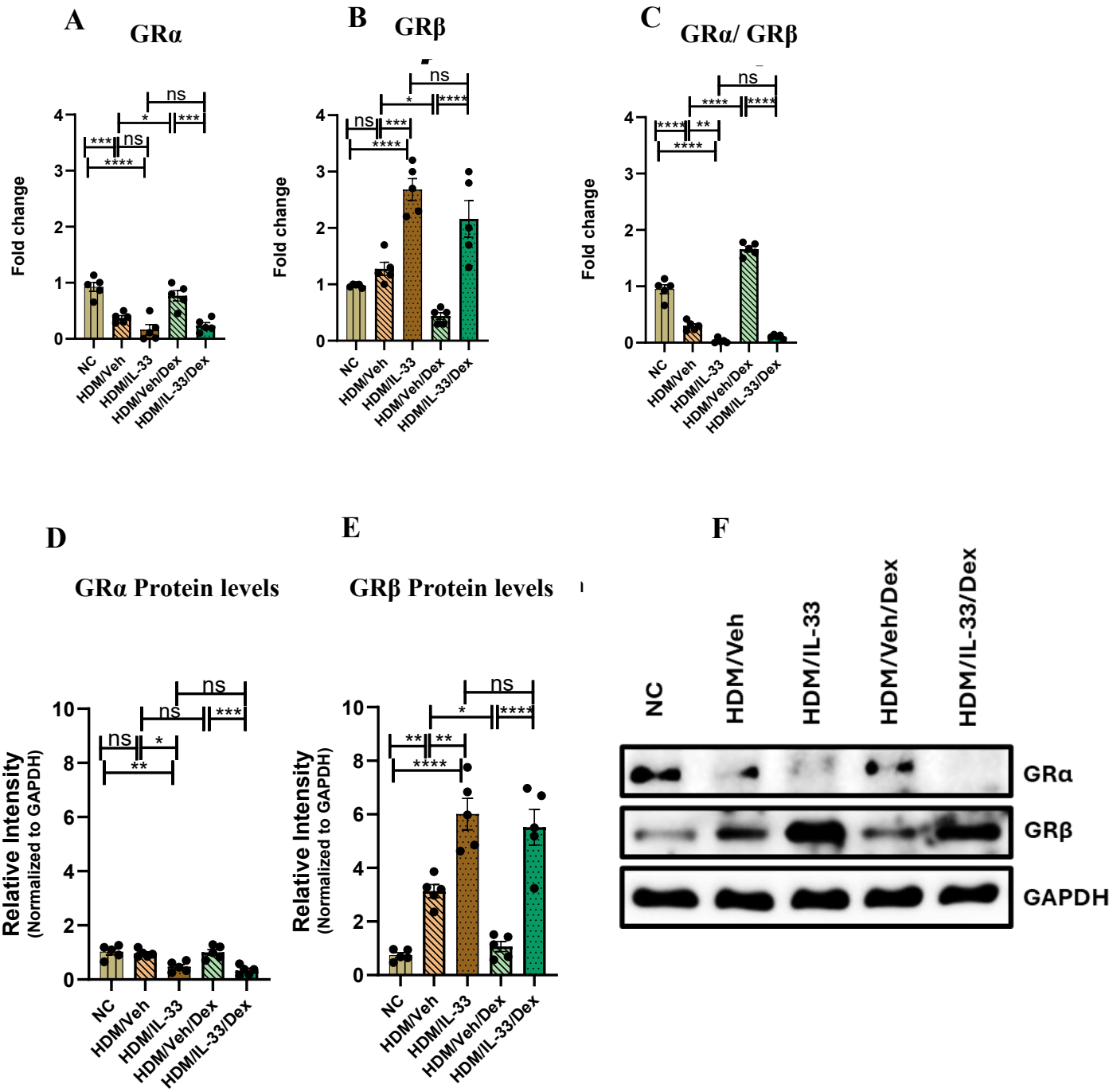
A
GRα
Fold change
B
GRβ
Fold change
C
GRα/ GRβ
Fold change
NC
HDM/Veh
HDM/IL-33
HDM/Veh/Dex
HDM/IL-33/Dex
D
GRα Protein levels
Relative Intensity
(Normalized to GAPDH)
E
GRβ Protein levels
Relative Intensity
(Normalized to GAPDH)
F
GRα
GRβ
GAPDH

Figure 3.4: IL-33/ST2 Signaling Induces Steroid Hypo-responsiveness by Regulating the GRα/GRβ Ratio

(A, D, F) GRα expression at mRNA and protein levels was significantly lower in the HDM/IL-33 group compared to the HDM-only group. (B, E, F) GRβ expression at mRNA and protein levels was significantly higher in the HDM/IL-33 group compared to the HDM-only group. (C) The GRα/GRβ ratio at mRNA levels shifted toward GRβ dominance in the HDM/IL-33 group. (A-F) Following DEX treatment, the HDM-only group—but not the HDM/IL-33 group—showed recovery in GR expression, with increased GRα levels and decreased GRβ levels. mRNA levels were quantified by qPCR using the ΔΔCt method, with gene expression normalized to β-actin. Protein levels were quantified by Western blot, with relative intensity normalized to GAPDH using ImageJ software. Data are presented as mean ± SEM (n = 5). Statistical analyses: Two-way comparisons used Student's t-test or Mann-Whitney test for skewed data. ns: non-significant, * $p < 0.05$, ** $p < 0.01$, *** $p < 0.001$, **** $p < 0.0001$. All analyses were performed using GraphPad Prism.

3.5 Development, Selection and Identification of Anti-ST2 Nanobody Clones

The development of nanobodies, derived from the heavy-chain-only antibodies (HCAbs) of camelids, has emerged as a powerful approach for generating highly specific and stable therapeutic candidates. These single-domain antibodies (VHHs) are unique to camelids. To identify nanobodies targeting human ST2, a receptor involved in various inflammatory pathways, we constructed a VHH library from camels immunized with recombinant human ST2 proteins.

To construct an immune VHH library, RNA was extracted from the blood of immunized camels and cDNA is synthesized from this RNA, the initial PCR produced two distinct products: one approximately 900 bp, corresponding to the VH + VL regions of conventional antibodies, and another approximately 700 bp, corresponding to the heavy-chain-only antibodies (HCAb) unique to camelids (**Figure 3.5 A**). The 700 bp HCAb product, representing the heavy-chain antibody, was purified and used as a template for nested PCR. This amplification yielded a single product of approximately 450 bp, representing the VHH region of the HCAb (**Figure 3.5 B**).

The VHH fragments were then cloned into a phagemid vector pMECS-GG (**Figure 3.5 C**) and transformed into E. coli TG1 cells to construct a bacterial library with an estimated capacity of 10^7 clones. Validation of the library was performed by PCR analysis of 36 randomly selected colonies. Amplification of the selected clones revealed clear bands corresponding to the expected size of the VHH fragment, confirming successful incorporation of VHH genes across all clones (**Figure 3.5 D**).

The TG1 bacterial library was infected with helper phage to rescue phage particles displaying the VHH fragments on their surfaces. These rescued phages were subjected to three rounds of bio-panning against immobilized recombinant human ST2 to enrich ST2-

specific nanobody candidates. ELISA analysis of the enriched phage clones demonstrated progressive enrichment of high-affinity binders, with a 2.76-fold and 2.77-fold increase in binding observed after the second and third rounds, respectively, compared to the original phage library. Minimal binding was observed for phages selected against the negative control, ST2-C, confirming the specificity of the enriched clones (**Figure 3.5 E**).

Following the bio-panning, individual colonies were randomly selected from each round for further characterization. To evaluate the binding efficiency of the expressed nanobodies to ST2, periplasmic ELISA was performed. The absorbance measurements demonstrated a progressive increase in binding efficiency across the panning rounds. Clones from Pan2 (B wells) and Pan3 (C and D wells) exhibited the highest absorbance values, indicating strong enrichment of high-affinity binders (**Figure 3.5 F**). In contrast, clones from Pan1 (A wells) displayed variable results, with some showing strong binding while others remained closer to baseline. Negative controls (E–H wells) consistently exhibited minimal absorbance, confirming negligible nonspecific binding. These trends are visually represented in a heatmap, where higher binding intensities are shown as lighter colors in Pan2 and Pan3 wells, while Pan1 and the negative controls appear darker (**Figure 3.5 F**).

Sequencing analysis identified three unique nanobody sequences—NB2, NB7, and NB21—that exhibited the highest homology (89–93%) to *Camelus dromedarius*, as determined by NCBI BLAST results. These nanobodies were selected for further assays to evaluate their potential as candidates for downstream applications. The amino acid sequences of the selected nanobodies are shown in (**Figure 3.5 G**).

The ligated VHH-pMECS-GG expression vector was transformed into E. coli WK6 cells for the production of soluble nanobodies. Colony PCR confirmed the successful

insertion of VHH sequences in all selected clones (**Figure 3.5 H.1**). His-tagged fusion nanobodies were expressed and purified using nickel affinity chromatography (Ni^{2+}-NTA). Purified fractions were pooled and dialyzed against PBS. SDS-PAGE analysis revealed single bands corresponding to the expected molecular weight of ~15 kDa, confirming successful expression (**Figure 3.5 H.2**). Western blot analysis, performed using anti-His HRP-conjugated antibodies and Ponceau staining, further verified the expression and structural integrity of the purified nanobodies (**Figure 3.5 H.3, H.4**).

The yield of purified nanobodies varied across clones, ranging from 10 to 30 mg per 500 mL of culture. These results highlight the efficient production and purification of ST2-specific nanobody candidates, with high yields and verified quality, enabling their use in subsequent functional evaluations.

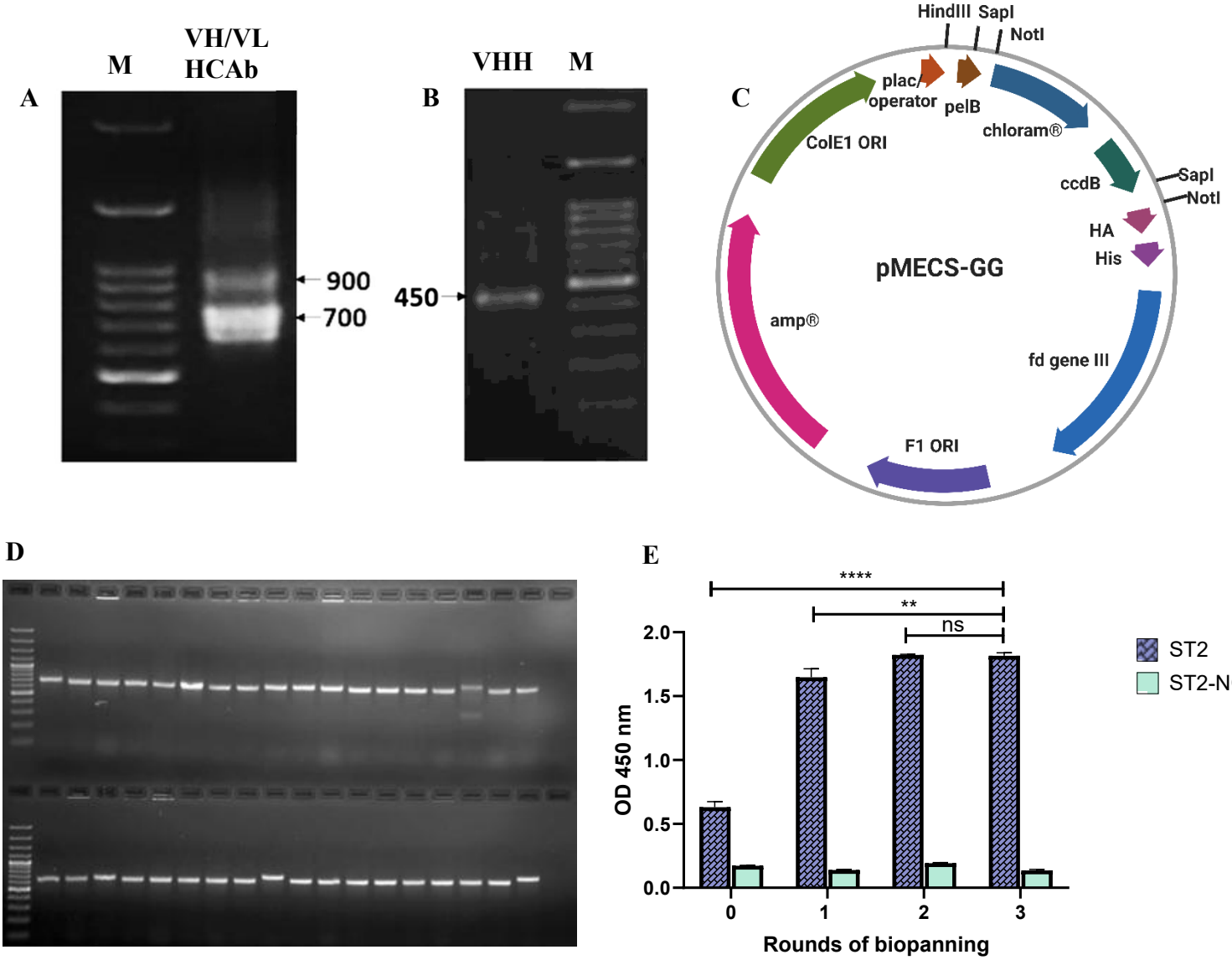
A
M
VH/VL
HCAb
900
700
B
VHH
M
450
C
HindIII
SapI
NotI
plac/
operator
pelB
chloram®
ColE1 ORI
ccdB
SapI
NotI
HA
His
pMECS-GG
amp®
fd gene III
F1 ORI
D
E
****
**
ns
OD 450 nm
2.0
1.5
1.0
0.5
0.0
0
1
2
3
Rounds of biopanning
ST2
ST2-NC
F
A
B
C
D
E
F
G
H
1
2
3
4
5
6
7
8
9
10
11
12
2.0
1.5
1.0
0.5

G

	FR1	CDR1	FR2	CDR2
NB2	QVQLQESGGGSVQAGGSLRLSC	EASAYAYS	MYCIGWFRQAPGKEREGV	AKINTGGAGAGTYYV
NB7	QVQLQESGGGSVQAGGSLRLSC	AASGFTFS	SNYMSWVRQAPGKGLEWX	-XTGIEGDGSITNYA
NB21	QVQLQESGGGSVQAGGSLRLSC	AASGYTYS	TYCLGWFRQRLGKEREGV	XXVIPKSGGGDTYYG

	FR3	CDR3
NB2	DAVKGRFTISQDPAKRTVYLQMNDLKPEDTGIYYCA	ASKPRTHCSATIYALKNDVYHYW
NB7	DSVKGRFTISRDNAKNTLYLQMNSLKSEDTALYYCA	T -GSX-XW - - - - XX - - - - - XSYR
NB21	DSVKGRFTISQDNAKNTVYLQMNDLKPEDTATYYCA	A-DSRSHC- - - - HMMQSYWYNYK

	FR4
NB2	GQGTQVTVSS
NB7	GQGTQVTVSS
NB21	GQGTQVTVSS

H.1

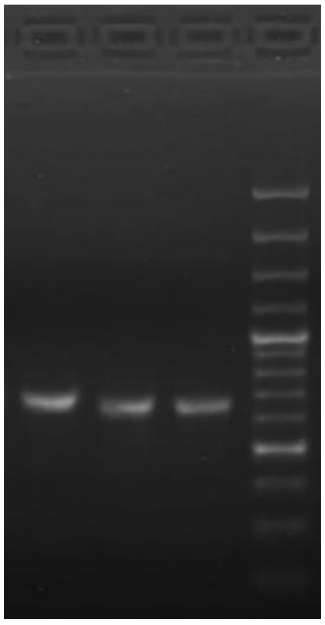

H.2

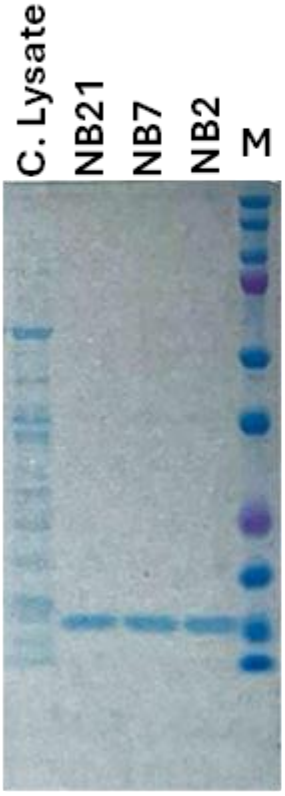

H.3

H.4

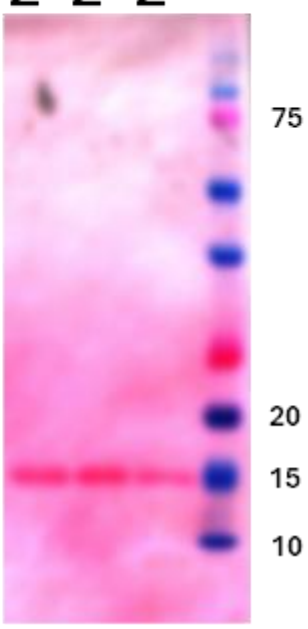

Figure 3.5: Development, Selection and Identification of Anti-ST2 Nanobody Clones

(A)RNA extracted from immunized camel blood was used to synthesize cDNA. Initial PCR amplified ~900 bp VH + VL fragments of conventional antibodies and ~700 bp heavy-chain-only antibody (HCAb) fragments. The 700 bp HCAb product was purified for nested PCR. (B) Nested PCR yielded a single ~450 bp product representing the VHH fragment of HCAb. (C) Schematic of the phagemid vector pMECS-GG used for VHH cloning. Constructs were electroporated into *E. coli* TG1 cells to generate the library. (D) Validation by colony PCR of 36 randomly selected clones confirmed consistent amplification of the VHH fragment. (E) Phage particles displaying VHH fragments were rescued and subjected to three rounds of bio-panning against recombinant human ST2 (3 µg/mL). ELISA demonstrated increased binding in the second and third rounds compared to the original library, with minimal binding to the negative control (ST2-NC), confirming specificity. (F) Heatmap visualization of periplasmic ELISA showed progressively stronger ST2 binding across panning rounds. Lighter colors in Pan2 (B wells) and Pan3 (C, D wells) indicated higher binding affinity, while darker colors in Pan1 (A wells) and negative controls (E–H wells) indicated lower or negligible binding. (G) The amino acid sequences of NB2, NB7, and NB21 were aligned using BLOSUM62 and analyzed for structural features characteristic of camelid nanobodies. (H.1) Colony PCR confirmed successful VHH insertion into *E. coli* WK6 cells. (H.2) Purified His-tagged nanobodies (~15 kDa) were verified by SDS-PAGE. (H.3, H.4) Western blot and Ponceau staining confirmed nanobody expression and structural integrity. Statistical analyses: Two-way comparisons used Student's t-test or Mann-Whitney test for skewed data. ns: non-significant, * $p < 0.05$, ** $p < 0.01$, *** $p < 0.001$, **** $p < 0.0001$. All analyses were performed using GraphPad Prism.

3.6 Binding Specificity, Affinity (KD), and IC_{50} Evaluation of Anti-ST2 Nanobodies

The binding specificity of anti-ST2 nanobodies was evaluated by ELISA against ST2 and a panel of control proteins from the same IL-1 receptor family, including IL-18Rα, IL-36R, IL-1R AcP, and BSA to assess potential cross-reactivity. The results demonstrated that three nanobody clones consistently exhibited significantly higher binding signals to ST2 compared to the control proteins (**Figure 3.6 A**). This strong and selective binding underscores the specificity of these nanobodies for ST2, with minimal off-target interactions, reinforcing their potential as precise candidates for further functional assays and therapeutic development.

The binding affinities of anti-ST2 nanobody clones were evaluated using direct ELISA and dissociation constant (KD) estimation based on the Hill equation. The binding affinities and Hill coefficients (h) were measured at two coating concentrations of ST2 (10 µg/ml and 1 µg/ml) to assess variations in nanobody binding characteristics (**Table 5, Figure 3.6 B**). At 10 µg/ml ST2 coating concentration, NB7 demonstrated the highest affinity with a KD of 9.67 nM (±0.075 SE, 0.75% SE%) and a Hill coefficient of 1.2 (±0.009 SE). This was followed by NB2, with a KD of 63.36 nM (±0.10 SE, 0.16% SE%) and a Hill coefficient of 2.04 (±0.006 SE). NB21 exhibited a KD of 99.9 nM (±0.075 SE, 0.08% SE%) and a Hill coefficient of 1.52 (±0.006 SE), ranking third (**Table 5**). When the ST2 coating concentration was reduced to 1 µg/ml, the binding affinities of the nanobodies shifted. NB7 retained its position as the top-performing nanobody, with a KD of 16.52 nM (±0.036 SE, 0.22% SE%) and a Hill coefficient of 1.62 (±0.013 SE). NB2's affinity decreased significantly to 287.9 nM (±0.132 SE, 0.05% SE%), with a Hill coefficient of 0.86 (±0.006 SE). Similarly, NB21 showed a KD of 289.2 nM (±0.151 SE, 0.05% SE%) and a Hill coefficient of 1.5 (±0.006

SE), ranking lowest under these conditions (**Table 5, Figure 3.6 B**). These results, summarized in Table 5 and illustrated in Figure 3.6, indicate that NB7 consistently demonstrated the highest binding affinity across both coating concentrations, confirming its potential as the most robust candidate for further therapeutic and functional studies.

The competitive ELISA assay evaluated the binding efficiency of anti-ST2 nanobodies by assessing their ability to inhibit the binding of immobilized ST2 in the presence of soluble ST2, with BSA as a negative control (**Table 6, Figure 3.6 C**). NB7 demonstrated the highest potency, with an IC_{50} of 0.1411 µg/mL and a Hill slope of -1.547, followed by NB2 (IC_{50}: 0.4115 µg/mL, slope: -1.271) and NB21 (IC_{50}: 0.4299 µg/mL, slope: -1.548). BSA exhibited minimal competition, serving as a baseline control (IC_{50}: 0.04169 µg/mL). These findings are summarized in (**Table 6**) and visualized in (**Figure 3.6 C)**, highlighting NB7 as the most potent and specific nanobody for ST2 binding.

A

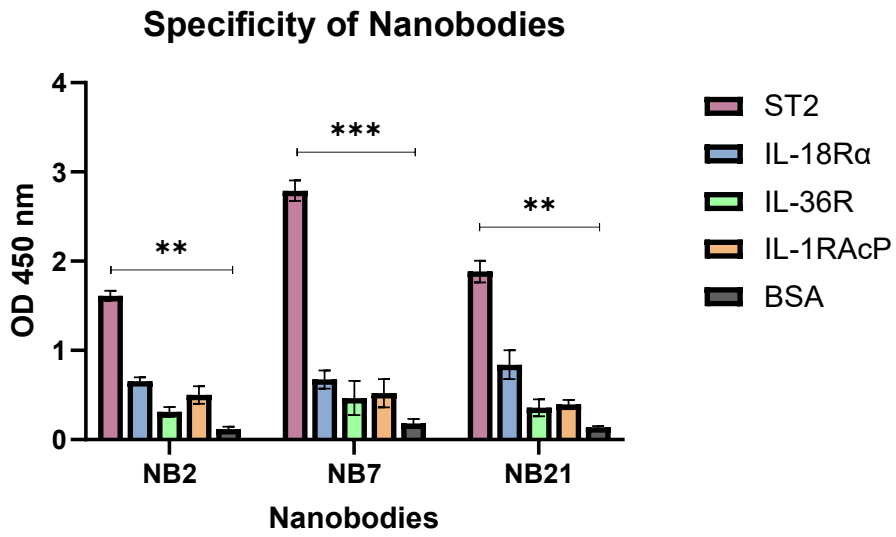

B

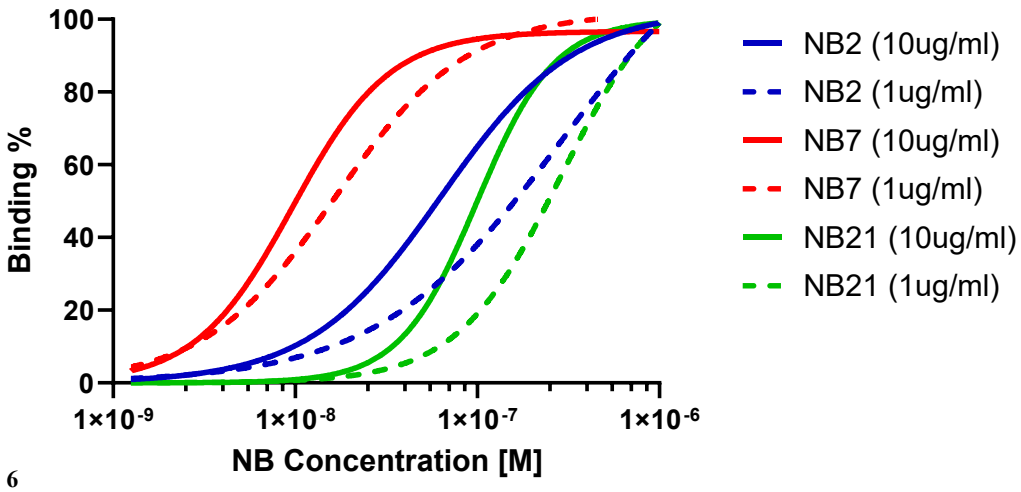

Table 6

Nanobody	Kd (nM)	SE±	SE%	Hill Coeff. (h)	SE ±	SE%	Rank (by Kd)
NB7 (10 µg/ml)	9.67	±0.075	0.75%	1.2	±0.009	0.75%	1st
NB7 (1 µg/ml)	16.52	±0.036	0.22%	1.62	±0.013	0.80%	2nd
NB2 (10 µg/ml)	63.36	±0.10	0.16%	2.04	±0.006	0.29%	3rd
NB21 (10 µg/ml)	99.9	±0.075	0.08%	1.52	±0.006	0.39%	4th
NB2 (1 µg/ml)	287.9	±0.132	0.05%	0.86	±0.006	0.69%	5th
NB21 (1 µg/ml)	289.2	±0.151	0.05%	1.5	±0.006	0.40%	6th

C

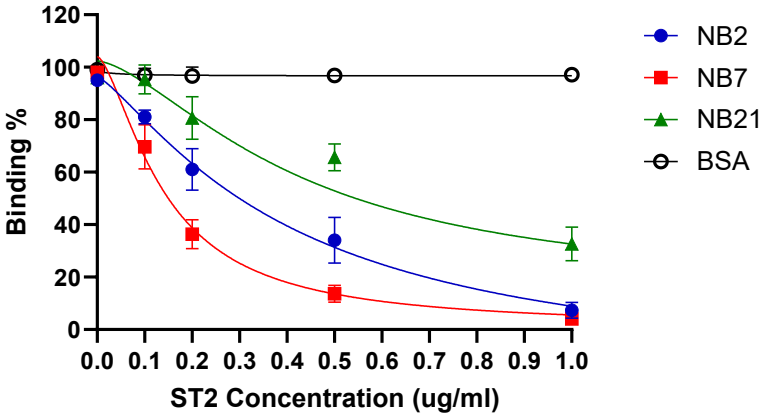

Table 5

Nanobody	IC50 (µg/mL)	Hill Slope
NB2	0.4115	-1.271
NB7	0.1411	-1.547
NB21	0.4299	-1.548
BSA	0.04169	-1.043

Figure 3.6: Binding specificity, affinity, and potency of anti-ST2 nanobodies.

(A) ELISA confirmed the specificity of NB2, NB7, and NB21 for ST2, with minimal cross-reactivity to control proteins (IL-18Rα, IL-36R, IL-1R AcP, BSA). (B) Direct ELISA showed NB7 had the highest binding affinity across ST2 coating concentrations (KD = 9.67 nM at 10 μg/mL; 16.52 nM at 1 μg/mL), followed by NB2 and NB21 (Table 5). (C) Competitive ELISA revealed NB7 as the most potent nanobody (IC_{50} = 0.1411 μg/mL), outperforming NB2 and NB21, with negligible inhibition by BSA (Table 6). Statistical analyses: Two-way comparisons used Student's t-test or Mann-Whitney test for skewed data for specificity and competitive ELISA. Nonlinear regression using the Hill equation for affinity measurements. Data are presented as mean ± SEM (n = 3 technical replicates per assay), and all analyses were performed using GraphPad Prism.

3.7 Functional Evaluation of NB7 in Human Lung Epithelial Cells: Comparable Efficacy to Astegolimab in Blocking ST2 Receptor and Modulating Inflammatory Pathways

After identifying the most promising nanobody candidate (NB7), we investigated its functional effects in a biologically relevant system. Given the critical role of airway epithelial cells in the pathogenesis of inflammatory diseases like asthma (Heijink et al., 2020), it was essential to evaluate NB7's ability to block the ST2 receptor in this cell type. Airway epithelial cells serve as the first line of defence and are pivotal in mediating immune responses through the release of cytokines and chemokines upon stimulation (Heijink et al., 2020).

Before proceeding into these functional experiments, it was crucial to confirm the safety of NB7 on the cells. To ensure that NB7 did not exhibit cytotoxic effects, we conducted a cell viability assay across a range of doses and time points. Primary human lung epithelial cells were treated with NB7 at concentrations of 1 µg/mL, 5 µg/mL, 10 µg/mL, and 50 µg/mL for 24 h, 48 h, and 72 h. Cell viability was normalized to the 0 µg/mL control, which was set as 100% viable. The results demonstrated no significant cytotoxic effects of NB7 at any of the tested concentrations or time points ($P>0.1$), confirming its safety and suitability for further investigation into its therapeutic potential (**Figure 3.7 A**)

To assess the therapeutic potential of NB7, we used primary human lung epithelial cells stimulated with HDM and IL-33. Upon stimulation, ST2 receptor expression was significantly elevated compared to the negative control, as confirmed by immunofluorescence imaging (**Figure 3.7 B**), protein expression analysis (**Figure 3.7 C, D**), and mRNA expression analysis (**Figure 3.7 E**). Protein levels showed a 2-fold increase ($p = 0.0002$),

while mRNA levels exhibited a 4-fold increase ($p < 0.0001$). This robust receptor upregulation provided a suitable platform to evaluate NB7's efficacy.

Treatment with NB7 demonstrated a significant reduction in ST2 receptor activity (2-fold decrease, $p = 0.004$), comparable to the effects observed with astegolimab, a monoclonal antibody targeting ST2 that has shown promise in clinical settings. Notably, no significant difference in efficacy was observed between NB7 and astegolimab ($p = 0.9$), underscoring NB7's potential as a targeted therapeutic agent (**Figure 3.7 C, D**).

Next, we investigated the signalling pathways downstream of the ST2 receptor to understand the molecular effects of NB7 treatment. Specifically, we focused on the MAPK/ERK and NF-κB pathways, critical mediators of inflammation and immune responses in airway epithelial cells. Upon stimulation with HDM and IL-33, both pathways were significantly activated compared to the negative control, as confirmed by Western blot analysis (MAPK/ERK: 5-fold increase, $p < 0.0001$; NF-κB: 7-fold increase, $p < 0.0001$) (**Figure 3.7 F-H**).

NB7 treatment significantly reduced MAPK/ERK activation (3-fold decrease, $p < 0.0001$) compared to untreated stimulated cells. Interestingly, this reduction was more pronounced with NB7 than with astegolimab (2-fold decrease, $p = 0.0004$), suggesting a potentially unique effect of NB7 on the MAPK/ERK pathway. In contrast, NF-κB activation was significantly decreased in both NB7- and astegolimab-treated cells, with no significant difference observed between the two treatments ($p = 0.09$) (**Figure 3.7 F-H**).

From previous studies, it is well-established that ST2 receptor stimulation in epithelial cells induces pro-inflammatory cytokines such as IL-17 and IL-8, which play a pivotal role in asthma pathogenesis (Fujita et al., 2012; H. Wu et al., 2014). To further evaluate NB7's therapeutic potential, we measured the expression levels of these cytokines at both mRNA and protein levels in the cell supernatant.

Stimulation with HDM and IL-33 resulted in significant upregulation of IL-17 (3-fold increase, $p = 0.0002$) and IL-8 (2-fold increase, $p = 0.0002$) at the mRNA level compared to the negative control. Similarly, protein levels in the supernatant were substantially increased, with IL-17 (8-fold increase, $p < 0.0001$) and IL-8 (3-fold increase, $p < 0.0001$) compared to the negative control, confirming pro-inflammatory activation of the epithelial cells (**Figure 3.7 I-J**).

Treatment with NB7 significantly reduced the expression of both cytokines. At the mRNA level, IL-17 decreased by 2-fold ($p =0.01$) and IL-8 by 2-fold ($p =0.02$) compared to the stimulated cells. Protein levels also showed similar reductions, with IL-17 reduced by 5-fold ($p < 0.0001$) and IL-8 by 3-fold ($p <0.0001$). Notably, the effects of NB7 were comparable to those of astegolimab at the mRNA level ($p > 0.05$) but significantly more effective than astegolimab at the protein level ($p =0.03$ and $p = 0.01$) respectively, demonstrating NB7's superior potential (**Figures 3.7 I-J**). These results highlight NB7's ability to effectively suppress key pro-inflammatory mediators downstream of ST2 activation. This further supports its potential as a targeted therapeutic agent for airway inflammation, with performance comparable to or even exceeding that of the monoclonal antibody astegolimab.

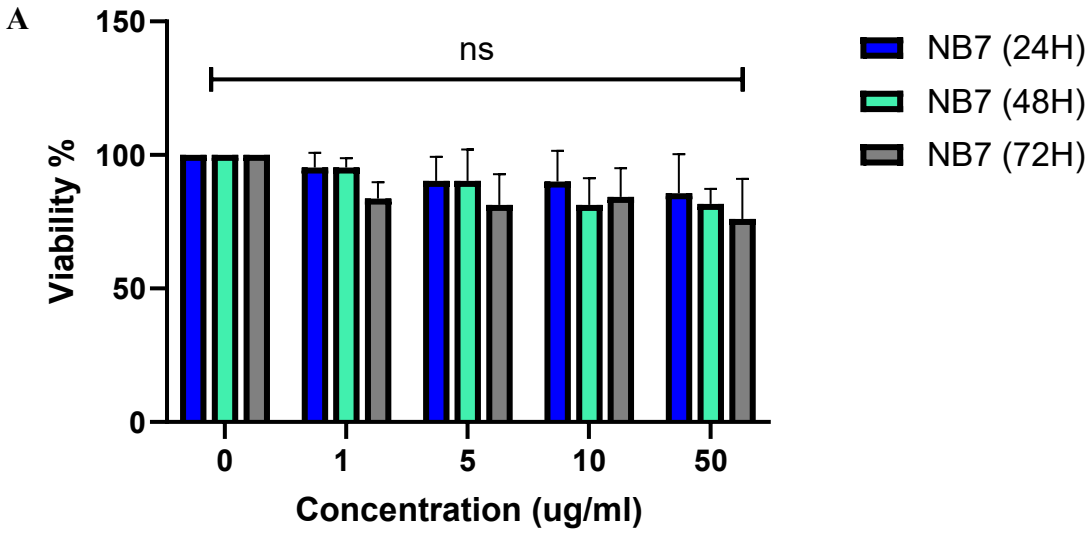
A
150
100
50
0
Viability %
ns
0
1
5
10
50
Concentration (ug/ml)
NB7 (24H)
NB7 (48H)
NB7 (72H)

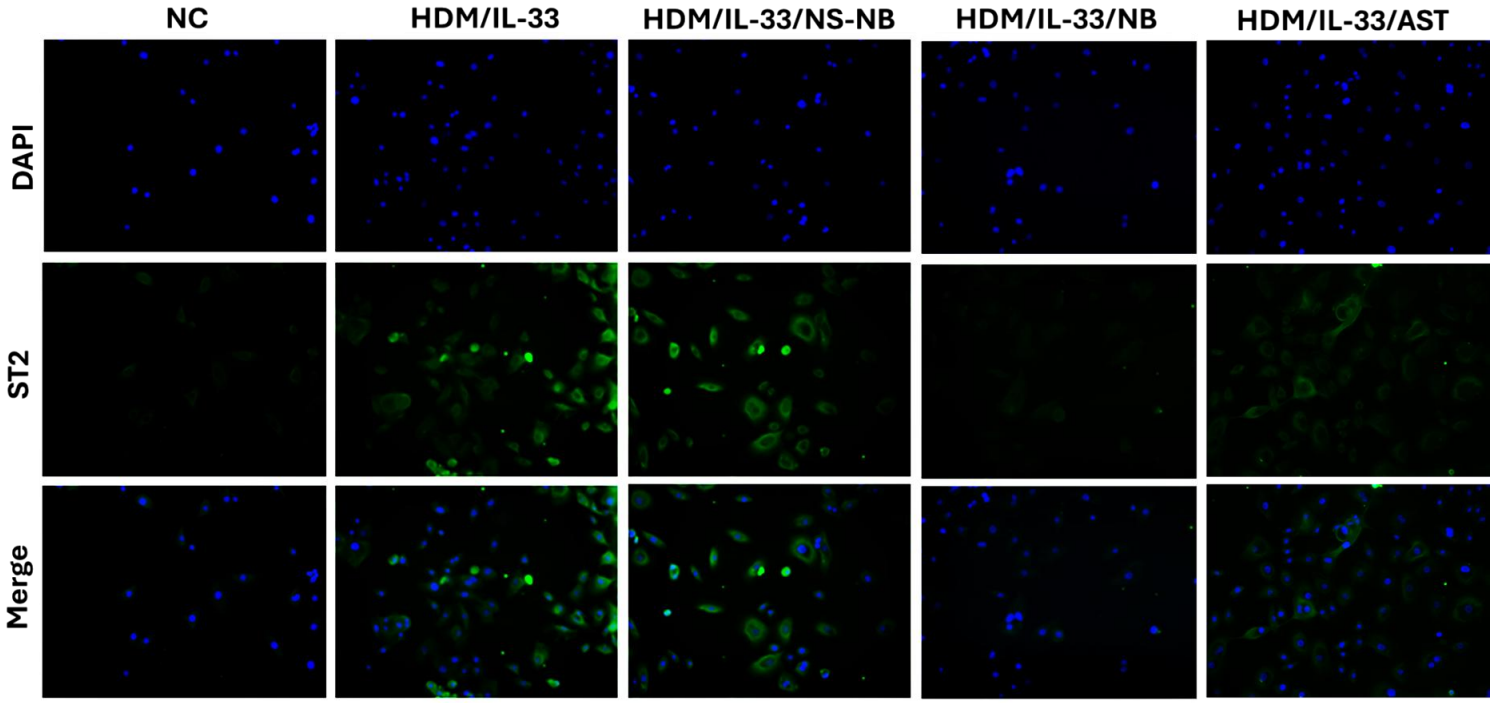
B
NC
HDM/IL-33
HDM/IL-33/NS-NB
HDM/IL-33/NB
HDM/IL-33/AST
DAPI
ST2
Merge

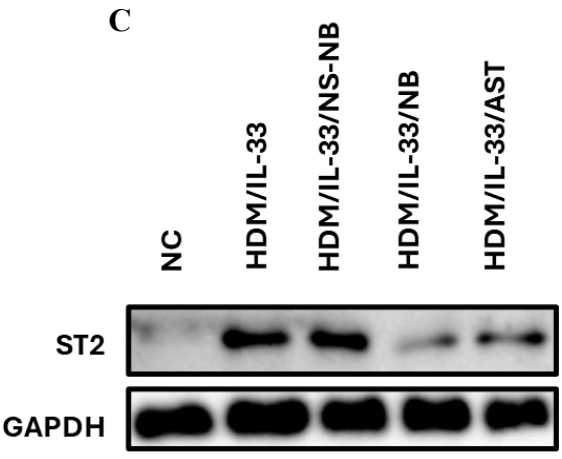
C
NC
HDM/IL-33
HDM/IL-33/NS-NB
HDM/IL-33/NB
HDM/IL-33/AST
ST2
GAPDH

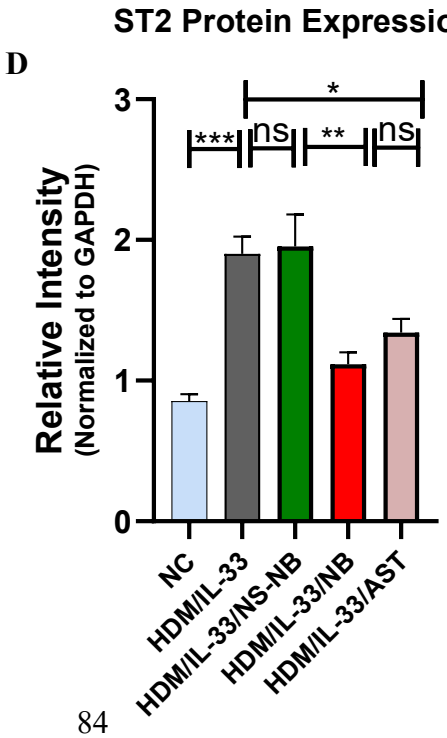
D
ST2 Protein Expression
Relative Intensity
(Normalized to GAPDH)
3
2
1
0
*
***
ns
**
ns
NC
HDM/IL-33
HDM/IL-33/NS-NB
HDM/IL-33/NB
HDM/IL-33/AST

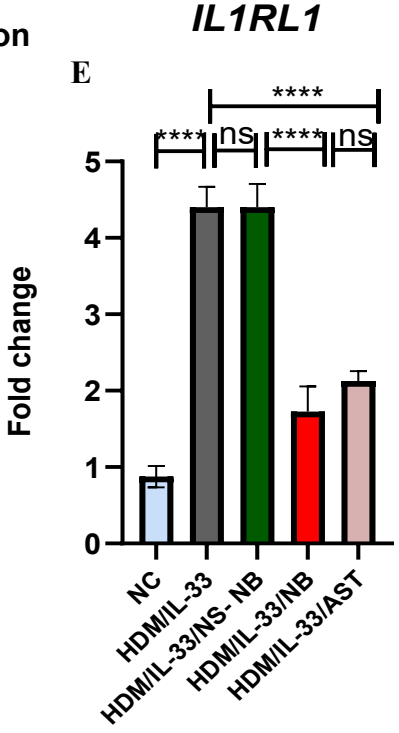
E
IL1RL1
Fold change
5
4
3
2
1
0
****
****
ns
****
ns
NC
HDM/IL-33
HDM/IL-33/NS- NB
HDM/IL-33/NB
HDM/IL-33/AST

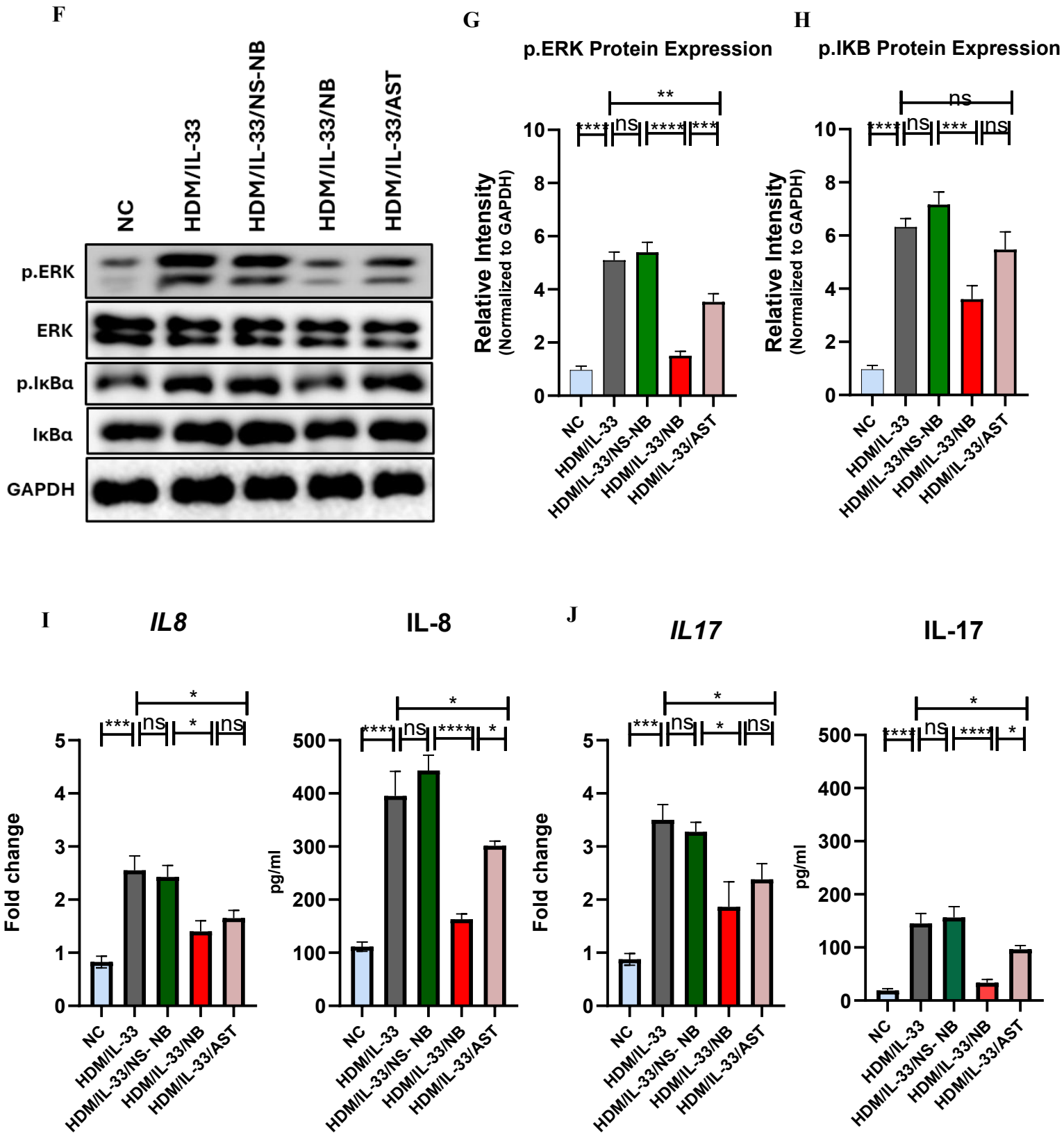
F
NC
HDM/IL-33
HDM/IL-33/NS-NB
HDM/IL-33/NB
HDM/IL-33/AST
p.ERK
ERK
p.IκBα
IκBα
GAPDH
G
p.ERK Protein Expression
Relative Intensity
(Normalized to GAPDH)
H
p.IKB Protein Expression
Relative Intensity
(Normalized to GAPDH)
I
IL8
IL-8
Fold change
pg/ml
J
IL17
IL-17
Fold change
pg/ml

Figure 3.7: Functional evaluation of NB7 in human lung epithelial cells: Comparable efficacy to Astegolimab in blocking ST2 receptor and modulating inflammatory pathways.

(A) CellTiter-Glo® assays confirmed no cytotoxic effects of NB7 (1–50 µg/mL) at 24, 48, and 72 hours. Luminescence was measured using a GloMax® luminometer, with untreated cells (0 µg/mL) serving as the 100% viability control. (B–E) Stimulation with HDM (50 µg/mL) and IL-33 (10 ng/mL) significantly increased ST2 expression at the protein and mRNA levels, assessed by immunofluorescence (Keyence BZ9000 BioRevo, 20× magnification), Western blot (normalized to GAPDH), and qPCR (fold change normalized to 18S). NB7 treatment reduced ST2 expression with efficacy comparable to astegolimab. NB7 at 1 µg/mL, astegolimab at 3 µg/mL as a positive control, or a non-specific nanobody at 1 µg/mL as a negative control. (F–H) Western blot analyses revealed significant activation of MAPK/ERK and NF-κB pathways upon stimulation. NB7 significantly reduced MAPK/ERK and NF-κB activation, with comparable efficacy to astegolimab for NF-κB but superior effects on MAPK/ERK. (I–J) Stimulation increased IL-17 and IL-8 levels in the supernatant, measured by ELISA. NB7 significantly reduced IL-17 and IL-8, outperforming astegolimab in both cases. Statistical Analysis: Two-way comparisons used Student's t-test or Mann-Whitney test for skewed data. Data are presented as mean ± SEM ($n = 3$). ns: non-significant, * $p < 0.05$, ** $p < 0.01$, *** $p < 0.001$, **** $p < 0.0001$. All analyses were performed using GraphPad Prism.

3.8 NB7 Restores GRα/GRβ Balance and Reverses IL-33-Induced Steroid Hypo-responsiveness in Human Bronchial Epithelial Cells

As we have previously shown, IL-33 increased steroid hypo-responsiveness through the dysregulation of GRα and GRβ expression in an HDM-induced asthma mouse model. Building on these findings, we sought to investigate whether a similar effect occurs in human bronchial epithelial cells. This approach aimed to better understand the role of IL-33 in modulating glucocorticoid receptor dynamics in a human-relevant system.

Upon stimulation with HDM and IL-33, GRα, the receptor responsible for mediating glucocorticoid effects, showed a significant 2-fold decrease ($p = 0.01$) at the mRNA level (**Figure 3.8 A**) and a 2-fold decrease ($p = 0.04$) at the protein level (**Figure 3.8 C, E**) in untreated stimulated cells compared to the negative control (NC), reflecting impaired steroid responsiveness. Treatment with NB7 or astegolimab significantly restored GRα expression, with approximately a 2-fold increase ($p < 0.01$) at the mRNA level (**Figure 3.8 A**) and approximately a 5-fold increase ($p < 0.001$) at the protein level, returning GRα levels to those comparable to NC (**Figure 3.8 C, E**).

Conversely, GRβ, the dominant-negative isoform that inhibits glucocorticoid signalling, was significantly upregulated in untreated stimulated cells, showing approximately a 2-fold increase ($p = 0.007$) at the mRNA level (**Figure 3.8 B**) and approximately a 2-fold increase ($p = 0.0015$) at the protein level compared to NC (**Figure 3.8 D, E**). This overexpression of GRβ further exacerbates the steroid-resistant environment induced by IL-17 and IL-8. Both NB7 and astegolimab treatments significantly reduced GRβ expression, with approximately a 2-fold decrease ($p = 0.01$) at the mRNA level (**Figure 3.8 B**) and approximately a 3-fold decrease ($p = 0.03$) at the protein level compared to untreated stimulated cells, mitigating the inhibitory effects of GRβ (**Figure 3.8 D, E**).

At the mRNA level, the GRα/GRβ ratio, a critical determinant of glucocorticoid responsiveness, was significantly reduced by approximately a 5-fold ($p = 0.001$) in untreated stimulated cells compared to NC (**Figure 3.8 C**). Both NB7 and astegolimab treatments restored the GRα/GRβ ratio, with NB7 and astegolimab showing approximately a 5-fold increase ($p < 0.001$) compared to untreated stimulated cells, bringing the ratio back to near-normal levels (**Figure 3.8 C**).

These findings confirm the steroid hypo-responsiveness effect of IL-33, which was effectively reversed upon treatment with anti-ST2 nanobody therapy. **Notably, treatment with NB7 demonstrated promising results, achieving comparable efficacy to astegolimab while using a dose three times lower.** NB7 not only suppressed IL-17 and IL-8 production but also effectively restored the balance of glucocorticoid receptors, highlighting its therapeutic potential in reversing steroid-resistant airway inflammation.

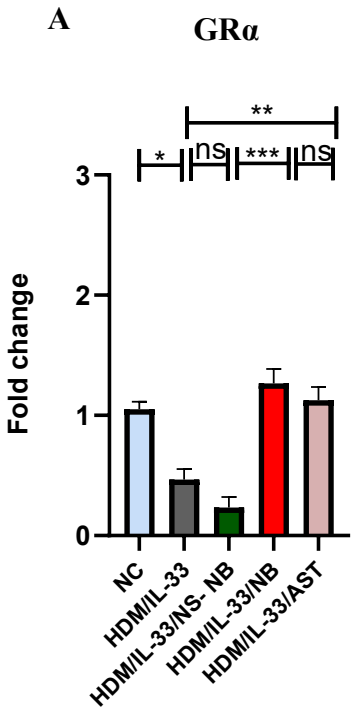
A
GRα
Fold change
NC
HDM/IL-33
HDM/IL-33/NS- NB
HDM/IL-33/NB
HDM/IL-33/AST

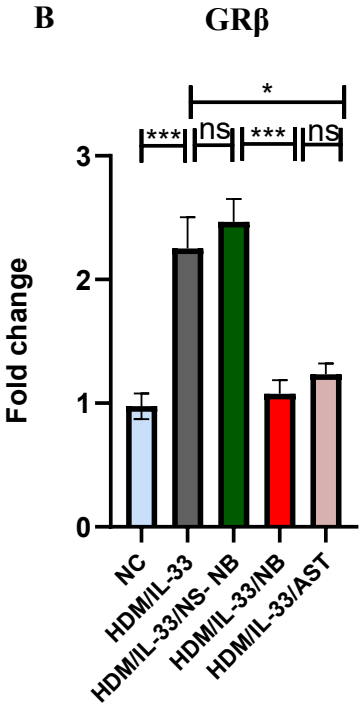
B
GRβ
Fold change
NC
HDM/IL-33
HDM/IL-33/NS- NB
HDM/IL-33/NB
HDM/IL-33/AST

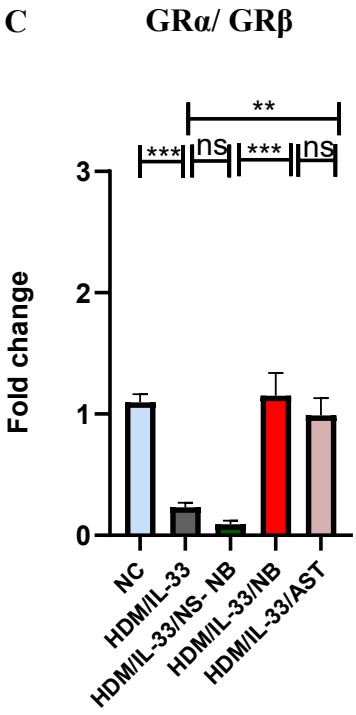
C
GRα/ GRβ
Fold change
NC
HDM/IL-33
HDM/IL-33/NS- NB
HDM/IL-33/NB
HDM/IL-33/AST

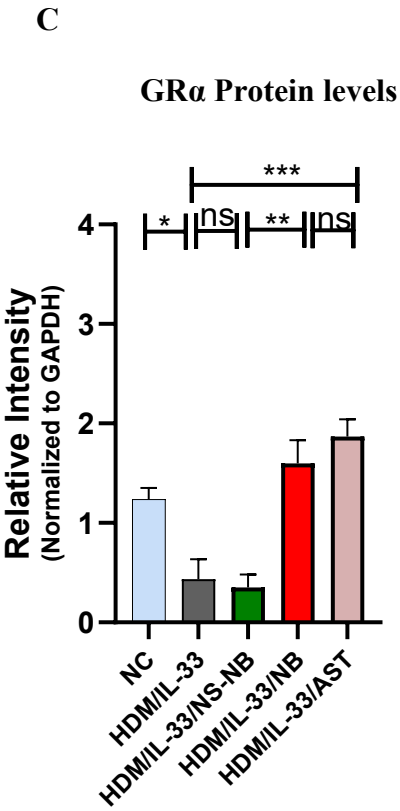
C
GRα Protein levels
Relative Intensity
(Normalized to GAPDH)
NC
HDM/IL-33
HDM/IL-33/NS-NB
HDM/IL-33/NB
HDM/IL-33/AST

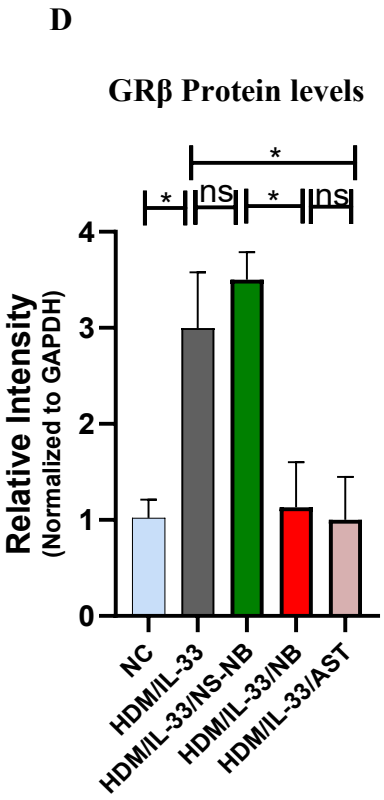
D
GRβ Protein levels
Relative Intensity
(Normalized to GAPDH)
NC
HDM/IL-33
HDM/IL-33/NS-NB
HDM/IL-33/NB
HDM/IL-33/AST

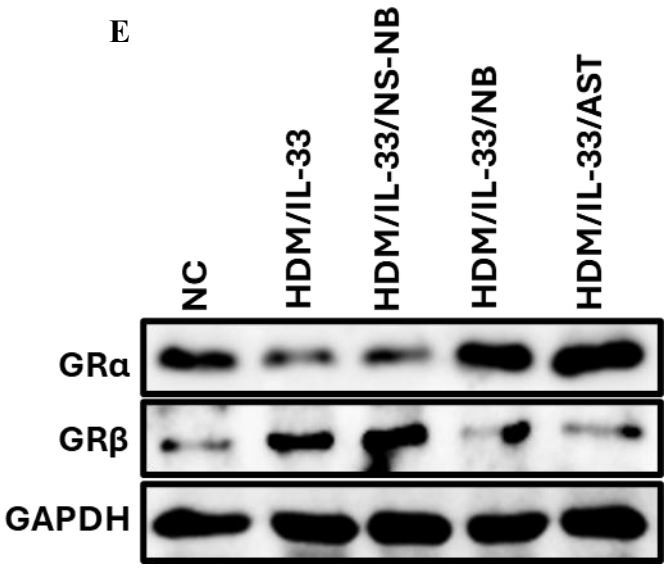
E
NC
HDM/IL-33
HDM/IL-33/NS-NB
HDM/IL-33/NB
HDM/IL-33/AST
GRα
GRβ
GAPDH

Figure 3.8: NB7 restores glucocorticoid receptor (GR) balance in human lung epithelial cells.

(A, C, E) GRα expression, reduced in untreated stimulated cells (HDM + IL-33), was restored by NB7 and astegolimab at both mRNA (qPCR normalized to 18S) and protein levels (Western blot normalized to GAPDH). (B, D, E) GRβ expression, elevated in untreated stimulated cells, was significantly reduced by NB7 and astegolimab at both mRNA and protein levels. (C) The GRα/GRβ ratio, decreased in untreated stimulated cells, was normalized by NB7 and astegolimab, as confirmed by qPCR. Statistical Analysis: Two-way comparisons used Student's t-test or Mann-Whitney test for skewed data. Data are presented as mean ± SEM (n = 3). ns: non-significant, * $p < 0.05$, ** $p < 0.01$, *** $p < 0.001$, **** $p < 0.0001$. All analyses were performed using GraphPad Prism.

3.9 Intranasal Delivery of NB7 Demonstrates Superior Efficacy in Reducing Airway Inflammation, Hyperresponsiveness, and Cytokine Levels, Outperforming Astegolimab in an HDM/IL-33 Asthma Mouse Model

Building on the promising *in vitro* findings with human lung epithelial cells, we next aimed to evaluate the efficacy of NB7 *in vivo*. To achieve this, we tested NB7 in the same HDM-induced asthma mouse model as schematically represented in (**Figure 3.9 A**), directly comparing its effects to those of astegolimab. This approach allowed us to assess the therapeutic potential of NB7 in a physiologically relevant setting, providing critical insights into its ability to modulate airway inflammation and steroid hypo-responsiveness *in vivo*.

The efficiency of the intranasal delivery of NB7 was first confirmed by demonstrating its presence in lung tissue over time using Western blot analysis. NB7 levels were high at 24 hours, moderate at 48 hours, and significantly reduced by 72 hours, suggesting that a dosing interval of every 48 hours is sufficient to maintain its presence in the lung tissue (**Figure 3.9 B**). Building on this, we examined the impact of NB7 on airway inflammation. Histological analysis showed that NB7 significantly reduced peri-bronchial and perivascular inflammation (3-fold decrease, $p < 0.0001$) compared to the untreated asthma group, outperforming astegolimab (1.5-fold decrease, $p = 0.01$) (**Figure 3.9 C, F**). This reduction in inflammation was accompanied by decreased mucus production, where NB7 reduced goblet cell hyperplasia and mucus accumulation by 6-fold ($p < 0.0001$), again exceeding the effect of astegolimab (2-fold decrease, $p <0.0001$) (**Figure 3.9 D, G**).

To further explore the inflammatory response, BALF was analyzed for immune cell infiltration and cytokine levels. Total inflammatory cell counts in BALF were also significantly decreased with NB7 treatment (3-fold reduction, $p < 0.0001$) compared to astegolimab (1.5-fold reduction, $p =0.0012$) (**Figure 3.9 E, H**). NB7 significantly reduced

eosinophil and neutrophil counts by 4.1-fold ($p < 0.001$) and 6-fold ($p < 0.0001$), respectively, compared to the untreated group, while astegolimab achieved a significant reduction in neutrophil counts 2-fold ($p < 0.0001$) but showed no significant effect on eosinophil counts ($p=0.9$) (**Figure 3.9 I-K**).

Cytokine analysis revealed elevated levels of IL-4, IL-5, IL-13, and IL-17 in the untreated group, which were significantly reduced by NB7 at both mRNA and protein levels. NB7 treatment resulted in reductions of 3.5-fold for IL-4 ($p < 0.0001$), 3-fold for IL-5 ($p = 0.0004$), 5-fold for IL-13 ($p < 0.0001$), and 8-fold for IL-17 ($p < 0.0001$) at the mRNA level. Similarly, at the protein level, NB7 reduced cytokine levels by 5-fold for IL-4 ($p < 0.0001$), 4-fold for IL-5 ($p <0.0001$), 5-fold for IL-13 ($p <0.0001$), and 5-fold for IL-17 ($p <0.0001$) (**Figure 3.9 M, N**).

Astegolimab also reduced these cytokines but to a lesser extent. At the mRNA level, astegolimab achieved reductions of 1.3-fold for IL-4 ($p = 0.02$), no significant change for IL-5 ($p = 0.7$), 2-fold for IL-13 ($p < 0.0001$), and 2-fold for IL-17 ($p = 0.0004$). At the protein level, astegolimab showed decreases of 2-fold for IL-4 ($p = 0.08$), 2-fold for IL-5 ($p = 0.03$), 2-fold for IL-13 ($p = 0.0005$), and 2-fold for IL-17 ($p = 0.01$) (**Figure 3.9 M, N**).

Functional improvements in lung mechanics were assessed using FlexiVent. NB7 treatment significantly reduced airway resistance by 6-fold ($p < 0.0001$), demonstrating superior efficacy compared to astegolimab, which reduced airway resistance by 3-fold ($p = 0.006$) (**Figure 3.9 L**). These functional improvements align with molecular findings, as shown in the subsequent figures, providing further support for the efficacy of NB7 in modulating key pathways involved in airway inflammation and mechanics.

NB7 demonstrated superior efficacy compared to astegolimab in reducing airway inflammation, mucus production, and pro-inflammatory cytokine levels, while significantly

improving lung mechanics. These findings underscore the therapeutic potential of NB7 delivered intranasally for addressing steroid hypo-responsiveness in asthma.

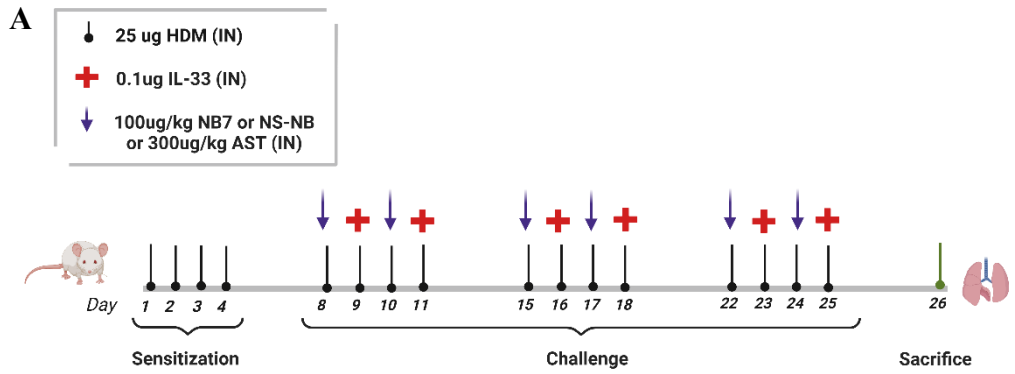
A
25 ug HDM (IN)
0.1ug IL-33 (IN)
100ug/kg NB7 or NS-NB
or 300ug/kg AST (IN)
Day
1 2 3 4
8 9 10 11
15 16 17 18
22 23 24 25
26
Sensitization
Challenge
Sacrifice

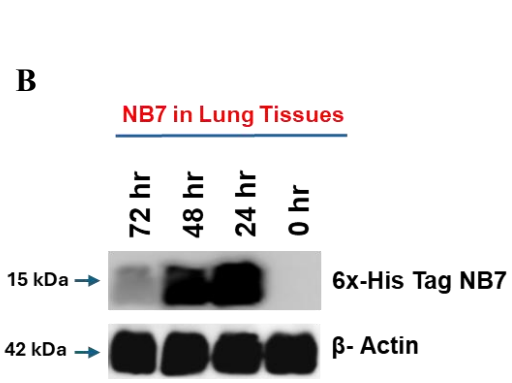
B
NB7 in Lung Tissues
72 hr
48 hr
24 hr
0 hr
15 kDa
6x-His Tag NB7
42 kDa
β- Actin

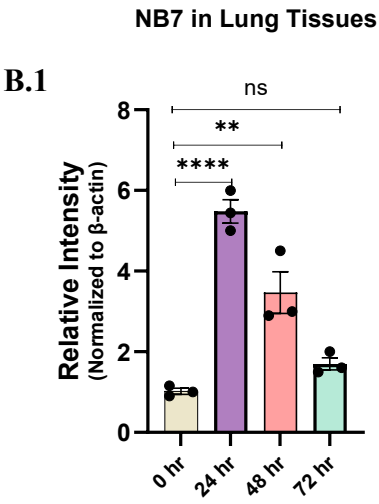
NB7 in Lung Tissues
B.1
ns
**
****
Relative Intensity
(Normalized to β-actin)
0
2
4
6
8
0 hr
24 hr
48 hr
72 hr

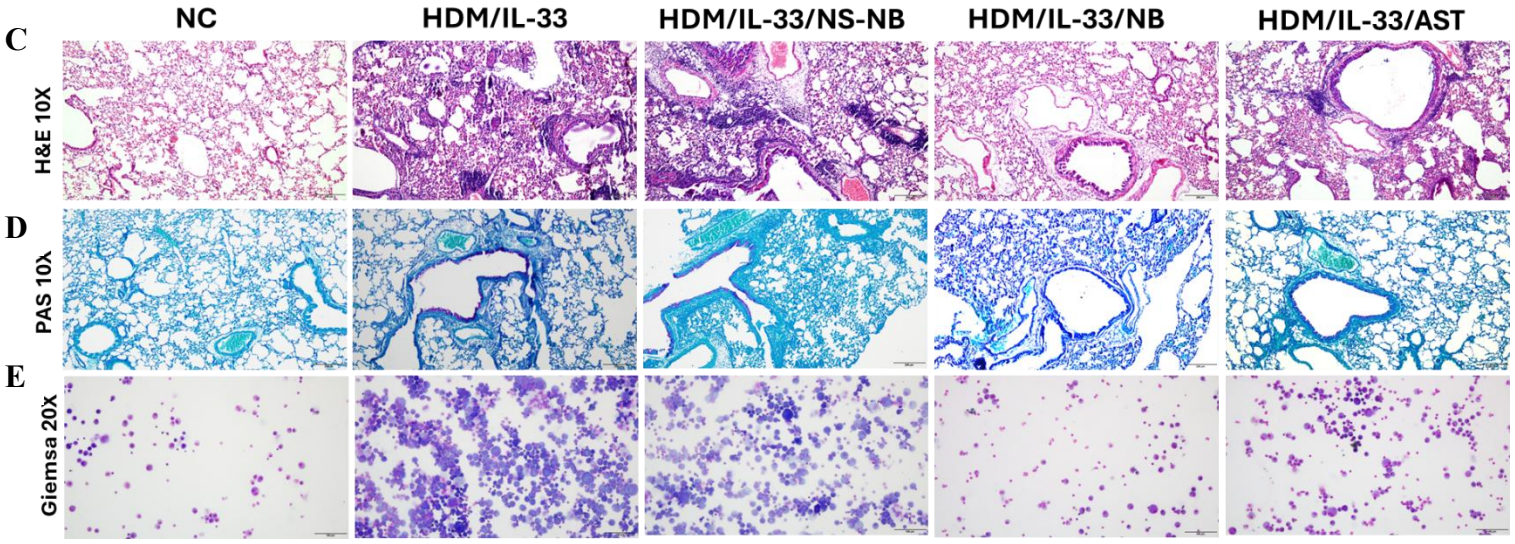
C
NC
HDM/IL-33
HDM/IL-33/NS-NB
HDM/IL-33/NB
HDM/IL-33/AST
H&E 10X
D
PAS 10X
E
Giemsa 20X

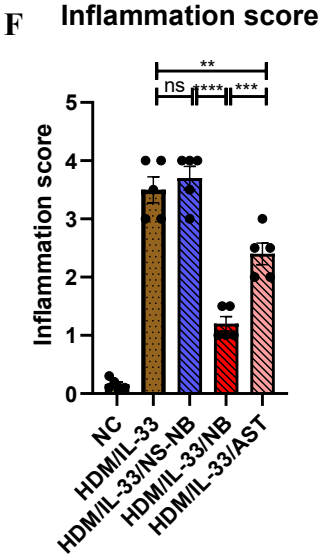
F
Inflammation score
Inflammation score
0
1
2
3
4
5
**
ns
****
***
NC
HDM/IL-33
HDM/IL-33/NS-NB
HDM/IL-33/NB
HDM/IL-33/AST

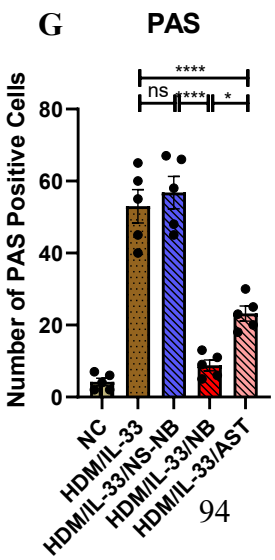
G
PAS
Number of PAS Positive Cells
0
20
40
60
80
****
ns
***
*
NC
HDM/IL-33
HDM/IL-33/NS-NB
HDM/IL-33/NB
HDM/IL-33/AST

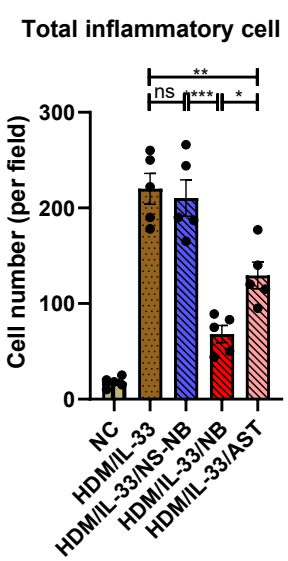
H
Total inflammatory cell count
Cell number (per field)
0
100
200
300
**
ns
***
*
NC
HDM/IL-33
HDM/IL-33/NS-NB
HDM/IL-33/NB
HDM/IL-33/AST

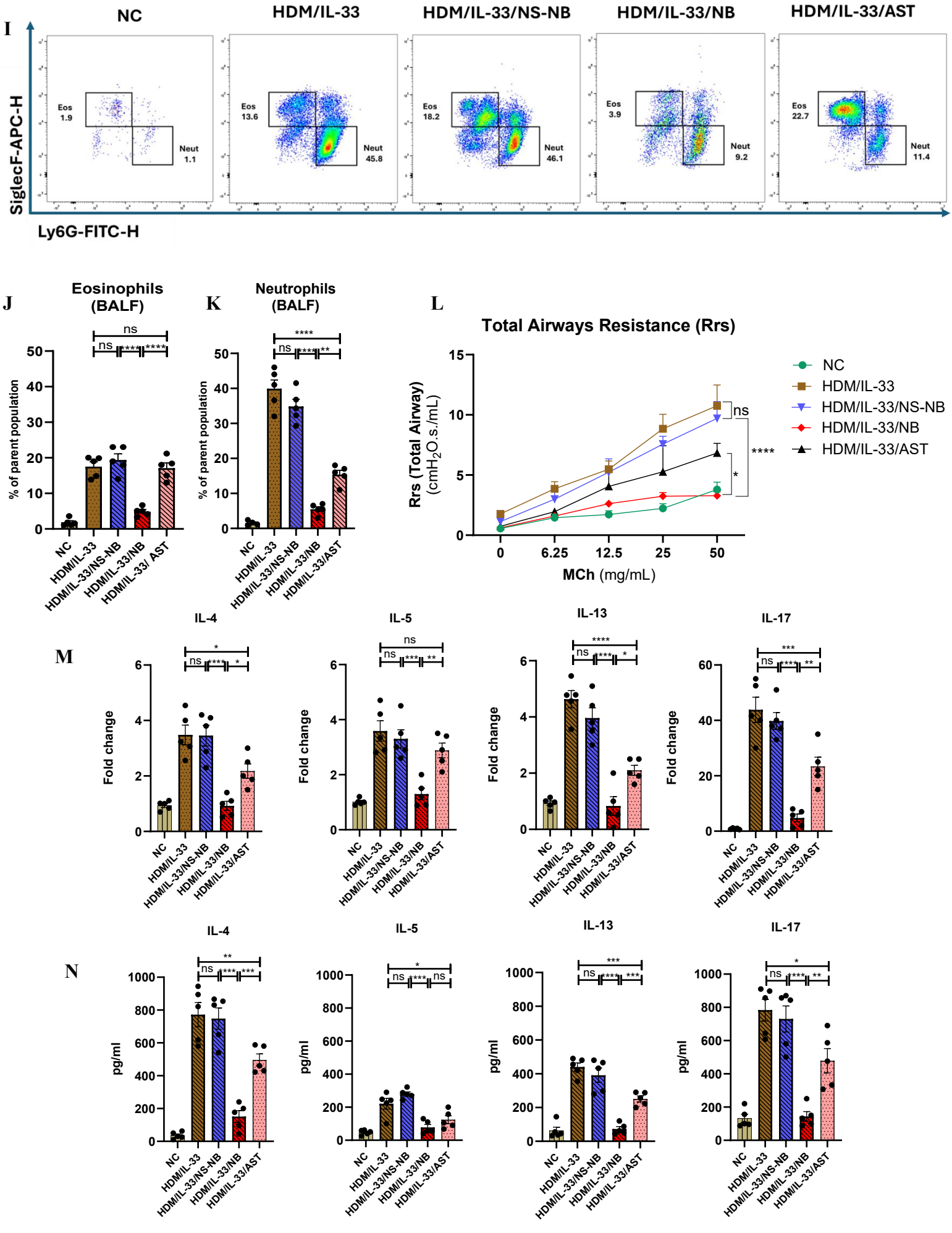
I
NC
HDM/IL-33
HDM/IL-33/NS-NB
HDM/IL-33/NB
HDM/IL-33/AST
SiglecF-APC-H
Ly6G-FITC-H
Eos 1.9
Neut 1.1
Eos 13.6
Neut 45.8
Eos 18.2
Neut 46.1
Eos 3.9
Neut 9.2
Eos 22.7
Neut 11.4
J
Eosinophils (BALF)
% of parent population
K
Neutrophils (BALF)
% of parent population
L
Total Airways Resistance (Rrs)
Rrs (Total Airway) (cmH2O.s./mL)
MCh (mg/mL)
M
IL-4
IL-5
IL-13
IL-17
Fold change
N
IL-4
IL-5
IL-13
IL-17
pg/ml

Figure 3.9: Intranasal delivery of NB7 demonstrates superior efficacy in reducing airway inflammation, immune responses, and airway hyperresponsiveness in an HDM/IL-33 asthma mouse model.

(A) Experimental protocol showing intranasal administration of NB7 (100 μg/kg) or astegolimab (300 μg/kg), delivered twice a week before each IL-33 stimulation. The nonspecific nanobody (Nb-ns) group received a control nanobody (100 μg/kg) on the same schedule. (B) Western blot analysis confirmed NB7 delivery to lung tissue, with high levels detected at 24 hours, moderate levels at 48 hours, and reduced levels by 72 hours, supporting a 48-hour dosing interval. (B.1) Relative intensity was normalized to β-actin. (C, F) H&E staining showed NB7 significantly reduced peri-bronchial and perivascular inflammation (0–4 scale) compared to untreated mice, outperforming astegolimab. (D, G) PAS staining demonstrated decreased goblet cell hyperplasia and mucus accumulation in NB7-treated mice, with greater efficacy than astegolimab (per visual field). (E, H) Giemsa staining revealed significant reductions in total inflammatory cell counts in BALF with NB7 treatment, outperforming astegolimab (per visual field). (I–K) Flow cytometry showed that NB7 reduced both eosinophil and neutrophil counts in BALF, while astegolimab primarily reduced neutrophils without significantly affecting eosinophils. Data were analyzed using FlowJo. (M, N) Cytokine analysis in lung tissue and BALF showed that NB7 reduced IL-4, IL-5, IL-13, and IL-17 at both mRNA (qPCR normalized to β-actin) and protein (ELISA) levels, with higher efficacy compared to astegolimab. (L) FlexiVent analysis showed NB7 significantly reduced airway resistance, demonstrating greater efficacy than astegolimab. Statistical Analysis: Two-way comparisons used Student's t-test or Mann-Whitney test for skewed data; multiple group comparisons used two-sided ANOVA with post hoc Bonferroni tests. Data are presented as mean ± SEM (n = 5). ns: non-significant, * $p < 0.05$, ** $p < 0.01$, *** $p < 0.001$, **** $p < 0.0001$. All analyses were performed using GraphPad Prism.

3.10 NB7 Inhibits ST2 Expression and Suppresses MAPK/ERK and NF-κB Pathways, Showing Greater Efficacy Than Astegolimab in an HDM/IL-33 Asthma Model

After demonstrating the efficacy of NB7, we further investigated its mechanism of action by examining its ability to inhibit ST2 expression and downstream signalling pathways in lung tissues. Immunohistochemistry (IHC) and Western blot analysis revealed that NB7 effectively inhibited ST2 expression in lung tissues, showing a 6-fold reduction ($p < 0.0001$) compared to the untreated group, with results comparable to those observed with astegolimab (6-fold reduction, $p < 0.0001$) (**Figure 3.10 A-D**). This confirms that NB7 successfully targets and blocks the ST2 receptor, a key driver of IL-33-mediated inflammation.

Building on these findings, we explored the impact of NB7 on the activation of downstream inflammatory signaling pathways. NB7 significantly inhibited the activation of the MAPK/ERK pathway, reducing phosphorylation levels by 6-fold ($p < 0.0001$) compared to the untreated group. In contrast, astegolimab exhibited a 3-fold reduction ($p <0.0001$) (**Figure 3.10 E, F**). Additionally, NB7 showed superior inhibition of NF-κB activation, with a 4-fold reduction in phosphorylation levels ($p < 0.0001$) compared to the untreated group, while astegolimab showed no significant effect ($p = 0.9$) (**Figure 3.10 E, G**).

These results provide deeper mechanistic insights into the anti-inflammatory effects of NB7, highlighting its ability to not only block ST2 receptor expression but also effectively suppress key signalling pathways that drive airway inflammation. This further supports its therapeutic potential as a targeted treatment for steroid-hyporesponsive asthma.

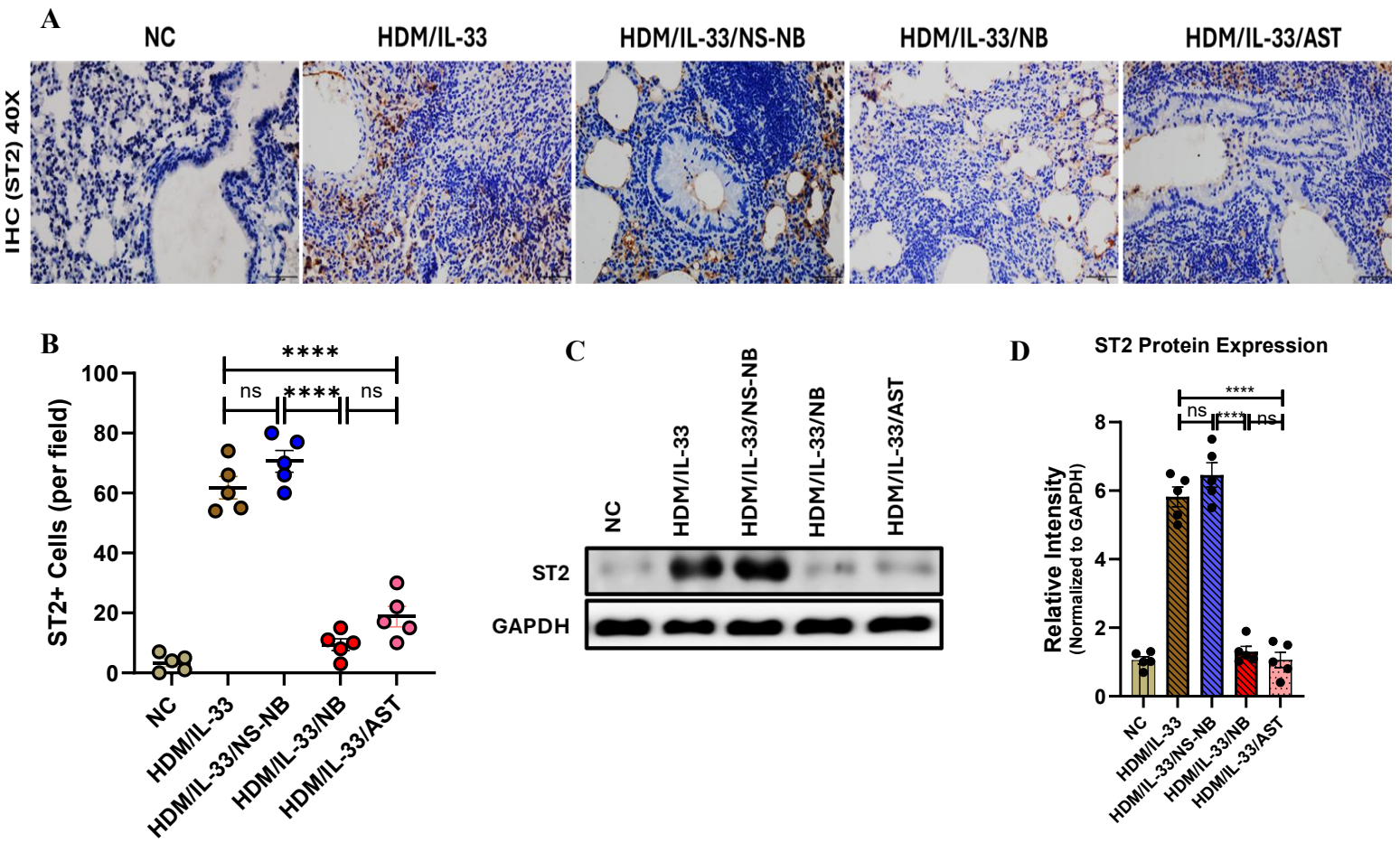
A
NC
HDM/IL-33
HDM/IL-33/NS-NB
HDM/IL-33/NB
HDM/IL-33/AST
IHC (ST2) 40X
B
ST2+ Cells (per field)
****
ns
****
ns
NC
HDM/IL-33
HDM/IL-33/NS-NB
HDM/IL-33/NB
HDM/IL-33/AST
C
NC
HDM/IL-33
HDM/IL-33/NS-NB
HDM/IL-33/NB
HDM/IL-33/AST
ST2
GAPDH
D
ST2 Protein Expression
Relative Intensity
(Normalized to GAPDH)
E
NC
HDM/IL-33
HDM/IL-33/NS-NB
HDM/IL-33/NB
HDM/IL-33/AST
p.ERK
ERK
p.IκBα
IκBα
GAPDH
F
p.ERK Protein Expression
Relative Intensity
(Normalized to GAPDH)
G
p.IKB Protein Expression
Relative Intensity
(Normalized to GAPDH)

Figure 3.10: NB7 inhibits ST2 expression and suppresses MAPK/ERK and NF-κB pathways with greater efficacy than Astegolimab in an HDM/IL-33 asthma model.

(A–D) Immunohistochemistry (40×, scale bar = 50 μm) and Western blot analysis demonstrated that NB7 effectively inhibited ST2 expression in lung tissues, achieving levels comparable to astegolimab. (E, F) Western blot analysis revealed that NB7 significantly reduced MAPK/ERK pathway activation, showing greater efficacy than astegolimab. (E, G) NB7 also suppressed NF-κB activation (phosphorylated IκBα), while astegolimab exhibited minimal effects. Statistical Analysis: Western blot relative intensity was normalized to GAPDH using ImageJ. Two-way comparisons used Student's t-test or Mann-Whitney test

3.11 NB7 Restores GRα/GRβ Balance and Reverses Steroid Hypo-responsiveness in an HDM/IL-33 Asthma Model, Surpassing Astegolimab

Building on these findings, we sought to investigate the downstream effects of NB7 treatment on glucocorticoid receptor dynamics, we aimed to assess whether NB7 could restore this balance.

At the mRNA level, NB7 significantly improved the GRα/GRβ ratio by a 6-fold increase ($p < 0.0001$) compared to the untreated group, outperforming astegolimab, which showed no significant change ($p = 0.2$) (**Figure 3.11 A-C**). At the protein level, NB7 restored GRα levels with a 6-fold increase ($p < 0.0001$) compared to the untreated group, exceeding the effects of astegolimab, which showed no significant change ($p = 0.1$) (**Figure 3.11 D, F**). Conversely, NB7 significantly reduced GRβ protein levels by a 6-fold decrease ($p < 0.0001$), demonstrating superior efficacy compared to astegolimab, which showed no significant change ($p = 0.2$) (**Figure 3.11 E, F**).

These results underscore NB7's superior ability to restore the GRα/GRβ balance, further supporting its potential to reverse steroid hypo-responsiveness in asthma, even at a dose three times lower than astegolimab.

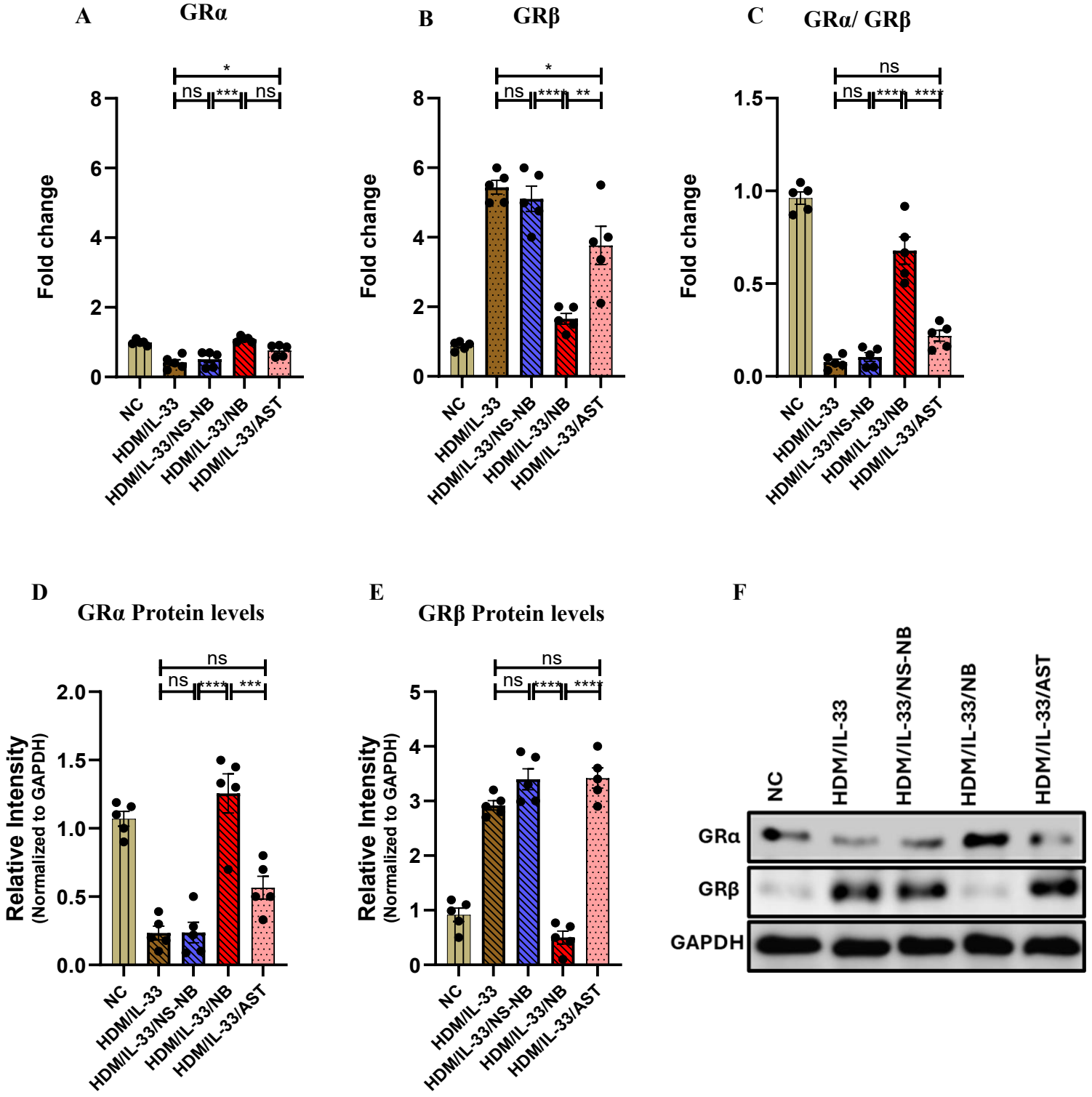
A
GRα
Fold change
B
GRβ
Fold change
C
GRα/ GRβ
Fold change
NC
HDM/IL-33
HDM/IL-33/NS-NB
HDM/IL-33/NB
HDM/IL-33/AST
D
GRα Protein levels
Relative Intensity
(Normalized to GAPDH)
E
GRβ Protein levels
Relative Intensity
(Normalized to GAPDH)
F
GRα
GRβ
GAPDH

Figure 3.11: NB7 restores GRα/GRβ balance and reverses steroid hypo-responsiveness, surpassing Astegolimab in an HDM/IL-33 asthma model.

(A–C) qPCR analysis demonstrated that NB7 significantly improved the GRα/GRβ ratio at the mRNA level (normalized to β-actin), outperforming astegolimab. (D–F) Western blot analysis showed that NB7 restored GRα protein levels (normalized to GAPDH) and reduced GRβ protein levels, exhibiting greater efficacy compared to astegolimab, which showed no significant changes. Statistical Analysis: Relative intensity was calculated using ImageJ. Two-way comparisons used Student's t-test or Mann-Whitney test

4. Discussion

This study highlights the pivotal role of IL-33/ST2 signalling in severe asthma, linking it to airway inflammation, mucus overproduction, and steroid hypo-responsiveness via MAPK/ERK and NF-κB activation and GR dysregulation. We developed and identified NB7, a novel anti-ST2 nanobody, as a highly effective therapeutic candidate. NB7 significantly reduced inflammation, cytokine production, and mucus hypersecretion, restored GRα/GRβ balance, and improved steroid responsiveness, outperforming astegolimab both *in vitro* and *in vivo*. These findings establish NB7 as a promising and cost-effective treatment for IL-33/ST2-driven asthma **(Figure 4.1).**

Our study emphasizes the critical involvement of IL-33/ST2 signalling in the pathogenesis of severe asthma. Through *in silico* analysis, we identified a significant upregulation of ST2 expression in airway samples from patients with moderate and severe asthma, with the most pronounced increase observed in severe cases. This finding highlights a strong correlation between ST2 expression and disease severity, reinforcing its role as a key driver of airway inflammation and asthma progression.

These findings are consistent with studies by Prefontaine et al. (Prefontaine et al., 2009) and Kearley et al. (Kearley et al., 2015), which demonstrated a direct link between increased IL-33/ST2 activation and asthma severity. Moreover, our observations align with evidence from chronic obstructive pulmonary disease (COPD) research (Kearley et al., 2015), which implicates maladaptive IL-33/ST2 signalling in recurrent infections, tissue damage, and lung function decline.

To explore the role of IL-33 in steroid hypo-responsiveness, we developed a novel chronic HDM-induced asthma mouse model and stimulated it with IL-33. The critical role of IL-33/ST2 signalling in steroid hypo-responsiveness was further demonstrated by our

findings on dexamethasone (DEX) treatment, aligning with previous studies that connect this pathway to glucocorticoid hypo-responsiveness (Prefontaine et al., 2009). The diminished efficacy of DEX in the HDM/IL-33 group, despite its effectiveness in the HDM-only group, highlights the role of IL-33 signalling in driving glucocorticoid hypo-responsiveness. IL-33-stimulated mice exhibited persistently high inflammatory cell counts in BALF, along with sustained lung inflammation and mucus production, despite dexamethasone administration. These observations suggest that IL-33 creates an inflammatory environment that is less susceptible to glucocorticoid control, likely through dysregulation of glucocorticoid receptor expression. Consistent with studies by Barnes et al. (Barnes & Adcock, 2009) and Corrigan, C. J., et al. (Corrigan & Loke, 2007), we observed a substantial reduction in GRα expression and an upregulation of GRβ, shifting the GRα/GRβ ratio toward GRβ dominance. The dominance of GRβ has been associated with glucocorticoid hypo-responsiveness in asthma, as it antagonizes GRα activity, preventing glucocorticoids from exerting their effects on inflammatory gene transcription (Hasan & Tory, 2024).

The persistence of IL-33 induced NF-κB and MAPK/ERK signalling despite Dexamethasone treatment further supports the mechanism of IL-33 induced steroid hypo-responsiveness (Yi, Lian, & Li, 2022). NF-κB and MAPK/ERK pathways are major drivers of inflammation in chronic respiratory diseases and are known to be less responsive to corticosteroids (T. Liu et al., 2017; van der Zwet et al., 2021). In this study, IL-33 stimulation led to sustained NF-κB activation, as shown by elevated levels of phosphorylated IκBα, which were not suppressed by Dexamethasone.

These findings emphasize the urgent need for targeted interventions to address the limitations of conventional corticosteroid therapies in IL-33/ST2-driven asthma. In addition to their limited efficacy in IL-33/ST2-driven asthma, corticosteroids are associated with significant side effects (Ericson-Neilsen & Kaye, 2014), particularly at high doses required

for severe cases. Prolonged corticosteroid use can lead to systemic complications such as osteoporosis, hyperglycaemia, hypertension, and increased susceptibility to infections, significantly affecting the quality of life of asthma patients (Da Silva et al., 2006; Saag et al., 1994; Yasir, Goyal, & Sonthalia, 2024). Moreover, corticosteroids do not directly target the underlying molecular drivers of IL-33/ST2 signalling, which means they address symptoms rather than the root cause of inflammation. These limitations highlight the need for novel therapeutic strategies that specifically inhibit the IL-33/ST2 axis. By addressing the source of inflammation and reducing reliance on high-dose corticosteroids, these interventions could significantly improve disease control, reduce side effects, and enhance the quality of life for patients with severe IL-33/ST2-driven asthma.

Targeted therapies, such as anti-ST2 monoclonal antibodies, which are still in clinical trials (Kelsen et al., 2021), offer significant potential to disrupt IL-33-driven inflammatory pathways and address the limitations of corticosteroids (Kelsen et al., 2021). However, the currently FDA-approved monoclonal antibodies for asthma—omalizumab, mepolizumab, reslizumab, benralizumab, dupilumab, and Tezepelumab (Agache et al., 2020; Kurihara, Kabata, Irie, & Fukunaga, 2023; Ridolo et al., 2020)—remain limited in their ability to fully control severe asthma in many patients. Despite their efficacy in specific asthma subtypes (Abe et al., 2021), challenges such as high production costs, limited tissue penetration, immunogenicity, and the need for repeated dosing and cold-chain logistics contribute to patient burden and healthcare costs (Kardas et al., 2022; Samaranayake et al., 2009). Moreover, these therapies often fail to address the multifactorial nature of asthma, leaving a significant gap in managing severe cases (Abe et al., 2021).

Nanobodies offer a promising solution, with advantages such as enhanced tissue penetration, reduced immunogenicity, and cost-effective production, marking a new era in targeted therapy (Abe et al., 2021; Hoey et al., 2019; Khodabakhsh et al., 2018). However,

nanobodies remain a focus of ongoing research, with no FDA-approved therapies for asthma currently available. Most preclinical trials have concentrated on Th2-driven asthma (Gevenois et al., 2021; L. Ma et al., 2022; Qiu et al., 2024; Shijie et al., 2024; Zhu et al., 2024), leaving other phenotypes underexplored. Recognizing these gaps, we developed a nanobody-based therapy targeting IL-33/ST2-driven asthma, a critical pathway implicated in severe asthma.

This novel approach has the potential to address the unmet needs of severe asthma management, offering an innovative and effective solution for patients unresponsive to current therapies. To achieve this, we developed and characterized novel anti-ST2 nanobodies, with NB7 emerging as the most promising candidate. Using a robust VHH library and a phage display-based screening process, we efficiently enriched high-affinity ST2-specific nanobodies, consistent with approaches used in previous studies (De Meyer, Muyldermans, & Depicker, 2014; Vincke et al., 2012) Binding affinity analysis confirmed NB7 as the top-performing nanobody, exhibiting superior binding characteristics, specificity, and potential compared to NB2 and NB21.

This study successfully utilized phage display technology to isolate and characterize high-affinity anti-ST2 nanobodies (Bazan, Całkosiński, & Gamian, 2012; Smith & Petrenko, 1997), underscoring the versatility of this platform in identifying and optimizing therapeutic candidates. Phage display remains a cornerstone technology in drug discovery, enabling the rapid screening of vast antibody libraries to identify molecules with desirable properties such as high specificity and binding affinity (Smith & Petrenko, 1997). The three-round panning approach employed here, with increasing stringency and the elimination of clones cross-reacting with a negative control, ensured the selection of nanobodies with exceptional specificity toward ST2 (Vincke et al., 2012).

The specificity of the identified anti-ST2 nanobodies was rigorously evaluated by ELISA against ST2 and other IL-1 receptor family members (Garlanda, Dinarello, & Mantovani, 2013), including IL-18Rα, IL-36R, and IL-1R AcP, in addition to BSA. The results demonstrated significantly higher binding signals to ST2 compared to the control proteins, reaffirming their selective binding. Notably, NB7 emerged as the most promising candidate, showcasing robust specificity with negligible off-target interactions. This level of selectivity is critical for therapeutic applications, as off-target effects can lead to unintended immunological consequences (Henrickson, Ruffner, & Kwan, 2016)

Binding affinity, a pivotal determinant of therapeutic efficacy, was assessed through direct ELISA and dissociation constant (KD) estimation, following the methodology described by previous study (Syedbasha et al., 2016). NB7 demonstrated the highest binding affinity among the clones, with a KD of 9.67 nM at 10 µg/ml ST2 coating concentration, outperforming NB2 and NB21, which exhibited KD values of 63.36 nM and 99.9 nM, respectively. Even at a lower ST2 coating concentration (1 µg/ml), NB7 retained its superior performance with a KD of 16.52 nM, compared to the significantly reduced affinities of NB2 (287.9 nM) and NB21 (289.2 nM). The high Hill coefficient of NB7 (1.2 at 10 µg/ml ST2 coating) indicates cooperative binding, a property that could enhance its therapeutic efficacy by stabilizing receptor-ligand complexes (Weiss, 1997). In competitive ELISA assays, NB7 further demonstrated superior potency, achieving the lowest IC_{50} (0.1411 µg/mL) compared to NB2 (0.4115 µg/mL) and NB21 (0.4299 µg/mL) following the methodology described by previous study (Naderi et al., 2020).

Functionally, NB7 demonstrated significant efficacy *in vitro*, using primary human epithelial cells by reducing MAPK/ERK and NF-κB activation, key pathways known to drive chronic inflammation in asthma. These findings are supported by previous research indicating that inhibiting the IL-33/ST2 axis suppresses these inflammatory pathways and lowers the

production of pro-inflammatory cytokines (Han et al., 2015; Y. Wu et al., 2020). This highlights NB7's potential as a targeted therapeutic to modulate these pathways. By targeting these inflammatory cascades, NB7 offers a novel approach to mitigating Th17-driven inflammation, a hallmark of severe and neutrophilic asthma (Xie, Abel, Casale, & Tu, 2022). Importantly, NB7 restored the balance of glucocorticoid receptor isoforms by increasing GRα expression while reducing GRβ levels. Unlike conventional therapies that fail to reverse this dysregulation, NB7's ability to normalize the GRα/GRβ ratio highlights its potential to restore steroid sensitivity (Marques, Silverman, & Sternberg, 2009), providing a mechanistic basis for NB7's therapeutic efficacy.

Building on these *in vitro* findings, we evaluated NB7 *in vivo* using a modified HDM-induced asthma mouse model, adapted from a previously reported protocol (Woo et al., 2018). Their model, involving 4 weeks of intranasal HDM administration (25 µg in 35 µl saline; 5 days/week), effectively induced airway hyperresponsiveness (AHR), inflammation, and remodeling comparable to the traditional 8-week model (Woo et al., 2018). We further adjusted this protocol to 4 days/week of HDM exposure, with the addition of IL-33 administration twice a week, creating an ideal model for studying the IL-33/ST2 pathway. This modified model was validated and compared against an HDM-only model to highlight the specific contributions of IL-33/ST2 signaling in asthma pathophysiology.

Intranasal delivery of NB7 demonstrated efficient lung tissue localization, a critical aspect of our study design. The intranasal route was chosen as a targeted delivery method to ensure direct deposition of NB7 in the lower respiratory tract, optimizing its therapeutic impact on lung tissues. Following a protocol similar to established methods, NB7 was administered intranasally using a micropipette, with a total volume of 50 µL applied drop by drop onto the nostrils to facilitate inhalation (Bushra Mdkhana, 2024). Previous studies, such as Tsuyuki et al., have shown that approximately 75% of a 50 µL intranasal instillation

deposits in the airways, underscoring the importance of instillation volume in achieving efficient pulmonary distribution (Tsuyuki, Tsuyuki, Einsle, Kopf, & Coyle, 1997). Factors such as anaesthesia and animal positioning were carefully controlled in our study to maximize delivery to the lower respiratory tract (Southam, Dolovich, O'Byrne, & Inman, 2002). The intranasal route is a well-established technique in murine models, providing direct access to the lungs while minimizing systemic absorption through the nasal mucosa. This method takes advantage of the anatomical connection between the upper and lower airways, enabling effective deposition in pulmonary tissues. The significant effects observed in the lungs in our study, including reductions in cytokine levels and inflammatory cell counts in BALF, provide strong evidence of successful NB7 delivery to the target site.

NB7 significantly reduced airway inflammation, mucus production, and immune cell infiltration, while also improving lung mechanics. These effects were associated with greater reductions in pro-inflammatory cytokines such as IL-4, IL-5, IL-13, and IL-17 compared to astegolimab, highlighting its broader anti-inflammatory capabilities. Mechanistically, NB7 effectively blocked ST2 receptor expression in lung tissues, achieving a six-fold reduction comparable to astegolimab. However, NB7 outperformed astegolimab in suppressing downstream signalling pathways. While astegolimab showed no significant effect on NF-κB activation, NB7 achieved a fourfold reduction, demonstrating its ability to comprehensively inhibit IL-33/ST2-driven inflammation. These findings highlight a critical distinction between NB7 and astegolimab, further establishing NB7 as a potentially superior therapeutic option. Building on the *in vitro* observations, NB7 demonstrated remarkable efficacy in restoring GR dynamics *in vivo*. By significantly increasing GRα expression and reducing GRβ levels, NB7 restored the GRα/GRβ balance, a critical determinant of glucocorticoid responsiveness. In contrast, astegolimab failed to restore GRα/GRβ dynamics, underscoring a unique therapeutic advantage of NB7. This is most likely due to the size of the monoclonal

antibody (Pillay & Muyldermans, 2021), which limits its ability to penetrate deeply into lung tissues. Nanobodies, such as NB7, are significantly smaller in size (Pillay & Muyldermans, 2021), enabling them to settle more effectively in the deeper regions of the lungs and exert their therapeutic effects directly at the site of inflammation. The ability of NB7 to improve steroid sensitivity, even at a dose three times lower than astegolimab, further highlights its potential as a cost-effective and efficient treatment option for steroid-resistant asthma.

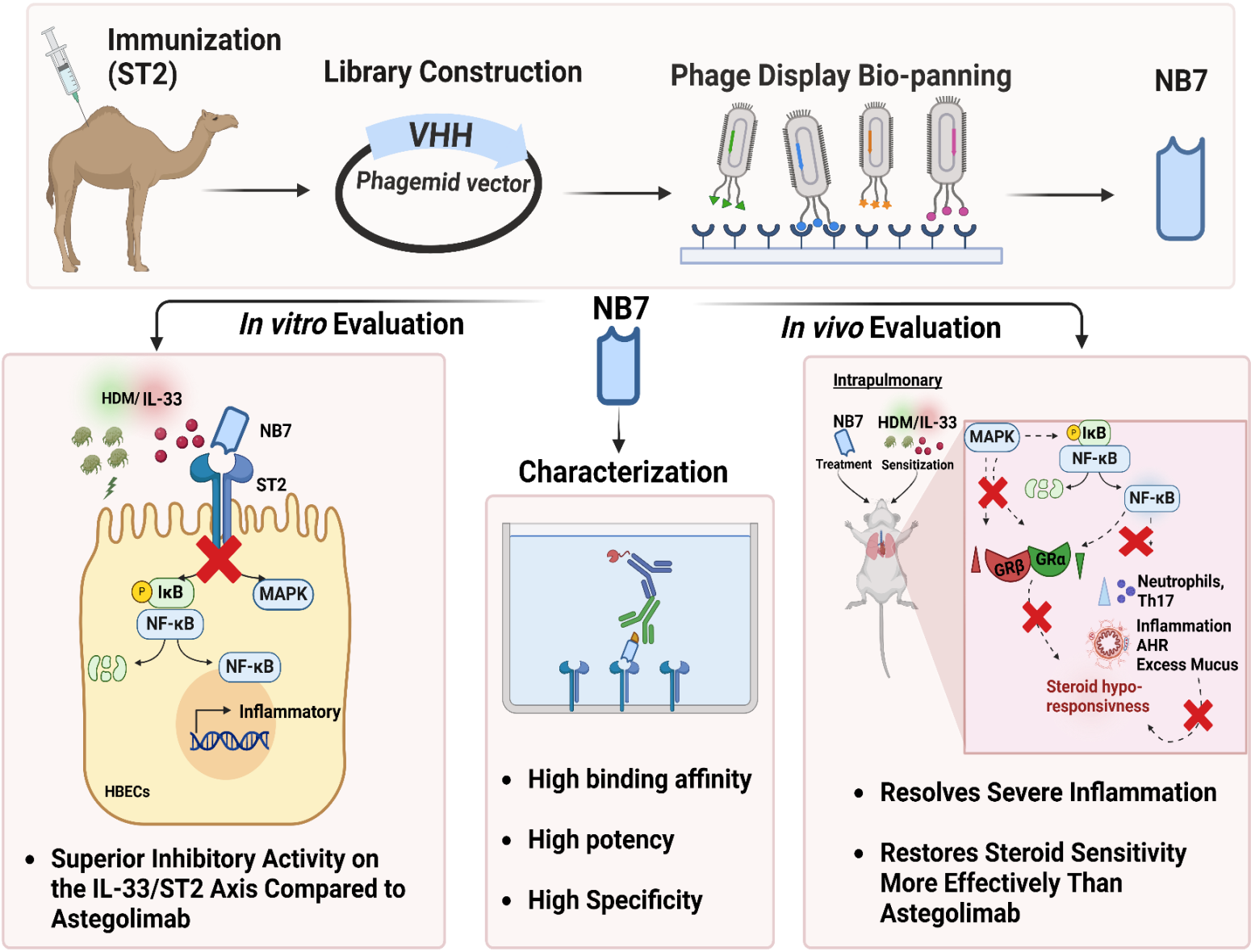

Figure 4.1: Schematic representation summarizing the key findings of this study, this figure illustrates the development and therapeutic effects of a nanobody (NB7) targeting the IL-33/ST2 axis in asthma. A camel is immunized with ST2, and its immune response is used to construct a VHH phagemid library, which undergoes phage display bio-panning to isolate high-affinity nanobodies, ultimately leading to the selection of NB7. In airway epithelial cells, NB7 effectively inhibits IL-33/ST2 signaling, blocking NF-κB and MAPK activation, thereby reducing inflammation more effectively than astegolimab. In an in vivo asthma model, NB7 administration alleviates severe inflammation, decreases neutrophil and Th17 recruitment, and restores steroid sensitivity better than astegolimab, making it a promising therapeutic candidate for severe asthma treatment.

5. Conclusion

In conclusion, this study underscores the pivotal role of IL-33/ST2 signaling in the pathogenesis of severe asthma, linking it to airway inflammation, mucus overproduction, and steroid hypo-responsiveness through MAPK/ERK and NF-κB activation and GR dysregulation. Through rigorous *in vitro* and *in vivo* analyses, we identified and characterized NB7, a novel anti-ST2 nanobody, as a highly effective therapeutic candidate. NB7 demonstrated superior efficacy compared to astegolimab, significantly reducing airway inflammation, cytokine production, and mucus hypersecretion, while restoring GRα/GRβ balance and improving glucocorticoid hypo-responsiveness. The targeted intranasal delivery of NB7 ensured efficient lung tissue localization and enhanced its therapeutic impact, addressing key mechanisms underlying severe, steroid-hyporesponsive asthma.

Mechanistically, NB7 effectively blocked ST2 receptor expression and downstream signalling pathways, offering comprehensive inhibition of IL-33/ST2-driven inflammation. Its ability to achieve these outcomes at a lower dose compared to astegolimab underscores its potential as a cost-effective and efficient therapeutic option. By targeting both inflammation and steroid hypo-responsiveness, NB7 represents a promising and innovative approach to managing IL-33/ST2-driven asthma, addressing critical unmet needs in the treatment of severe asthma phenotypes.

5.1 Limitations

Despite the promising findings, this study has several limitations. Being preclinical in nature, the results are based on *in vitro* and animal models, which may not fully replicate the complexity of human asthma, necessitating further validation in clinical trials. While the focus on the IL-33/ST2 axis provided valuable insights, asthma is a multifactorial disease,

and this approach may not address all phenotypes, particularly non-IL-33/ST2-driven asthma or mixed inflammatory profiles. Additionally, the study primarily examined acute or short-term outcomes, leaving long-term efficacy, safety, and potential immunogenicity of NB7 unexplored. The intranasal delivery method, although effective in this controlled setting, may require optimization for real-world clinical application, such as via inhalers, which could affect dosage and efficacy. Addressing these limitations will be critical for translating NB7 into a viable treatment option for severe asthma.

5.2 Future work

Future preclinical work should focus on evaluating the long-term efficacy and safety of NB7 in animal models, including its sustained anti-inflammatory effects, potential immunogenicity, and tolerance development. Expanding studies to include diverse asthma phenotypes, such as mixed Th2/Th17-driven and non-IL-33/ST2-driven asthma, will help assess the broader applicability of NB7. Investigating the interplay of the IL-33/ST2 axis with other key pathways, such as TSLP and IL-25, could provide deeper mechanistic insights and identify potential combinatory therapeutic strategies. Lastly, incorporating pharmacological modifications, such as PEGylation, to extend NB7's half-life will enhance dosing efficiency and therapeutic potential, paving the way for its eventual clinical translation.

6. References

Abe, Y., Suga, Y., Fukushima, K., Ohata, H., Niitsu, T., Nabeshima, H., . . . Kumanogoh, A. (2021). Advances and Challenges of Antibody Therapeutics for Severe Bronchial Asthma. *Int J Mol Sci, 23*(1). doi:10.3390/ijms23010083

Abrams, E. M., Becker, A. B., & Szefler, S. J. (2018). Current State and Future of Biologic Therapies in the Treatment of Asthma in Children. *Pediatr Allergy Immunol Pulmonol, 31*(3), 119-131. doi:10.1089/ped.2018.0901

Adcock, I. M., Ford, P. A., Bhavsar, P., Ahmad, T., & Chung, K. F. (2008). Steroid resistance in asthma: mechanisms and treatment options. *Curr Allergy Asthma Rep, 8*(2), 171-178. doi:10.1007/s11882-008-0028-4

Agache, I., Beltran, J., Akdis, C., Akdis, M., Canelo-Aybar, C., Canonica, G. W., . . . Jutel, M. (2020). Efficacy and safety of treatment with biologicals (benralizumab, dupilumab, mepolizumab, omalizumab and reslizumab) for severe eosinophilic asthma. A systematic review for the EAACI Guidelines - recommendations on the use of biologicals in severe asthma. *Allergy, 75*(5), 1023-1042. doi:10.1111/all.14221

Akar-Ghibril, N., Casale, T., Custovic, A., & Phipatanakul, W. (2020). Allergic Endotypes and Phenotypes of Asthma. *J Allergy Clin Immunol Pract, 8*(2), 429-440. doi:10.1016/j.jaip.2019.11.008

Al Heialy, S., Gaudet, M., Ramakrishnan, R. K., Mogas, A., Salameh, L., Mahboub, B., & Hamid, Q. (2020). Contribution of IL-17 in Steroid Hyporesponsiveness in Obese Asthmatics Through Dysregulation of Glucocorticoid Receptors alpha and beta. *Front Immunol, 11*, 1724. doi:10.3389/fimmu.2020.01724

Alam, R., & Gorska, M. M. (2011). Mitogen-activated protein kinase signalling and ERK1/2 bistability in asthma. *Clin Exp Allergy, 41*(2), 149-159. doi:10.1111/j.1365-2222.2010.03658.x

Andrade, M. V., Iwaki, S., Ropert, C., Gazzinelli, R. T., Cunha-Melo, J. R., & Beaven, M. A. (2011). Amplification of cytokine production through synergistic activation of NFAT and AP-1 following stimulation of mast cells with antigen and IL-33. *Eur J Immunol, 41*(3), 760-772. doi:10.1002/eji.201040718

Araújo, P., Resende, R., Corrêa, P., Andrade, L., Almeida, V., Silva, J., . . . Schwarz, M. (2023). *In silico design of therapeutic single domain antibodies for asthma*.

Arbabi-Ghahroudi, M. (2017). Camelid Single-Domain Antibodies: Historical Perspective and Future Outlook. *Front Immunol, 8*, 1589. doi:10.3389/fimmu.2017.01589

Arbabi-Ghahroudi, M. (2022). Camelid Single-Domain Antibodies: Promises and Challenges as Lifesaving Treatments. *Int J Mol Sci, 23*(9). doi:10.3390/ijms23095009

Athari, S. S. (2019). Targeting cell signaling in allergic asthma. *Signal Transduction and Targeted Therapy, 4*(1), 45. doi:10.1038/s41392-019-0079-0

Auckland, T. U. o. (2018). Global Asthma Report.

Ayroldi, E., Cannarile, L., Migliorati, G., Nocentini, G., Delfino, D. V., & Riccardi, C. (2012). Mechanisms of the anti-inflammatory effects of glucocorticoids: genomic and nongenomic interference with MAPK signaling pathways. *FASEB J, 26*(12), 4805-4820. doi:10.1096/fj.12-216382

Banafea, G. H., Bakhashab, S., Alshaibi, H. F., Natesan Pushparaj, P., & Rasool, M. (2022). The role of human mast cells in allergy and asthma. *Bioengineered, 13*(3), 7049-7064. doi:10.1080/21655979.2022.2044278

Barnes, P. J. (2006). How corticosteroids control inflammation: Quintiles Prize Lecture 2005. *Br J Pharmacol, 148*(3), 245-254. doi:10.1038/sj.bjp.0706736
Barnes, P. J., & Adcock, I. M. (2009). Glucocorticoid resistance in inflammatory diseases. *Lancet, 373*(9678), 1905-1917. doi:10.1016/S0140-6736(09)60326-3
Bauernfeind, C., Zettl, I., Ivanova, T., Goryainova, O., Weijler, A. M., Pranz, B., . . . Flicker, S. (2024). Trimeric Bet v 1-specific nanobodies cause strong suppression of IgE binding. *Front Immunol, 15*, 1343024. doi:10.3389/fimmu.2024.1343024
Bazan, J., Całkosiński, I., & Gamian, A. (2012). Phage display--a powerful technique for immunotherapy: 1. Introduction and potential of therapeutic applications. *Hum Vaccin Immunother, 8*(12), 1817-1828. doi:10.4161/hv.21703
Bergstrand, M., Hansson, E., Delaey, B., Callewaert, F., De Passos Sousa, R., & Sargentini-Maier, M. L. (2022). Caplacizumab Model-Based Dosing Recommendations in Pediatric Patients With Acquired Thrombotic Thrombocytopenic Purpura. *J Clin Pharmacol, 62*(3), 409-421. doi:10.1002/jcph.1991
Bleecker, E. R., FitzGerald, J. M., Chanez, P., Papi, A., Weinstein, S. F., Barker, P., . . . investigators, S. s. (2016). Efficacy and safety of benralizumab for patients with severe asthma uncontrolled with high-dosage inhaled corticosteroids and long-acting beta(2)-agonists (SIROCCO): a randomised, multicentre, placebo-controlled phase 3 trial. *Lancet, 388*(10056), 2115-2127. doi:10.1016/S0140-6736(16)31324-1
Borish, L., & Culp, J. A. (2008). Asthma: a syndrome composed of heterogeneous diseases. *Annals of Allergy, Asthma & Immunology, 101*(1), 1-9. doi:https://doi.org/10.1016/S1081-1206(10)60826-5
Bushra Mdkhana, N. S. S.-A., Roberta Cagliani, Baraa Khalid Al-Sheakly, Rakhee K. Ramakrishnan, Fatemeh Saheb Sharif-Askari, Ibrahim Yaseen Hachim, Qutayba Hamid, Mutasem Rawas-Qalaji, and Rabih Halwani. (2024). Inhibiting DNA Sensing Pathway Controls Steroid Hyporesponsive Lung Inflammation *Advanced Biology*. doi:10.1002/adbi.202400230
Busse, W., Corren, J., Lanier, B. Q., McAlary, M., Fowler-Taylor, A., Cioppa, G. D., . . . Gupta, N. (2001). Omalizumab, anti-IgE recombinant humanized monoclonal antibody, for the treatment of severe allergic asthma. *J Allergy Clin Immunol, 108*(2), 184-190. doi:10.1067/mai.2001.117880
Busse, W. W., Maspero, J. F., Rabe, K. F., Papi, A., Wenzel, S. E., Ford, L. B., . . . Teper, A. (2018). Liberty Asthma QUEST: Phase 3 Randomized, Double-Blind, Placebo-Controlled, Parallel-Group Study to Evaluate Dupilumab Efficacy/Safety in Patients with Uncontrolled, Moderate-to-Severe Asthma. *Adv Ther, 35*(5), 737-748. doi:10.1007/s12325-018-0702-4
Calderon, A. A., Dimond, C., Choy, D. F., Pappu, R., Grimbaldeston, M. A., Mohan, D., & Chung, K. F. (2023). Targeting interleukin-33 and thymic stromal lymphopoietin pathways for novel pulmonary therapeutics in asthma and COPD. *Eur Respir Rev, 32*(167). doi:10.1183/16000617.0144-2022
Caminati, M., Vaia, R., Furci, F., Guarnieri, G., & Senna, G. (2021). Uncontrolled Asthma: Unmet Needs in the Management of Patients. *J Asthma Allergy, 14*, 457-466. doi:10.2147/JAA.S260604
Carr, T. F., & Bleecker, E. (2016). Asthma heterogeneity and severity. *World Allergy Organ J, 9*(1), 41. doi:10.1186/s40413-016-0131-2
Castillo, J. R., Peters, S. P., & Busse, W. W. (2017). Asthma Exacerbations: Pathogenesis, Prevention, and Treatment. *J Allergy Clin Immunol Pract, 5*(4), 918-927. doi:10.1016/j.jaip.2017.05.001
Cayrol, C., & Girard, J. P. (2018). Interleukin-33 (IL-33): A nuclear cytokine from the IL-1 family. *Immunol Rev, 281*(1), 154-168. doi:10.1111/imr.12619

Chapman, D. G., & Irvin, C. G. (2015). Mechanisms of airway hyper-responsiveness in asthma: the past, present and yet to come. *Clin Exp Allergy, 45*(4), 706-719. doi:10.1111/cea.12506

Cheng, X., Wang, J., Kang, G., Hu, M., Yuan, B., Zhang, Y., & Huang, H. (2019). *Homology Modeling-Based in Silico Affinity Maturation Improves the Affinity of a Nanobody*. Int J Mol Sci. Retrieved from https://www.ncbi.nlm.nih.gov/pubmed/31461846

Cheng, X., Xie, Q., & Sun, Y. (2023). Advances in nanomaterial-based targeted drug delivery systems. *Front Bioeng Biotechnol, 11*, 1177151. doi:10.3389/fbioe.2023.1177151

Cherry, W. B., Yoon, J., Bartemes, K. R., Iijima, K., & Kita, H. (2008). A novel IL-1 family cytokine, IL-33, potently activates human eosinophils. *J Allergy Clin Immunol, 121*(6), 1484-1490. doi:10.1016/j.jaci.2008.04.005

Cho, K. A., Suh, J. W., Sohn, J. H., Park, J. W., Lee, H., Kang, J. L., . . . Cho, Y. J. (2012). IL-33 induces Th17-mediated airway inflammation via mast cells in ovalbumin-challenged mice. *Am J Physiol Lung Cell Mol Physiol, 302*(4), L429-440. doi:10.1152/ajplung.00252.2011

Ciprandi, G., Tosca, M. A., Silvestri, M., & Ricciardolo, F. L. M. (2017). Inflammatory biomarkers for asthma endotyping and consequent personalized therapy. *Expert Rev Clin Immunol, 13*(7), 715-721. doi:10.1080/1744666x.2017.1313117

Corren, J., Parnes, J. R., Wang, L., Mo, M., Roseti, S. L., Griffiths, J. M., & van der Merwe, R. (2017). Tezepelumab in Adults with Uncontrolled Asthma. *N Engl J Med, 377*(10), 936-946. doi:10.1056/NEJMoa1704064

Corrigan, C. J., & Loke, T. K. (2007). Clinical and molecular aspects of glucocorticoid resistant asthma. *Ther Clin Risk Manag, 3*(5), 771-787.

Curren, B., Ahmed, T., Howard, D. R., Ashik Ullah, M., Sebina, I., Rashid, R. B., . . . Phipps, S. (2023). IL-33-induced neutrophilic inflammation and NETosis underlie rhinovirus-triggered exacerbations of asthma. *Mucosal Immunol, 16*(5), 671-684. doi:10.1016/j.mucimm.2023.07.002

Da Silva, J. A., Jacobs, J. W., Kirwan, J. R., Boers, M., Saag, K. G., Inês, L. B., . . . Bijlsma, J. W. (2006). Safety of low dose glucocorticoid treatment in rheumatoid arthritis: published evidence and prospective trial data. *Ann Rheum Dis, 65*(3), 285-293. doi:10.1136/ard.2005.038638

de Marco, A. (2020). Recombinant expression of nanobodies and nanobody-derived immunoreagents. *Protein Expr Purif, 172*, 105645. doi:10.1016/j.pep.2020.105645

De Meyer, T., Muyldermans, S., & Depicker, A. (2014). Nanobody-based products as research and diagnostic tools. *Trends Biotechnol, 32*(5), 263-270. doi:10.1016/j.tibtech.2014.03.001

Deiteren, A., Krupka, E., Imberdis, K., Patel, N., Staudinger, H., & Suratt, B. T. (2023). *Targeting of TSLP and IL-13 by the Novel NANOBODY ® Molecule SAR443765 Reduces FeNO in Asthma Following Single Dose Exposure*.

Deng, C., Peng, N., Tang, Y., Yu, N., Wang, C., Cai, X., . . . Lu, L. (2021). Roles of IL-25 in Type 2 Inflammation and Autoimmune Pathogenesis. *12*. doi:10.3389/fimmu.2021.691559

Derendorf, H., Nave, R., Drollmann, A., Cerasoli, F., & Wurst, W. (2006). Relevance of pharmacokinetics and pharmacodynamics of inhaled corticosteroids to asthma. *Eur Respir J, 28*(5), 1042-1050. doi:10.1183/09031936.00074905

Detalle, L., Stohr, T., Palomo, C., Piedra, P. A., Gilbert, B. E., Mas, V., . . . Depla, E. (2016). Generation and Characterization of ALX-0171, a Potent Novel Therapeutic Nanobody for the Treatment of Respiratory Syncytial Virus Infection. *Antimicrob Agents Chemother, 60*(1), 6-13. doi:10.1128/AAC.01802-15

Dingus, J. G., Tang, J. C. Y., Amamoto, R., Wallick, G. K., & Cepko, C. L. (2022). A general approach for stabilizing nanobodies for intracellular expression. *eLife, 11*, e68253. doi:10.7554/eLife.68253

Dougherty, R. H., & Fahy, J. V. (2009). Acute exacerbations of asthma: epidemiology, biology and the exacerbation-prone phenotype. *Clin Exp Allergy, 39*(2), 193-202. doi:10.1111/j.1365-2222.2008.03157.x

Drake, L. Y., & Kita, H. (2017). IL-33: biological properties, functions, and roles in airway disease. *Immunol Rev, 278*(1), 173-184. doi:10.1111/imr.12552

Drake, M. G., Cook, M., Fryer, A. D., Jacoby, D. B., & Scott, G. D. (2021). Airway Sensory Nerve Plasticity in Asthma and Chronic Cough. *Front Physiol, 12*, 720538. doi:10.3389/fphys.2021.720538

Dua, K., Shukla, S. D., & Hansbro, P. M. (2017). Aspiration techniques for bronchoalveolar lavage in translational respiratory research: Paving the way to develop novel therapeutic moieties. *J Biol Methods, 4*(3), e73. doi:10.14440/jbm.2017.174

Ericson-Neilsen, W., & Kaye, A. D. (2014). Steroids: pharmacology, complications, and practice delivery issues. *Ochsner J, 14*(2), 203-207.

Faul, F., Erdfelder, E., Buchner, A., & Lang, A. G. (2009). Statistical power analyses using G*Power 3.1: tests for correlation and regression analyses. *Behav Res Methods, 41*(4), 1149-1160. doi:10.3758/brm.41.4.1149

Fei, Q., Bentley, I., Ghadiali, S. N., & Englert, J. A. (2023). Pulmonary drug delivery for acute respiratory distress syndrome. *Pulm Pharmacol Ther, 79*, 102196. doi:10.1016/j.pupt.2023.102196

Fridy, P. C., Li, Y., Keegan, S., Thompson, M. K., Nudelman, I., Scheid, J. F., . . . Rout, M. P. (2014). A robust pipeline for rapid production of versatile nanobody repertoires. *Nat Methods, 11*(12), 1253-1260. doi:10.1038/nmeth.3170

Fujita, J., Kawaguchi, M., Kokubu, F., Ohara, G., Ota, K., Huang, S. K., . . . Hizawa, N. (2012). Interleukin-33 induces interleukin-17F in bronchial epithelial cells. *Allergy, 67*(6), 744-750. doi:10.1111/j.1398-9995.2012.02825.x

Garlanda, C., Dinarello, C. A., & Mantovani, A. (2013). The interleukin-1 family: back to the future. *Immunity, 39*(6), 1003-1018. doi:10.1016/j.immuni.2013.11.010

Gaurav, R., & Poole, J. A. (2022). Interleukin (IL)-33 immunobiology in asthma and airway inflammatory diseases. *J Asthma, 59*(12), 2530-2538. doi:10.1080/02770903.2021.2020815

Gauvreau, G. M., Bergeron, C., Boulet, L. P., Cockcroft, D. W., Côté, A., Davis, B. E., . . . Sehmi, R. (2023). Sounding the alarmins-The role of alarmin cytokines in asthma. *Allergy, 78*(2), 402-417. doi:10.1111/all.15609

Gevenois, P. J. Y., De Pauw, P., Schoonooghe, S., Delporte, C., Sebti, T., Amighi, K., . . . Wauthoz, N. (2021). Development of Neutralizing Multimeric Nanobody Constructs Directed against IL-13: From Immunization to Lead Optimization. *J Immunol, 207*(10), 2608-2620. doi:10.4049/jimmunol.2100250

Guo, Y., Bera, H., Shi, C., Zhang, L., Cun, D., & Yang, M. (2021). Pharmaceutical strategies to extend pulmonary exposure of inhaled medicines. *Acta Pharm Sin B, 11*(8), 2565-2584. doi:10.1016/j.apsb.2021.05.015

Hamid, Q., Tulic, M. K., Liu, M. C., & Moqbel, R. (2003). Inflammatory cells in asthma: mechanisms and implications for therapy. *J Allergy Clin Immunol, 111*(1 Suppl), S5-S12; discussion S12-17. doi:10.1067/mai.2003.22

Han, P., Liu, S., Zhang, M., Zhao, J., Wang, Y., Wu, G., & Mi, W. (2015). Inhibition of Spinal Interlukin-33/ST2 Signaling and Downstream ERK and JNK Pathways in Electroacupuncture Analgesia in Formalin Mice. *PLoS One, 10*(6), e0129576. doi:10.1371/journal.pone.0129576

Hansi, R. K., Ranjbar, M., Whetstone, C. E., & Gauvreau, G. M. (2024). Regulation of Airway Epithelial-Derived Alarmins in Asthma: Perspectives for Therapeutic Targets. *12*(10), 2312.

Hasan, M. M., & Tory, S. (2024). Association between glucocorticoid receptor beta and steroid resistance: A systematic review. *Immun Inflamm Dis, 12*(1), e1137. doi:10.1002/iid3.1137

Hashmi, M. F., & Cataletto, M. E. (2024). Asthma. In *StatPearls*. Treasure Island (FL) ineligible companies. Disclosure: Mary Cataletto declares no relevant financial relationships with ineligible companies.: StatPearls Publishing

He, R., & Geha, R. S. (2010). Thymic stromal lymphopoietin. *Ann N Y Acad Sci, 1183*, 13-24. doi:10.1111/j.1749-6632.2009.05128.x

Heijink, I. H., Kuchibhotla, V. N. S., Roffel, M. P., Maes, T., Knight, D. A., Sayers, I., & Nawijn, M. C. (2020). Epithelial cell dysfunction, a major driver of asthma development. *Allergy, 75*(8), 1902-1917. doi:10.1111/all.14421

Henderson, I., Caiazzo, E., McSharry, C., Guzik, T. J., & Maffia, P. (2020). Why do some asthma patients respond poorly to glucocorticoid therapy? *Pharmacol Res, 160*, 105189. doi:10.1016/j.phrs.2020.105189

Henrickson, S. E., Ruffner, M. A., & Kwan, M. (2016). Unintended Immunological Consequences of Biologic Therapy. *Curr Allergy Asthma Rep, 16*(6), 46. doi:10.1007/s11882-016-0624-7

Hoey, R. J., Eom, H., & Horn, J. R. (2019). Structure and development of single domain antibodies as modules for therapeutics and diagnostics. *Exp Biol Med (Maywood), 244*(17), 1568-1576. doi:10.1177/1535370219881129

Holland, A., Smith, F., Penny, K., McCrossan, G., Veitch, L., & Nicholson, C. (2013). Metered dose inhalers versus nebulizers for aerosol bronchodilator delivery for adult patients receiving mechanical ventilation in critical care units. *Cochrane Database Syst Rev, 2013*(6), CD008863. doi:10.1002/14651858.CD008863.pub2

Hoshino, M., Nakamura, Y., Sim, J. J., Yamashiro, Y., Uchida, K., Hosaka, K., & Isogai, S. (1998). Inhaled corticosteroid reduced lamina reticularis of the basement membrane by modulation of insulin-like growth factor (IGF)-I expression in bronchial asthma. *Clin Exp Allergy, 28*(5), 568-577. doi:10.1046/j.1365-2222.1998.00277.x

Hough, K. P., Curtiss, M. L., Blain, T. J., Liu, R. M., Trevor, J., Deshane, J. S., & Thannickal, V. J. (2020). Airway Remodeling in Asthma. *Front Med (Lausanne), 7*, 191. doi:10.3389/fmed.2020.00191

Hsu, C. L., & Bryce, P. J. (2012). Inducible IL-33 expression by mast cells is regulated by a calcium-dependent pathway. *J Immunol, 189*(7), 3421-3429. doi:10.4049/jimmunol.1201224

Hudey, S. N., Ledford, D. K., & Cardet, J. C. (2020). Mechanisms of non-type 2 asthma. *Curr Opin Immunol, 66*, 123-128. doi:10.1016/j.coi.2020.10.002

Hunt, A., Qian, V., Olds, H., & Daveluy, S. (2023). The Current Clinical Trial Landscape for Hidradenitis Suppurativa: A Narrative Review. *Dermatol Ther (Heidelb), 13*(7), 1391-1407. doi:10.1007/s13555-023-00935-x

Hussain, M., & Liu, G. (2024). Eosinophilic Asthma: Pathophysiology and Therapeutic Horizons. *Cells, 13*(5). doi:10.3390/cells13050384

Ikeuchi, E., Kuroda, D., Nakakido, M., Murakami, A., & Tsumoto, K. (2021). Delicate balance among thermal stability, binding affinity, and conformational space explored by single-domain V(H)H antibodies. *Sci Rep, 11*(1), 20624. doi:10.1038/s41598-021-98977-8

Ito, K., Barnes, P. J., & Adcock, I. M. (2000). Glucocorticoid receptor recruitment of histone deacetylase 2 inhibits interleukin-1beta-induced histone H4 acetylation on lysines 8 and 12. *Mol Cell Biol, 20*(18), 6891-6903. doi:10.1128/MCB.20.18.6891-6903.2000

Jin, B. K., Odongo, S., Radwanska, M., & Magez, S. (2023). NANOBODIES®: A Review of Diagnostic and Therapeutic Applications. *Int J Mol Sci, 24*(6). doi:10.3390/ijms24065994

Jonckheere, A. C., Bullens, D. M. A., & Seys, S. F. (2019). Innate lymphoid cells in asthma: pathophysiological insights from murine models to human asthma phenotypes. *Curr Opin Allergy Clin Immunol, 19*(1), 53-60. doi:10.1097/aci.0000000000000497

Jovcevska, I., & Muyldermans, S. (2020). The Therapeutic Potential of Nanobodies. *BioDrugs, 34*(1), 11-26. doi:10.1007/s40259-019-00392-z

Jovčevska, I., & Muyldermans, S. (2020). The Therapeutic Potential of Nanobodies. *BioDrugs, 34*(1), 11-26. doi:10.1007/s40259-019-00392-z

Kakkar, R., & Lee, R. T. (2008). The IL-33/ST2 pathway: therapeutic target and novel biomarker. *Nature Reviews Drug Discovery, 7*(10), 827-840. doi:10.1038/nrd2660

Kardas, G., Panek, M., Kuna, P., Damiański, P., & Kupczyk, M. (2022). Monoclonal antibodies in the management of asthma: Dead ends, current status and future perspectives. *Front Immunol, 13*, 983852. doi:10.3389/fimmu.2022.983852

Katsaounou, P., Buhl, R., Brusselle, G., Pfister, P., Martinez, R., Wahn, U., & Bousquet, J. (2019). Omalizumab as alternative to chronic use of oral corticosteroids in severe asthma. *Respir Med, 150*, 51-62. doi:10.1016/j.rmed.2019.02.003

Kearley, J., Silver, J. S., Sanden, C., Liu, Z., Berlin, A. A., White, N., . . . Humbles, A. A. (2015). Cigarette smoke silences innate lymphoid cell function and facilitates an exacerbated type I interleukin-33-dependent response to infection. *Immunity, 42*(3), 566-579. doi:10.1016/j.immuni.2015.02.011

Kelsen, S. G., Agache, I. O., Soong, W., Israel, E., Chupp, G. L., Cheung, D. S., . . . Brightling, C. E. (2021). Astegolimab (anti-ST2) efficacy and safety in adults with severe asthma: A randomized clinical trial. *J Allergy Clin Immunol, 148*(3), 790-798. doi:10.1016/j.jaci.2021.03.044

Khodabakhsh, F., Behdani, M., Rami, A., & Kazemi-Lomedasht, F. (2018). Single-Domain Antibodies or Nanobodies: A Class of Next-Generation Antibodies. *Int Rev Immunol, 37*(6), 316-322. doi:10.1080/08830185.2018.1526932

Kunz, P., Zinner, K., Mucke, N., Bartoschik, T., Muyldermans, S., & Hoheisel, J. D. (2018). The structural basis of nanobody unfolding reversibility and thermoresistance. *Sci Rep, 8*(1), 7934. doi:10.1038/s41598-018-26338-z

Kurihara, M., Kabata, H., Irie, M., & Fukunaga, K. (2023). Current summary of clinical studies on anti-TSLP antibody, Tezepelumab, in asthma. *Allergol Int, 72*(1), 24-30. doi:10.1016/j.alit.2022.11.006

Kuruvilla, M. E., Lee, F. E., & Lee, G. B. (2019). Understanding Asthma Phenotypes, Endotypes, and Mechanisms of Disease. *Clin Rev Allergy Immunol, 56*(2), 219-233. doi:10.1007/s12016-018-8712-1

Labiris, N. R., & Dolovich, M. B. (2003a). Pulmonary drug delivery. Part I: physiological factors affecting therapeutic effectiveness of aerosolized medications. *Br J Clin Pharmacol, 56*(6), 588-599. doi:10.1046/j.1365-2125.2003.01892.x

Labiris, N. R., & Dolovich, M. B. (2003b). Pulmonary drug delivery. Part II: the role of inhalant delivery devices and drug formulations in therapeutic effectiveness of aerosolized medications. *Br J Clin Pharmacol, 56*(6), 600-612. doi:10.1046/j.1365-2125.2003.01893.x

Lambrecht, B. N., & Hammad, H. (2012). The airway epithelium in asthma. *Nat Med, 18*(5), 684-692. doi:10.1038/nm.2737

Lambrecht, B. N., Hammad, H., & Fahy, J. V. (2019). The Cytokines of Asthma. *Immunity, 50*(4), 975-991. doi:10.1016/j.immuni.2019.03.018
Law, C. W., Chen, Y., Shi, W., & Smyth, G. K. (2014). voom: Precision weights unlock linear model analysis tools for RNA-seq read counts. *Genome Biol, 15*(2), R29. doi:10.1186/gb-2014-15-2-r29
Li, L. B., Leung, D. Y., Martin, R. J., & Goleva, E. (2010). Inhibition of histone deacetylase 2 expression by elevated glucocorticoid receptor beta in steroid-resistant asthma. *Am J Respir Crit Care Med, 182*(7), 877-883. doi:10.1164/rccm.201001-0015OC
Liew, F. Y., Girard, J. P., & Turnquist, H. R. (2016). Interleukin-33 in health and disease. *Nat Rev Immunol, 16*(11), 676-689. doi:10.1038/nri.2016.95
Lingel, A., Weiss, T. M., Niebuhr, M., Pan, B., Appleton, B. A., Wiesmann, C., . . . Fairbrother, W. J. (2009). Structure of IL-33 and its interaction with the ST2 and IL-1RAcP receptors--insight into heterotrimeric IL-1 signaling complexes. *Structure, 17*(10), 1398-1410. doi:10.1016/j.str.2009.08.009
Liu, P., Chen, G., & Zhang, J. (2022). A Review of Liposomes as a Drug Delivery System: Current Status of Approved Products, Regulatory Environments, and Future Perspectives. *Molecules, 27*(4). doi:10.3390/molecules27041372
Liu, T., Zhang, L., Joo, D., & Sun, S. C. (2017). NF-kappaB signaling in inflammation. *Signal Transduct Target Ther, 2*, 17023-. doi:10.1038/sigtrans.2017.23
Liu, X., Kenkare, K., Li, S., Desai, V., Wong, J., Luo, X., . . . Wang, Q. M. (2015). Increased Th17/Treg Ratio in Poststroke Fatigue. *Mediators Inflamm, 2015*, 931398. doi:10.1155/2015/931398
Liu, X., Xiao, Y., Pan, Y., Li, H., Zheng, S. G., & Su, W. (2019). The role of the IL-33/ST2 axis in autoimmune disorders: Friend or foe? *Cytokine & Growth Factor Reviews, 50*, 60-74. doi:https://doi.org/10.1016/j.cytogfr.2019.04.004
Löhning, M., Stroehmann, A., Coyle, A. J., Grogan, J. L., Lin, S., Gutierrez-Ramos, J. C., . . . Kamradt, T. (1998). T1/ST2 is preferentially expressed on murine Th2 cells, independent of interleukin 4, interleukin 5, and interleukin 10, and important for Th2 effector function. *Proc Natl Acad Sci U S A, 95*(12), 6930-6935. doi:10.1073/pnas.95.12.6930
Lommatzsch, M., & Virchow, J. C. (2014). Severe asthma: definition, diagnosis and treatment. *Dtsch Arztebl Int, 111*(50), 847-855. doi:10.3238/arztebl.2014.0847
Ma, J., Sun, X., Wang, X., Liu, B., & Shi, K. (2023). Factors Affecting Patient Adherence to Inhalation Therapy: An Application of SEIPS Model 2.0. *Patient Prefer Adherence, 17*, 531-545. doi:10.2147/PPA.S395327
Ma, L., Zhu, M., Li, G., Gai, J., Li, Y., Gu, H., . . . Wan, Y. (2022). Preclinical development of a long-acting trivalent bispecific nanobody targeting IL-5 for the treatment of eosinophilic asthma. *Respir Res, 23*(1), 316. doi:10.1186/s12931-022-02240-1
Mahemuti, G., Zhang, H., Li, J., Tieliwaerdi, N., & Ren, L. (2018). Efficacy and side effects of intravenous theophylline in acute asthma: a systematic review and meta-analysis. *Drug Des Devel Ther, 12*, 99-120. doi:10.2147/DDDT.S156509
Mahmood, T., & Yang, P. C. (2012). Western blot: technique, theory, and trouble shooting. *N Am J Med Sci, 4*(9), 429-434. doi:10.4103/1947-2714.100998
Marques, A. H., Silverman, M. N., & Sternberg, E. M. (2009). Glucocorticoid dysregulations and their clinical correlates. From receptors to therapeutics. *Ann N Y Acad Sci, 1179*, 1-18. doi:10.1111/j.1749-6632.2009.04987.x
Mato, N., Hirahara, K., Ichikawa, T., Kumagai, J., Nakayama, M., Yamasawa, H., . . . Nakayama, T. (2017). Memory-type ST2(+)CD4(+) T cells participate in the steroid-resistant pathology of eosinophilic pneumonia. *Sci Rep, 7*(1), 6805. doi:10.1038/s41598-017-06962-x

Matthews, J. G., Ito, K., Barnes, P. J., & Adcock, I. M. (2004). Defective glucocorticoid receptor nuclear translocation and altered histone acetylation patterns in glucocorticoid-resistant patients. *J Allergy Clin Immunol, 113*(6), 1100-1108. doi:10.1016/j.jaci.2004.03.018

McGovern, T. K., Robichaud, A., Fereydoonzad, L., Schuessler, T. F., & Martin, J. G. (2013). Evaluation of respiratory system mechanics in mice using the forced oscillation technique. *J Vis Exp*(75), e50172. doi:10.3791/50172

Miller, A. M. (2011). Role of IL-33 in inflammation and disease. *Journal of Inflammation, 8*(1), 22. doi:10.1186/1476-9255-8-22

Mir, M. A., Mehraj, U., Sheikh, B. A., & Hamdani, S. S. (2020). Nanobodies: The "Magic Bullets" in therapeutics, drug delivery and diagnostics. *Human Antibodies, 28*(1), 29-51. doi:10.3233/HAB-190390

Moussion, C., Ortega, N., & Girard, J. P. (2008). The IL-1-like cytokine IL-33 is constitutively expressed in the nucleus of endothelial cells and epithelial cells in vivo: a novel 'alarmin'? *PLoS One, 3*(10), e3331. doi:10.1371/journal.pone.0003331

Murakami-Satsutani, N., Ito, T., Nakanishi, T., Inagaki, N., Tanaka, A., Vien, P. T., . . . Nomura, S. (2014). IL-33 promotes the induction and maintenance of Th2 immune responses by enhancing the function of OX40 ligand. *Allergol Int, 63*(3), 443-455. doi:10.2332/allergolint.13-OA-0672

Murdaca, G., Greco, M., Tonacci, A., Negrini, S., Borro, M., Puppo, F., & Gangemi, S. (2019). IL-33/IL-31 Axis in Immune-Mediated and Allergic Diseases. *20*(23), 5856.

Mustafa, M., & Ahmed, A. (2023). *Nanobodies as Spray and Aerosol Particles: A Breakthrough in Treating Respiratory Viral Infections*.

Muyldermans, S. (2013). Nanobodies: natural single-domain antibodies. *Annu Rev Biochem, 82*, 775-797. doi:10.1146/annurev-biochem-063011-092449

Naderi, S., Roshan, R., Ghaderi, H., Behdani, M., Mahmoudi, S., Habibi-Anbouhi, M., . . . Kazemi-Lomedasht, F. (2020). Selection and characterization of specific nanobody against neuropilin-1 for inhibition of angiogenesis. *Mol Immunol, 128*, 56-63. doi:10.1016/j.molimm.2020.10.004

Nair, P., Pizzichini, M. M., Kjarsgaard, M., Inman, M. D., Efthimiadis, A., Pizzichini, E., . . . O'Byrne, P. M. (2009). Mepolizumab for prednisone-dependent asthma with sputum eosinophilia. *N Engl J Med, 360*(10), 985-993. doi:10.1056/NEJMoa0805435

Nair, P., Surette, M. G., & Virchow, J. C. (2021). Neutrophilic asthma: misconception or misnomer? *Lancet Respir Med, 9*(5), 441-443. doi:10.1016/s2213-2600(21)00023-0

Nakagome, K., & Nagata, M. (2024). The Possible Roles of IL-4/IL-13 in the Development of Eosinophil-Predominant Severe Asthma. *Biomolecules, 14*(5). doi:10.3390/biom14050546

Nakamura, Y., Sugano, A., Ohta, M., & Takaoka, Y. (2017). Docking analysis and the possibility of prediction efficacy for an anti-IL-13 biopharmaceutical treatment with tralokinumab and lebrikizumab for bronchial asthma. *PLoS One, 12*(11), e0188407. doi:10.1371/journal.pone.0188407

Nannini, L. J., Lasserson, T. J., & Poole, P. (2012). Combined corticosteroid and long-acting beta(2)-agonist in one inhaler versus long-acting beta(2)-agonists for chronic obstructive pulmonary disease. *Cochrane Database Syst Rev, 2012*(9), Cd006829. doi:10.1002/14651858.CD006829.pub2

Newcomb, D. C., & Peebles, R. S., Jr. (2013). Th17-mediated inflammation in asthma. *Curr Opin Immunol, 25*(6), 755-760. doi:10.1016/j.coi.2013.08.002

Norzila, M. Z., Fakes, K., Henry, R. L., Simpson, J., & Gibson, P. G. (2000). Interleukin-8 secretion and neutrophil recruitment accompanies induced sputum eosinophil

activation in children with acute asthma. *Am J Respir Crit Care Med, 161*(3 Pt 1), 769-774. doi:10.1164/ajrccm.161.3.9809071

O'Byrne, P. M., & Inman, M. D. (2003). Airway hyperresponsiveness. *Chest, 123*(3 Suppl), 411s-416s. doi:10.1378/chest.123.3_suppl.411s

Olguín-Martínez, E., Muñoz-Paleta, O., Ruiz-Medina, B. E., Ramos-Balderas, J. L., Licona-Limón, I., & Licona-Limón, P. (2022). IL-33 and the PKA Pathway Regulate ILC2 Populations Expressing IL-9 and ST2. *13*. doi:10.3389/fimmu.2022.787713

Onyedum, C., Ukwaja, K., Desalu, O., & Ezeudo, C. (2013). Challenges in the management of bronchial asthma among adults in Nigeria: a systematic review. *Ann Med Health Sci Res, 3*(3), 324-329. doi:10.4103/2141-9248.117927

Papi, A., Blasi, F., Canonica, G. W., Morandi, L., Richeldi, L., & Rossi, A. (2020). Treatment strategies for asthma: reshaping the concept of asthma management. *Allergy Asthma Clin Immunol, 16*, 75. doi:10.1186/s13223-020-00472-8

Pardon, E., Laeremans, T., Triest, S., Rasmussen, S. G., Wohlkönig, A., Ruf, A., . . . Steyaert, J. (2014). A general protocol for the generation of Nanobodies for structural biology. *Nat Protoc, 9*(3), 674-693. doi:10.1038/nprot.2014.039

Paul, P., Ghosh, N., Mitra, S., Banerjee, E., & Ghorui, S. (2023). Camelid derived anti IgE nanoantibodies block Th2 response in induced acute allergic lung inflammation of BALB/c mice. *INDIAN JOURNAL OF ANIMAL HEALTH, 62*. doi:10.36062/ijah.2023.spl.02123

Pavord, I. D., Korn, S., Howarth, P., Bleecker, E. R., Buhl, R., Keene, O. N., . . . Chanez, P. (2012). Mepolizumab for severe eosinophilic asthma (DREAM): a multicentre, double-blind, placebo-controlled trial. *Lancet, 380*(9842), 651-659. doi:10.1016/S0140-6736(12)60988-X

Pelaia, C., Heffler, E., Crimi, C., Maglio, A., Vatrella, A., Pelaia, G., & Canonica, G. W. (2022). Interleukins 4 and 13 in Asthma: Key Pathophysiologic Cytokines and Druggable Molecular Targets. *Front Pharmacol, 13*, 851940. doi:10.3389/fphar.2022.851940

Peters, M. C., Kerr, S., Dunican, E. M., Woodruff, P. G., Fajt, M. L., Levy, B. D., . . . Blood Institute Severe Asthma Research, P. (2019). Refractory airway type 2 inflammation in a large subgroup of asthmatic patients treated with inhaled corticosteroids. *J Allergy Clin Immunol, 143*(1), 104-113 e114. doi:10.1016/j.jaci.2017.12.1009

Piehler, D., Eschke, M., Schulze, B., Protschka, M., Müller, U., Grahnert, A., . . . Alber, G. (2016). The IL-33 receptor (ST2) regulates early IL-13 production in fungus-induced allergic airway inflammation. *Mucosal Immunology, 9*(4), 937-949. doi:10.1038/mi.2015.106

Pillay, T. S., & Muyldermans, S. (2021). Application of Single-Domain Antibodies ("Nanobodies") to Laboratory Diagnosis. *Ann Lab Med, 41*(6), 549-558. doi:10.3343/alm.2021.41.6.549

Pinto, S. M., Subbannayya, Y., Rex, D. A. B., Raju, R., Chatterjee, O., Advani, J., . . . Pandey, A. (2018). A network map of IL-33 signaling pathway. *J Cell Commun Signal, 12*(3), 615-624. doi:10.1007/s12079-018-0464-4

Poon, A. H., & Hamid, Q. (2016). Severe Asthma: Have We Made Progress? *Ann Am Thorac Soc, 13 Suppl 1*, S68-77. doi:10.1513/AnnalsATS.201508-514MG

Prefontaine, D., Lajoie-Kadoch, S., Foley, S., Audusseau, S., Olivenstein, R., Halayko, A. J., . . . Hamid, Q. (2009). Increased expression of IL-33 in severe asthma: evidence of expression by airway smooth muscle cells. *J Immunol, 183*(8), 5094-5103. doi:10.4049/jimmunol.0802387

Qiu, W., Meng, J., Su, Z., Xie, W., & Song, G. (2024). Structural insight into interleukin-4Ralpha and interleukin-5 inhibition by nanobodies from a bispecific antibody. *MedComm (2020), 5*(9), e700. doi:10.1002/mco2.700

Ramakrishnan, R. K., Al Heialy, S., & Hamid, Q. (2019). Role of IL-17 in asthma pathogenesis and its implications for the clinic. *Expert Rev Respir Med, 13*(11), 1057-1068. doi:10.1080/17476348.2019.1666002

Ramamoorthy, S., & Cidlowski, J. A. (2016). Corticosteroids: Mechanisms of Action in Health and Disease. *Rheum Dis Clin North Am, 42*(1), 15-31, vii. doi:10.1016/j.rdc.2015.08.002

Ridolo, E., Pucciarini, F., Nizi, M. C., Makri, E., Kihlgren, P., Panella, L., & Incorvaia, C. (2020). Mabs for treating asthma: omalizumab, mepolizumab, reslizumab, benralizumab, dupilumab. *Hum Vaccin Immunother, 16*(10), 2349-2356. doi:10.1080/21645515.2020.1753440

Rinaldi, M., Denayer, T., Thiolloy, S., Perez Tosar, L. C., Buyse, M.-A., De Decker, P., . . . Holz, J.-B. (2013). ALX-0962, an anti-IgE Nanobody® with a dual mode of action. *42*(Suppl 57), 1765.

Robins, S., Roussel, L., Schachter, A., Risse, P. A., Mogas, A. K., Olivenstein, R., . . . Rousseau, S. (2011). Steroid-insensitive ERK1/2 activity drives CXCL8 synthesis and neutrophilia by airway smooth muscle. *Am J Respir Cell Mol Biol, 45*(5), 984-990. doi:10.1165/rcmb.2010-0450OC

Robinson, D., Humbert, M., Buhl, R., Cruz, A. A., Inoue, H., Korom, S., . . . Nair, P. (2017). Revisiting Type 2-high and Type 2-low airway inflammation in asthma: current knowledge and therapeutic implications. *Clin Exp Allergy, 47*(2), 161-175. doi:10.1111/cea.12880

Saag, K. G., Koehnke, R., Caldwell, J. R., Brasington, R., Burmeister, L. F., Zimmerman, B., . . . Furst, D. E. (1994). Low dose long-term corticosteroid therapy in rheumatoid arthritis: an analysis of serious adverse events. *Am J Med, 96*(2), 115-123. doi:10.1016/0002-9343(94)90131-7

Saleh, J. A. (2008). Combination therapy in asthma: a review. *Niger J Med, 17*(3), 238-243. doi:10.4314/njm.v17i3.37377

Samaranayake, H., Wirth, T., Schenkwein, D., Räty, J. K., & Ylä-Herttuala, S. (2009). Challenges in monoclonal antibody-based therapies. *Ann Med, 41*(5), 322-331. doi:10.1080/07853890802698842

Samarasinghe, R. A., Witchell, S. F., & DeFranco, D. B. (2012). Cooperativity and complementarity: synergies in non-classical and classical glucocorticoid signaling. *Cell Cycle, 11*(15), 2819-2827. doi:10.4161/cc.21018

Scherzer, R., & Grayson, M. H. (2018). Heterogeneity and the origins of asthma. *Ann Allergy Asthma Immunol, 121*(4), 400-405. doi:10.1016/j.anai.2018.06.009

Schmitz, J., Owyang, A., Oldham, E., Song, Y., Murphy, E., McClanahan, T. K., . . . Kastelein, R. A. (2005). IL-33, an interleukin-1-like cytokine that signals via the IL-1 receptor-related protein ST2 and induces T helper type 2-associated cytokines. *Immunity, 23*(5), 479-490. doi:10.1016/j.immuni.2005.09.015

Scully, M., Cataland, S. R., Peyvandi, F., Coppo, P., Knobl, P., Kremer Hovinga, J. A., . . . Investigators, H. (2019). Caplacizumab Treatment for Acquired Thrombotic Thrombocytopenic Purpura. *N Engl J Med, 380*(4), 335-346. doi:10.1056/NEJMoa1806311

Serdar, C. C., Cihan, M., Yücel, D., & Serdar, M. A. (2021). Sample size, power and effect size revisited: simplified and practical approaches in pre-clinical, clinical and laboratory studies. *Biochem Med (Zagreb), 31*(1), 010502. doi:10.11613/bm.2021.010502

Shijie, L. I., Weiyan, D. A. I., Xuelian, W., Chang, L. I. U., Yaoji, L., Zhonghu, B. A. I., & Yongqi, C. (2024). Anti-IL-5 Nanobody Screening and Activity Detection. *China Biotechnology, 44*(2-3), 59-68. doi:10.13523/j.cb.2307036

Sim, S., Choi, Y., & Park, H. S. (2024). Update on Inflammatory Biomarkers for Defining Asthma Phenotype. *Allergy Asthma Immunol Res, 16*(5), 462-472. doi:10.4168/aair.2024.16.5.462

Smith, G. P., & Petrenko, V. A. (1997). Phage Display. *Chem Rev, 97*(2), 391-410. doi:10.1021/cr960065d

Sobieraj, D. M., Weeda, E. R., Nguyen, E., Coleman, C. I., White, C. M., Lazarus, S. C., . . . Baker, W. L. (2018). Association of Inhaled Corticosteroids and Long-Acting beta-Agonists as Controller and Quick Relief Therapy With Exacerbations and Symptom Control in Persistent Asthma: A Systematic Review and Meta-analysis. *JAMA, 319*(14), 1485-1496. doi:10.1001/jama.2018.2769

Southam, D. S., Dolovich, M., O'Byrne, P. M., & Inman, M. D. (2002). Distribution of intranasal instillations in mice: effects of volume, time, body position, and anesthesia. *Am J Physiol Lung Cell Mol Physiol, 282*(4), L833-839. doi:10.1152/ajplung.00173.2001

Stanbery, A. G., Shuchi, S., Jakob von, M., Tait Wojno, E. D., & Ziegler, S. F. (2022). TSLP, IL-33, and IL-25: Not just for allergy and helminth infection. *J Allergy Clin Immunol, 150*(6), 1302-1313. doi:10.1016/j.jaci.2022.07.003

Svecova, D., Lubell, M. W., Casset-Semanaz, F., Mackenzie, H., Grenningloh, R., & Krueger, J. G. (2019). A randomized, double-blind, placebo-controlled phase 1 study of multiple ascending doses of subcutaneous M1095, an anti-interleukin 17A/F nanobody, in moderate-to-severe psoriasis. *J Am Acad Dermatol, 81*(1), 196-203. doi:10.1016/j.jaad.2019.03.056

Syedbasha, M., Linnik, J., Santer, D., O'Shea, D., Barakat, K., Joyce, M., . . . Egli, A. (2016). An ELISA Based Binding and Competition Method to Rapidly Determine Ligand-receptor Interactions. *J Vis Exp*(109). doi:10.3791/53575

Tai, A., Tran, H., Roberts, M., Clarke, N., Wilson, J., & Robertson, C. F. (2014). The association between childhood asthma and adult chronic obstructive pulmonary disease. *Thorax, 69*(9), 805-810. doi:10.1136/thoraxjnl-2013-204815

Talabot-Ayer, D., Calo, N., Vigne, S., Lamacchia, C., Gabay, C., & Palmer, G. (2012). The mouse interleukin (Il)33 gene is expressed in a cell type- and stimulus-dependent manner from two alternative promoters. *J Leukoc Biol, 91*(1), 119-125. doi:10.1189/jlb.0811425

Tarraf, H., Aydin, O., Mungan, D., Albader, M., Mahboub, B., Doble, A., . . . El Hasnaoui, A. (2018). Prevalence of asthma among the adult general population of five Middle Eastern countries: results of the SNAPSHOT program. *BMC Pulm Med, 18*(1), 68. doi:10.1186/s12890-018-0621-9

Thomas, R. J. (2013). Particle size and pathogenicity in the respiratory tract. *Virulence, 4*(8), 847-858. doi:10.4161/viru.27172

Toskala, E., & Kennedy, D. W. (2015). Asthma risk factors. *Int Forum Allergy Rhinol, 5 Suppl 1*(Suppl 1), S11-16. doi:10.1002/alr.21557

Tsuda, H., Komine, M., Karakawa, M., Etoh, T., Tominaga, S., & Ohtsuki, M. (2012). Novel splice variants of IL-33: differential expression in normal and transformed cells. *J Invest Dermatol, 132*(11), 2661-2664. doi:10.1038/jid.2012.180

Tsuyuki, S., Tsuyuki, J., Einsle, K., Kopf, M., & Coyle, A. J. (1997). Costimulation through B7-2 (CD86) is required for the induction of a lung mucosal T helper cell 2 (TH2) immune response and altered airway responsiveness. *J Exp Med, 185*(9), 1671-1679. doi:10.1084/jem.185.9.1671

Ukena, D., Fishman, L., & Niebling, W. B. (2008). Bronchial asthma: diagnosis and long-term treatment in adults. *Dtsch Arztebl Int, 105*(21), 385-394. doi:10.3238/arztebl.2008.0385

van der Zwet, J. C. G., Buijs-Gladdines, J., Cordo, V., Debets, D. O., Smits, W. K., Chen, Z., . . . Meijerink, J. P. P. (2021). MAPK-ERK is a central pathway in T-cell acute lymphoblastic leukemia that drives steroid resistance. *Leukemia, 35*(12), 3394-3405. doi:10.1038/s41375-021-01291-5

Van Heeke, G., Allosery, K., De Brabandere, V., De Smedt, T., Detalle, L., & de Fougerolles, A. (2017). Nanobodies(R) as inhaled biotherapeutics for lung diseases. *Pharmacol Ther, 169*, 47-56. doi:10.1016/j.pharmthera.2016.06.012

Van Roy, M., Ververken, C., Beirnaert, E., Hoefman, S., Kolkman, J., Vierboom, M., . . . Ulrichts, H. (2015). The preclinical pharmacology of the high affinity anti-IL-6R Nanobody(R) ALX-0061 supports its clinical development in rheumatoid arthritis. *Arthritis Res Ther, 17*(1), 135. doi:10.1186/s13075-015-0651-0

Vazquez-Tello, A., Halwani, R., Hamid, Q., & Al-Muhsen, S. (2013). Glucocorticoid receptor-beta up-regulation and steroid resistance induction by IL-17 and IL-23 cytokine stimulation in peripheral mononuclear cells. *J Clin Immunol, 33*(2), 466-478. doi:10.1007/s10875-012-9828-3

Vazquez-Tello, A., Semlali, A., Chakir, J., Martin, J. G., Leung, D. Y., Eidelman, D. H., & Hamid, Q. (2010). Induction of glucocorticoid receptor-beta expression in epithelial cells of asthmatic airways by T-helper type 17 cytokines. *Clin Exp Allergy, 40*(9), 1312-1322. doi:10.1111/j.1365-2222.2010.03544.x

Vincke, C., Gutiérrez, C., Wernery, U., Devoogdt, N., Hassanzadeh-Ghassabeh, G., & Muyldermans, S. (2012). Generation of single domain antibody fragments derived from camelids and generation of manifold constructs. *Methods Mol Biol, 907*, 145-176. doi:10.1007/978-1-61779-974-7_8

von Mutius, E., & Smits, H. H. (2020). Primary prevention of asthma: from risk and protective factors to targeted strategies for prevention. *Lancet, 396*(10254), 854-866. doi:10.1016/S0140-6736(20)31861-4

Wadhwa, R., Dua, K., Adcock, I. M., Horvat, J. C., Kim, R. Y., & Hansbro, P. M. (2019). Cellular mechanisms underlying steroid-resistant asthma. *Eur Respir Rev, 28*(153). doi:10.1183/16000617.0096-2019

Wadsworth, S., Sin, D., & Dorscheid, D. (2011). Clinical update on the use of biomarkers of airway inflammation in the management of asthma. *J Asthma Allergy, 4*, 77-86. doi:10.2147/JAA.S15081

Ward, C., Pais, M., Bish, R., Reid, D., Feltis, B., Johns, D., & Walters, E. H. (2002). Airway inflammation, basement membrane thickening and bronchial hyperresponsiveness in asthma. *Thorax, 57*(4), 309-316. doi:10.1136/thorax.57.4.309

Weiss, J. N. (1997). The Hill equation revisited: uses and misuses. *Faseb j, 11*(11), 835-841.

Wenzel, S. E. (2012). Asthma phenotypes: the evolution from clinical to molecular approaches. *Nat Med, 18*(5), 716-725. doi:10.1038/nm.2678

Whetstone, C. E., Ranjbar, M., Omer, H., Cusack, R. P., & Gauvreau, G. M. (2022). The Role of Airway Epithelial Cell Alarmins in Asthma. *Cells, 11*(7). doi:10.3390/cells11071105

Woo, L. N., Guo, W. Y., Wang, X., Young, A., Salehi, S., Hin, A., . . . Chow, C. W. (2018). A 4-Week Model of House Dust Mite (HDM) Induced Allergic Airways Inflammation with Airway Remodeling. *Scientific Reports, 8*(1), 6925. doi:10.1038/s41598-018-24574-x

Wu, H., Yang, S., Wu, X., Zhao, J., Zhao, J., Ning, Q., . . . Xie, J. (2014). Interleukin-33/ST2 signaling promotes production of interleukin-6 and interleukin-8 in systemic

inflammation in cigarette smoke-induced chronic obstructive pulmonary disease mice. *Biochem Biophys Res Commun, 450*(1), 110-116. doi:10.1016/j.bbrc.2014.05.073

Wu, Y., Shi, W., Wang, H., Yue, J., Mao, Y., Zhou, W., . . . Wang, Y. (2020). Anti-ST2 Nanoparticle Alleviates Lung Inflammation by Targeting ILC2s-CD4(+)T Response. *Int J Nanomedicine, 15*, 9745-9758. doi:10.2147/ijn.S268282

Xie, Y., Abel, P. W., Casale, T. B., & Tu, Y. (2022). T(H)17 cells and corticosteroid insensitivity in severe asthma. *J Allergy Clin Immunol, 149*(2), 467-479. doi:10.1016/j.jaci.2021.12.769

Yasir, M., Goyal, A., & Sonthalia, S. (2024). Corticosteroid Adverse Effects. In *StatPearls*. Treasure Island (FL) ineligible companies. Disclosure: Amandeep Goyal declares no relevant financial relationships with ineligible companies. Disclosure: Sidharth Sonthalia declares no relevant financial relationships with ineligible companies.

Ye, Y., Ma, Y., & Zhu, J. (2022). The future of dry powder inhaled therapy: Promising or discouraging for systemic disorders? *Int J Pharm, 614*, 121457. doi:10.1016/j.ijpharm.2022.121457

Yi, X. M., Lian, H., & Li, S. (2022). Signaling and functions of interleukin-33 in immune regulation and diseases. *Cell Insight, 1*(4), 100042. doi:10.1016/j.cellin.2022.100042

Yousuf, A. J., Mohammed, S., Carr, L., Yavari Ramsheh, M., Micieli, C., Mistry, V., . . . Brightling, C. E. (2022). Astegolimab, an anti-ST2, in chronic obstructive pulmonary disease (COPD-ST2OP): a phase 2a, placebo-controlled trial. *The Lancet Respiratory Medicine, 10*(5), 469-477. doi:10.1016/S2213-2600(21)00556-7

Zhu, M., Ma, L., Zhong, P., Huang, J., Gai, J., Li, G., . . . Wan, Y. (2024). A novel inhalable nanobody targeting IL-4Ralpha for the treatment of asthma. *J Allergy Clin Immunol, 154*(4), 1008-1021. doi:10.1016/j.jaci.2024.05.027

7. Acknowledgments

I would like to express my sincere gratitude to Prof. Jennifer Hundt at the University of Lübeck, whose guidance and endless support have been a beacon of hope during my time in a new environment. Her understanding and encouragement kept me grounded, and her mentorship enriched my research in ways words cannot fully capture. I am also immensely thankful to Nadine, the lab technician, for her incredible patience and kindness. She guided me step by step when I felt lost and alone, helping me navigate the challenges of adapting to an unfamiliar environment. A special note of thanks to Marieke, the coordinator, for her constant support and care, ensuring that every hurdle was easier to overcome. I am deeply grateful to all Hundt lab members.

I would also like to thank my co-supervisor in Lübeck, Dr. Yves Laumonnier, for his invaluable support and guidance throughout my research journey.

I am deeply grateful to my mentor, Prof. Rabih Halwani, whose exceptional leadership, insightful advice, and continuous support have been invaluable throughout my journey. His encouragement, patience, and belief in my potential have not only shaped this research but also contributed significantly to my personal and academic growth.

My heartfelt thanks go to Dr. Fatemeh, whose steadfast support, guidance, and encouragement during the most challenging phases of this journey have been a source of immense strength for me. Your mentorship was truly invaluable, and I am beyond grateful for everything you have done. To Dr. Narjes, thank you for your meticulous attention to detail, constructive feedback, and thoughtful insights that greatly enhanced my work. You both have been more than mentors—you have been like sisters to me, always there with warmth, understanding, and inspiration.

I also want to express my gratitude to Dr. Adel Zakari, our collaborator, for his profound knowledge, remarkable patience, and invaluable training during my time in Saudi Arabia. Your warm welcome and dedication to teaching made the experience both meaningful and enriching.

I am deeply grateful to Dr. Priya for her expertise in microbiology, which added a significant dimension to my work. My heartfelt thanks also go to Dr. Ibrahim, a pathologist, for his support and insights throughout this journey. Additionally, I would like to extend my sincere gratitude to Dr. Bala for his invaluable advice and thoughtful guidance.

To my fellow researchers and lab colleagues your unwavering support and encouragement have been a source of strength throughout this journey. The countless late nights we spent working together, thank you for being more than colleagues—you became family on this path.

Special thanks to the incredible team at the tissue bank for their exceptional technical assistance, unwavering support, and kindness. Your help has been instrumental in the progress and success of my research.

I would also like to thank my colleagues in the dual-degree program between the University of Sharjah and the University of Lübeck for making the academic and cultural exchange experience enjoyable.

We sincerely acknowledge Prof. Serge Muyldermans from the Cellular and Molecular Immunology, Vrije Universiteit Brussel, Pleinlaan 2, 1050 Brussel, Belgium, for kindly providing us with the pMECS-GG phagemid vector.

Lastly, I express my deepest appreciation to my family. To my husband, for his constant support. To my parents, brothers, uncle, sisters-in-law and parents-in-law I could not have reached this point without your continuous help and encouragement.

8. Publications associated with this research

1. Baraa Khalid Al-Sheakly, Fatemeh Saheb Sharif-Askari, Narjes Saheb Sharif-Askari, Jennifer E. Hundt, Rabih Halwani. Nanobodies: A Promising Strategy for Asthma Therapy. **Accepted**

2. Baraa Khalid Salah Al-Sheakly, Fatemeh Saheb Sharif-Askari, Narjes Saheb Sharif-Askari, Bushra Mdkhana, Mariam Wed Eladham, Bariaa A Khalil, Ibrahim Hachim, Adel M. Zakri, Jennifer E. Hundt, Rabih Halwani. IL-33 Induces Steroid Hyporesponsive Asthma in a Chronic HDM-Induced Asthma Mouse Model. **Submitted**

3. Baraa Khalid Salah Al-Sheakly, Fatemeh Saheb Sharif-Askari, Narjes Saheb Sharif-Askari, Rabih Halwani. Intranasal Astegolimab Mitigates Steroid Hypo-responsiveness and Airway Remodeling in Severe Asthma. **In preparation**

4. Baraa Khalid Salah Al-Sheakly, Fatemeh Saheb Sharif-Askari, Narjes Saheb Sharif-Askari, Adel M. Zakri, Rabih Halwani. Selection and characterization of specific nanobody against ST2. **In preparation**

5. Baraa Khalid Salah Al-Sheakly, Fatemeh Saheb Sharif-Askari, Narjes Saheb Sharif-Askari, Adel M. Zakri, Rabih Halwani. Novel Anti-ST2 Therapy Reverses Steroid Hypo-Responsiveness in Severe Asthma. **In preparation**

6. A **patent application has been submitted** based on the innovative findings presented in this study, aiming to protect the intellectual property associated with the therapeutic potential of the NB7 nanobody.